University of Veterinary Medicine Hannover Foundation
Small Animal Clinic

Molecular Characterisation of Feline Mammary Tumours

Thesis
Submitted in partial fulfilment of the requirements for the degree

Doctor of Philosophy (PhD)
Veterinary Research and Animal Biology

José Luis Granados-Soler
(Born in Bogotá, Colombia)
Published in Hannover, Germany
2019

University of Veterinary Medicine Hannover Foundation
Small Animal Clinic

Molecular Characterisation of Feline Mammary Tumours

Thesis
Submitted in partial fulfilment of the requirements for the degree

Doctor of Philosophy (PhD)
Veterinary Research and Animal Biology

by

José Luis Granados-Soler
(Born in Bogotá, Colombia)
Published in Hannover, Germany
2019

"Supervision group"

Main Supervisor	**Prof. Dr. Ingo Nolte**
Advisory Committee	**Prof. Dr. Ingo Nolte** **PD Dr. rer. nat. habil. Hugo Murua Escobar** **Prof. Dr. Marion Hewicker-Trautwein**
First evaluation	**Prof. Dr. Ingo Nolte** Klinik für Kleintiere Stiftung Tierärztliche Hochschule Hannover. **PD Dr. rer. nat. habil. Hugo Murua Escobar** Medizinische Klinik III, Klinik für Hämatologie, Onkologie und Palliativmedizin Universitätsmedizin Rostock **Prof. Dr. Marion Hewicker-Trautwein** Institut für Pathologie Stiftung Tierärztliche Hochschule Hannover.
Second Evaluation	**Prof. Dr. Arnold Ganser** Medizinische Hochschule Hannover Klinik für Hämatologie, Hämostaseologie, Onkologie und Stammzelltransplantation
Date of final exam:	**04.04.2019**

"This study was partially funded by the German Academic Exchange Service (DAAD) by a research scholarship awarded to José Luis Granados-Soler"

Dedicated to my family

"Manuscripts included"

The following manuscript has been published in the journal Scientific Reports:

TiHo-0906: a new feline mammary cancer cell line with molecular, morphological, and immunocytological characteristics of epithelial to mesenchymal transition.
José Luis Granados-Soler, Johannes Junginger, Marion Hewicker-Trautwein, Kirsten Bornemann-Kolatzki, Julia Beck, Bertram Brenig, Daniela Betz, Jan Torben Schille, Hugo Murua Escobar, Ingo Nolte. Scientific Reports | (2018) 8:13231 | DOI:10.1038/s41598-018-31682-1.

The following manuscript have been submitted for publication:

Analysis of Somatic Copy-Number Variations and Feline Mammary Carcinoma Survival.
José Luis Granados-Soler, Kirsten Bornemann-Kolatzki, Julia Beck, Bertram Brenig, Ekkehard Schütz, Daniela Betz, Johannes Junginger, Marion Hewicker-Trautwein, Hugo Murua Escobar, Ingo Nolte. Journal, Scientific reports | manuscript tracking number, SREP-19-00005 | submission date, 11th January 2019 | current stage, manuscript assigned to peer-reviewers

The following manuscript is under preparation to be submitted for publication:

High-Resolution Transcriptome Profiling of Feline Mammary Carcinomas.
José Luis Granados-Soler, Kirsten Bornemann-Kolatzki, Julia Beck, Bertram Brenig, Ekkehard Schütz, Daniela Betz, Johannes Junginger, Marion Hewicker-Trautwein, Hugo Murua Escobar, Ingo Nolte.

"Conferences and posters"

Parts of this thesis were presented at the following meetings and conferences:

Conferences

Copy number variations analysis and feline mammary carcinoma survival
European Society of Veterinary Oncology (ESVONC), ESVONC-Congress. 23–26 May 2018, Las Palmas de Gran Canaria, Spain

Copy number variations analysis and feline mammary cancer survival: a multivariable prognostic study
26th Internal Medicine and Laboratory Meeting (InnLab). German Society of Veterinary Medicine (DVG). 02–03 February 2018, Hannover, Germany

Establishment and characterization of a cell line derived from a feline mammary adenocarcinoma
25th Internal Medicine and Laboratory Meeting (InnLab). German Society of Veterinary Medicine (DVG). 03–04 February 2017, Göttingen, Germany

Molecular and cytogenetic characterization of feline mammary tumours
9th Graduate School Days, University of Veterinary Medicine Hannover, Foundation. 02–03 December 2016, Hannover, Germany

Posters

TiHo-0906: a new feline mammary cancer cell line with characteristics of epithelial to mesenchymal transition
10th Graduate School Days, University of Veterinary Medicine Hannover, Foundation. 01–02 December 2017, Hannover, Germany

"Contents"

"Realising feline mammary cancer heterogeneity"

Mammary cancer is one of the most common malignancies observed in humans, dogs and cats, and a major health problem in human and small animal medicine. In recent years, there has been substantial progress in the molecular portraying of human breast cancer, leading to a more detailed classification—beyond the histological diagnosis[1–7]. Molecular studies using different approaches (e.g. genomic, transcriptomic, proteomic and metabolomics) suggest that human breast cancer represents a heterogeneous group of diseases with distinctive molecular traits influencing therapeutic response, disease-free survival (DFS), and overall survival (OS)[1,2,7–12]. Next-generation sequencing (NGS) allows rapid high-resolution characterisation of potentially clinically relevant genomic and transcriptomic features of cancer[6,7,13–16]. In small animal medicine, the heterogeneity of the feline and canine mammary cancers—and cells composing the tumour microenvironment—have been realised through the conventional histopathological examination and immunohistochemical profiling[17–22]. Nonetheless, the actual extent of diversity among mammary cancer in dogs and cats can be appreciated only through extensive molecular analyses.

The feline mammary tissue encompasses three tissue lineages: the luminal epithelial, the myoepithelial (or basal epithelial), and the mesenchymal. Feline mammary tumours are typically invasive adenocarcinomas—approximately 80–90% of feline mammary tumours are malignant luminal epithelial tumours usually referred to as feline mammary carcinomas (FMCs)[23–25]. Until now, only the expression of single or few potentially related marker genes has been analysed in FMCs—mostly via immunohistochemistry[17,20,24,26–32]. The identification of individual targets as potential markers for FMCs is fundamental. However, a comprehensive analysis of structural genomic rearrangements and gene expression patterns in correlation with survival intervals (DFS and OS) and well-documented prognostic factors (i.e. histological malignancy grade [HMG] and lymph node invasion) is pivotal but has not been conducted so far.

"Factors influencing prognosis of FMCs"

Biological behaviour. FMCs are characterised by early lymph node/lymphovascular invasion and distant metastasis[24,25,33]. Cats affected usually have a reduced DFS and OS, and a poor response to treatment[34–37]. Most of the animals affected are older individuals with a mean age of presentation between 10–12 years[24,25,38–40]. Affected cats have a poor prognosis due to the early metastasis to regional lymph nodes, lungs, liver and pleura[24,33,41,42]. An association between early spaying and a reduced risk of developing FMCs has been reported[43]. However, the biological behaviour of FMCs affecting intact and spayed cats do not differ[44,45]. A considerable amount of FMCs are triple-negative tumours (i.e. oestrogen receptor [ER] negative, progesterone receptor [PR] negative, and human epidermal growth factor receptor 2 (HER2) negative) [17,25,46], this typical feature may be a determining factor explaining FMCs aggressiveness and poor survival.

Clinical staging, lymph node invasion and histological grading. Various parameters have been applied for prognostication of FMCs including the size of tumours, HMG, and lymph node involvement at diagnosis[24,47,48]. Traditional classifications including histological diagnosis and clinical staging are used to guide patient management. The current clinical staging system, commonly referred to as "tumour, node, metastasis" or TNM staging system[49] is based on the evaluation of three clinically approachable parameters: tumour size, lymph node invasion, and distant metastases. However, according to a literature review by Zappulli et al. (2015)—evaluating around 200 manuscripts—the most reliable prognostic parameters for FMCs are the HMG and the lymph node status at diagnosis[24]. Bigger tumours have been associated with poor prognosis and higher HMGs[50–52]; nonetheless, small tumours have been also reported to have high HMGs[53,54]. Accordingly, it appears reasonable to consider that specific malignancy features can be directly correlated with the molecular characteristics of distinctive subtypes of FMCs and not necessarily with the disease progression.

Suitable therapies availability. The current standard therapy for FMCs is the complete excision of the tumour by removing one or preferably both mammary chains and associated lymph nodes[55,37]. The median survival time in untreated cats after tumour detection is varying from four months to three years depending on the tumour size and the clinical staging[24,41,42,51]. Thus, early diagnosis and treatment are important for improving prognosis[51]. Some clinical studies have investigated the benefit of different chemotherapeutic regimens with variable results[34,49,56,36]. However, due to the lack of information about which subset of patients would specifically benefit from the proposed chemotherapeutic and adjuvant-therapy regimes[34,49,56,36,38] most of them are not commonly used in the clinical practice.

"Molecular and immunohistochemical features of FMCs"

In addition to clinical and histological parameters, potential molecular markers can provide further prognostic relevant information and may help to understand the molecular pathogenesis of the neoplastic change[25,33,57]. Most of the literature characterising the FMC expression of relevant molecular markers (i.e. HER2, ER, PR, Ki67, etc.) —commonly used in human breast cancer—has been based on immunohistochemistry. However, different factors including sample size, lack of protocols standardization, molecular tool cross-reactivity, and consensus on data analysis make published data on FMCs less reliable and hard to compare[24].

FMCs are commonly hormone-independent tumours (ER-negative and PR-negative)[46,55,58,59]. In some cases the PR status is initially positive, but has been shown to decrease in invasive carcinomas[59,60] suggesting loss of steroid dependency during malignant progression[58,61,62]. Additionally, a large group of hormone receptor-negative FMCs do not express HER2[46]. Considering the lack of hormone dependency and the common HER2-negative status, triple-negative FMCs may share important molecular features with the human late-stage hormone receptor-independent triple-negative breast cancer (hTNBC)—characterised by a highly aggressive behaviour and poor prognosis[55,60].

Until now, a limited number of human breast cancer-related genes have been investigated in FMCs—mostly via immunohistochemistry. Those targets include: *ER*, *PR*[33], *HER2*[28,63], *EGFR*[25], *PI3K*[33], *pAKT*[53], *PTEN*[33], *CDH1*[20,29], *CLDN2*[32], *COX2*[64], *CK5/6/14*[25], *BRCA1*[25], *BRCA2*[25], and *STAT3*[65,66]. In some cases, the aforementioned targets showed similar results to studies in human breast cancer, but also contradictory findings were reported. In addition, some molecular markers have only been analysed in human breast cancer such as *HMGA2*[67–69], *CD44*[70,71], *SNAIL*[72,73], *FOXC1*[74], and *STAT1*[74]. As 90% of putative feline genes are homologue to the human counterpart[75] it is likely that those potential markers in human breast cancer might play a key role in FMCs as well. In addition to immunohistochemical and molecular studies focusing on single or few potentially related markers, mass-parallel NGS-based studies are necessary to validate previous findings, generate an overview of the genomic and transcriptomic landscape of FMCs, and provide a solid base for the generation of further prognostic and therapeutic relevant information. Moreover, a detailed understanding of the biological processes and molecular pathway alterations underlying FMC dysregulation may help to understand the molecular pathogenesis of the disease.

"Reliable cellular models development"

Only few cell lines derived from primary FMCs or metastatic lesions have been established and characterised[76–82]. Despite the similarities between original tumours and derived cell lines, important differences influencing the relevance of cell lines to reliably model specific aspects of the original tumours dysregulation have been previously pointed-out in multiple types of cancer[14,83–88]. In most of the reports characterising FMC-derived cell lines, the molecular characteristics of the cell lines were not compared with those of the original tumours. Moreover, the evaluation of specific molecular characteristics during primary and long-term culture is essential, as cell lines are prone to genotypic and phenotypic changes over time [14,84,89]. Therefore, understanding the suitability of available FMC cell lines through the appropriate pairing with tumour counterparts based on their genomic and transcriptomic similarities during prolonged subculturing is still necessary. Although immortalised cell lines are essential for the testing of novel treatment modalities, their direct applicability to study specific characteristics of the neoplastic process highly depend on the individual characteristics of each cell line[84,88]. Considering the lack of comparisons between FMC-derived cell lines and original tumours, determine which aspects of the FMC dysregulation process may be reliably modelled with the available cell lines is difficult.

Despite the relatively frequent occurrence of FMCs, cytogenetic and genomic data are scarce and little is known about the chromosomal aberrations within these tumours and derived cell lines[90,91]. Several repeatedly occurring numerical and structural alterations such as chromosomal gains and deletions have play an important role in human breast cancer elicitation, and some of them are correlated with specific subsets of patients displaying poor outcome and chemotherapy resistance[92–97]. Thus, the detection of structural chromosomal rearrangements in FMCs is critical to identify patients with poor prognosis, and furthermore to disclose new candidate genes within the rearranged chromosome regions and to confirm the involvement of currently discussed target genes in FMCs.

The cat has a highly conserved karyotype, closely resembling those of the ancestral mammals which facilitates comparison with the human karyotype[98,99]. Additionally, and considering the close evolutionary relationship between the human and feline karyotypes[98], the identification of chromosomal aberrations in FMCs will provide valuable data to understand the similarities between human and feline mammary cancers. In this context, NGS-based techniques offer increased resolution in comparison with previously reported cytogenetic- and microarray-based approaches facilitating comparative read-depth analysis of gains and losses of any sizes[90,100] between derived cell lines and original tumours.

"Justification and objectives"

Genomic and transcriptomic studies using NGS are useful to identify reliable biomarkers with prognostic and therapeutic potential[8,101,102], and suitable *in vitro* models for the testing of specifically-addressed therapies[14,103,104]. Furthermore, NGS-based studies will contribute to understand the molecular pathogenesis of the neoplastic change and biological processes governing the FMC dysregulation. On the other hand, the comparative analysis of distinctive genomic and transcriptomic traits between human and feline mammary cancers may help to understand the suitability of therapeutic strategies proposed for human breast cancer in FMCs.

Considering the recent advances in mass-parallel sequencing technologies and its suitability for future applications in the daily clinical practice, an NGS-based approach was used in this study to examine the genomic and transcriptomic traits of FMC tissues and cell lines. This thesis aimed to promote the identification of prognostic molecular markers and suitable therapeutic targets. With this goal in mind, the first specific objective proposed was to establish and characterise FMC-derived cell lines. Next, to identify and compare chromosomal rearrangements within FMCs and cell lines established. Afterward, to correlate the genomic characteristics of FMCs with survival intervals (DFS and OS) and identify candidate genes as reliable prognostic markers within the rearranged genomic regions. Finally, to compare the gene expression patterns of neoplastic samples to healthy reference samples in order to detect differentially expressed genes (DEGs) participating in important molecular pathways and biological processes characterising the FMC dysregulation.

"Cell lines establishment and characterisation"

Tissue samples for primary culture were collected from five patients included in this study (Table 1), from which the following cell lines were derived: TiHo-0906, TiHo-1403, TiHo-1604, TiHo-1605 and TiHo-1702. Among those, only TiHo-0906 growth during prolonged subculturing (over 120 passages) and were further characterised, the remaining cell lines did not growth over passage 20.

Breed	Age*	RS	Tumour size	Lymph node invasion	Clinical Stage	Diagnosis	HMG	Cell line		Last passage cultured
								Full name	Short name	
BS	13	I	T3	Y	3	TC	III	TiHoCMglAdcar0906	TiHo-0906	130
Ps	11	I	T1	N	1	IPC	I	TiHoCMglAdcar1403	TiHo-1403	13
DSH	13	S	T1	N	1	IPC	II	TiHoCMglAdcar1605	TiHo-1605	11
DSH	13	S	T1	N	1	TC	I	TiHoCMglAdcar1609	TiHo-1609	7
DSH	8	I	T2	Y	3	SC	II	TiHoCMglSolcar1702	TiHo-1702	8

BS, British shorthair; DSH, Domestic Shorthair; Ps, Persian; RS, reproductive status; I, intact; S, spayed; T1, < 2 cm; T2, 2-3 cm; T3, > 3 cm; N, no; Y, yes; HMG, histological malignancy grade; TC, tubulopapillary carcinomas; IPC, intraductal papillary carcinomas; SC, solid carcinomas; and CC, comedocarcinomas. *years

Table 1. Characteristics of cats and tumours from which samples were obtained for cell culturing.

The protocol for tissue collection and cell culture establishment was the same in all cases and is further described in the manuscript entitled "**TiHo-0906: a new feline mammary cancer cell line with molecular, morphological, and immunocytological characteristics of epithelial to mesenchymal transition**" SCIENTIFIC REPORTS | (2018) 8:13231 | DOI:10.1038/s41598-018-31682-1 https://www.nature.com/articles/s41598-018-31682-1

SCIENTIFIC REPORTS

OPEN

Received: 25.04.2018
Accepted: 21.08.2018
Published online: 05.09.2018

TiHo-0906: a new feline mammary cancer cell line with molecular, morphological, and immunocytological characteristics of epithelial to mesenchymal transition

José Luis Granados-Soler[1,5], Johannes Junginger[2], Marion Hewicker-Trautwein[2], Kirsten Bornemann-Kolatzki[3], Julia Beck[3], Bertram Brenig[4], Daniela Betz[1], Jan Torben Schille[1,5], Hugo Murua Escobar[1,5 &] Ingo Nolte[1&]

Feline mammary carcinomas (FMCs) with anaplastic and malignant spindle cells histologically resemble the human metaplastic breast carcinoma (hMBC), spindle-cell subtype. hMBCs display epithelial-to-mesenchymal transition (EMT) characteristics. Herein we report the establishment and characterization of a cell line (TiHoCMglAdca0906; TiHo-0906) exhibiting EMT-like properties derived from an FMC with anaplastic and malignant spindle cells. Copy-number variations (CNVs) by next-generation sequencing and immunohistochemical characteristics of the cell line and the tumour were compared. The absolute qPCR expression of EMT-related markers HMGA2 and CD44 was determined. The growth, migration, and sensitivity to doxorubicin were assessed. TiHo-0906 CNVs affect several genomic regions harbouring known EMT-, breast cancer-, and hMBCs-associated genes as AKT1, GATA3, CCND2, CDK4, ZEB1, KRAS, HMGA2, ESRP1, MTDH, YWHAZ, and MYC. Most of them were located in amplified regions of feline chromosomes (FCAs) B4 and F2. TiHo-0906 cells displayed an epithelial/mesenchymal phenotype, and high HMGA2 and CD44 expression. Growth and migration remained comparable during subculturing. Low-passaged cells were two-fold more resistant to doxorubicin than high-passaged cells (IC50: 99.97 nM, and 41.22 nM, respectively). The TiHo-0906 cell line was derived from a poorly differentiated cellular subpopulation of the tumour consistently displaying EMT traits. The cell line presents excellent opportunities for studying EMT on FMCs.

[1]Small Animal Clinic, University of Veterinary Medicine Hannover Foundation, Hannover, Germany. [2]Department of Pathology, University of Veterinary Medicine Hannover Foundation, Hannover, Germany. [3]Chronix Biomedical, Göttingen, Germany. [4]Institute of Veterinary Medicine, University of Göttingen, Göttingen, Germany. [5]Department of Internal Medicine, Medical Clinic III, Clinic for Haematology, Oncology and Palliative Care, University Medical Center Rostock, Rostock, Germany. Hugo Murua Escobar and Ingo Nolte contributed equally. Correspondence and requests for materials should be addressed to I.N. (email: Ingo.Nolte@tiho-hannover.de)

Introduction

Feline mammary tumours are the third most common neoplasms in female cats[1]. The feline mammary tissue encompasses three tissue lineages, the luminal epithelial, the myoepithelial, and the mesenchymal[2]. Around 90% of feline mammary neoplasms are luminal epithelial tumours usually referred to as FMCs[2,3]. FMCs are invasive tumours characterized by early metastasis[3,4]. FMCs with anaplastic and malignant spindle cells are uncommon, and their distinctive morphologic features are not described in any of the subtypes included in the latest classification published by the World Health Organization (WHO)[2]. The genetic determinants of the neoplastic spindle-cell component in FMCs are still unclear, and little is known about the biological behaviour of these tumours and prognosis of the affected animals. The EMT is regulated by several cytokines and growth factors[9,15,21]. Consequently, it has been induced in cell culture by different methods[13,14,22,23]. The High-mobility group AT-hook 2 protein (HMGA2) activates a range of EMT transcription factors implicated in the repression of epithelial genes, and mesenchymal genes up-regulation[24,25]. Therefore, EMT-derived cells are usually characterized by a higher HMGA2 expression[9,26], loss or reduced expression of E-cadherin (E-cad), up-regulation of vimentin (Vim)[7,9], and co-expression of epithelial markers (cytokeratins [CKs]) and mesenchymal markers (calponin [CALP], smooth muscle actin [SMA], and Vim)[7,27]. Other markers like CD44 participate in the downregulation of E-cad[12,28]. Consequently, EMT-derived cells are characterized by a higher CD44 expression[8,28]. The overexpression of this cell surface protein leads to enhanced cell migration, cancer invasion and metastasis[28]. Additionally, a higher CD44 expression in combination with other surface markers is used for CSCs identification[29,30].

CNVs (copy-number gains [CNGs], and copy-number losses [CNLs]) are structural aberrations usually affecting extensive regions of the genome[31]. CNVs affect the gene expression patterns by altering the gene dosage in human breast cancer[32–34], hMBCs[7,32], and breast cancer cell lines[35]. Additionally, specific CNGs are concordant with EMT-related genes up-regulation in multiple human cancer types[36]. Cancer cell lines are characterized by genomic instability and structural dynamism[37–39], which makes CNVs a suitable tool to understand cancer cell adaptation to the *in vitro* environment during cell culture establishment and clonal selection during subculturing. To the extent of our knowledge, this is the first study characterizing CNVs in an FMC cell line. This study reports on the establishment and comprehensive characterization of a cell line TiHo-0906 derived from a poorly differentiated FMC with anaplastic and spindle cells. The original tumour and the derived cell line were enriched with EMT-associated traits.

Results

Histopathological description of the tumour. Histologically, the tumour was mainly composed of malignant spindle cells, malignant tubular epithelial cells, and small areas with anaplastic polygonal cells. The mammary gland was infiltrated by a multinodular invasive growing neoplasm. Some areas were characterized by cuboidal to columnar epithelial cells that formed irregular tubular structures by palisading along a basement membrane (Fig. 1a).

These cells showed distinct cytoplasmic borders, moderate amounts of eosinophilic cytoplasm and central round basophilic nuclei with finely stippled chromatin and distinct nucleoli. In addition, there were multifocal areas in which neoplastic cells were arranged in solid nests of variable size with anaplastic morphology lacking tubular differentiation (Fig. 1b). Cells in these areas were featured by a polygonal shape with mostly well-defined cell borders and low to moderate amounts of eosinophilic cytoplasm. Their large prominent centrally arranged basophilic round to oval nuclei revealed a finely to coarsely stippled chromatin pattern and distinct prominent nucleoli. In contrast, some areas were dominated by closely packed spindle cells with low amounts of cytoplasm and oval to elongated basophilic nuclei containing finely stippled chromatin and indistinct nucleoli (Fig. 1c). Predominating within the anaplastic foci, the cells were featured by moderate anisokaryosis and anisocytosis and occasionally contained multiple nuclei. Mitotic figures averaged three per high power field. Clusters of tumour cells were also present within some lymphatic vessels. Multifocally, there were single cells or coalescing necrosis characterized by hypereosinophilia and nuclear pyknosis, rhexis and lysis. Neoplastic cells were supported by low to moderate amounts of collagen-rich fibrovascular stroma that showed multifocal infiltration by moderate numbers of lymphocytes and plasma cells as well as variable numbers of neutrophils.

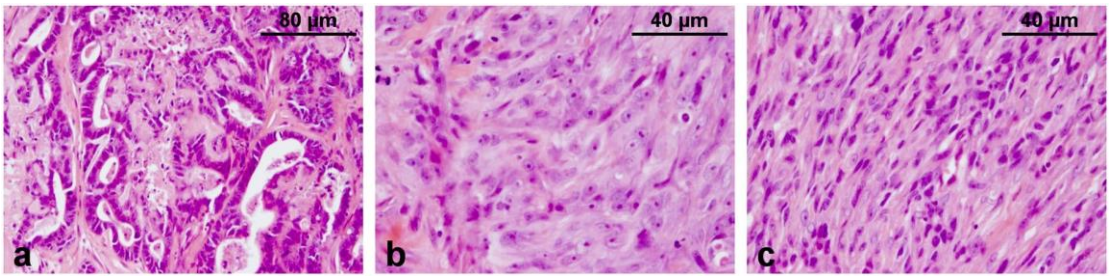

Figure 1. Histopathology. Tumour paraffin sections, H&E. The neoplasm, of which the cell line TiHo-0906 is derived, was characterized by (**a**) tubular, (**b**) solid anaplastic, and (**c**) spindle areas.

FMCs with malignant anaplastic and spindle cells share some histological characteristics with the highly malignant hMBCs, spindle-cell subtype. Histologically, hMBCs display epithelial differentiation towards mesenchymal elements (chondroid, osseous, rhabdoid, and spindle)[5]. Around 80% of hMBCs are spindle-cell tumours frequently enriched in EMT features[6–8]. EMT is an embryonic process reactivated in adult tissues during cicatrization, fibrosis, and cancer[9]. During EMT, epithelial cells lose expression of cell-cell junction proteins and gain the expression of mesenchymal proteins[10]. Afterwards, the EMT-derived cells secrete proteolytic enzymes (metalloproteinases), which degrade the extracellular matrix and cell-cell junctions, facilitating detachment, mobility, and metastasis[11]. EMT results in enhanced migratory capacity[7,10], cancer stem cells (CSCs) properties[9,12–15], and drug resistance[9,16,17]. Usually, neoplastic cells do not experience a full EMT, instead, they assume different phenotypes along the epithelial-mesenchymal axis[17–20].

Cytomorphologic features of the cell line. After cell culture establishment, TiHo-0906 cells proliferated in a monolayer. Subconfluent cells were spindle-shaped with a bipolar to multipolar morphology (Fig. 2a). At confluence, cells revealed a more epithelioid morphology with polygonal to bipolar shape (Fig. 2b). Cellular morphology and proliferation rate remained stable during prolonged subculturing (over 100 passages). Microscopic examination of TiHo-0906 cells in H&E stained paraffin sections from pellets revealed round to polygonal cells and a moderate to partly abundant cytoplasm. They had large, prominent, round to oval nuclei that showed moderate to severe atypia and contained coarsely stippled to vesiculated chromatin and distinct nucleoli. TiHo-0906 cells were further characterized by marked anisokaryosis and anisocytosis, atypical mitotic figures and several large multinucleated syncytia (Fig. 2c).

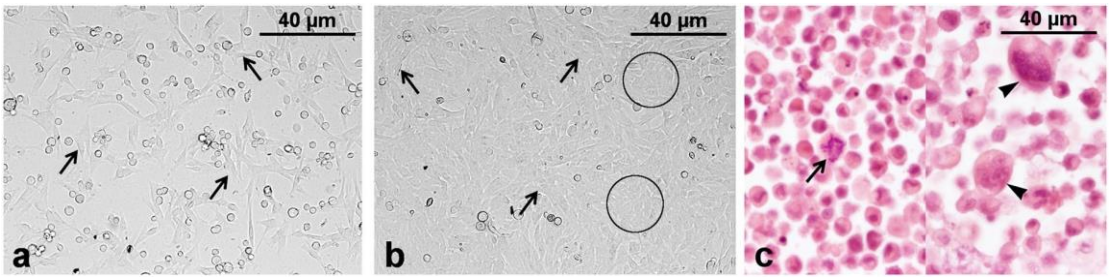

Figure 2. Cellular morphology. (**a**) TiHo-0906 P76 cell culture at subconfluence, inverted microscopy. Bipolar to multipolar shaped cells (arrows). (**b**) TiHo-0906 P76 cell culture at confluence, inverted microscopy. Monolayer of epithelial-like cells characterized by polygonal (circles) to bipolar morphology (arrows). (**c**) TiHo0906 P79 pellet; paraffin sections, H&E. Round to polygonal shaped cells characterised by marked anisokaryosis and anisocytosis, atypical mitotic figure (arrow) and large multinucleated syncytia (arrowheads).

Marker	Tubuli-forming cells	Polygonal cells	Spindle cells
E-cad	+	–	–
CK8/18	+	+	–
pan-CK	+	+	–
CK14	+	+	–
CK5/6	–	–	–
p63	–	–	–
SMA	–	+	+
CALP	–	+	+
Vim	+	+	+
CD44	+	+	+

Table 1. Comparative expression profile of the original tumour. +Positive, –Negative.

Tumour immunophenotyping. Tumours displaying EMT features usually express epithelial and mesenchymal markers concurrently[7]. In general, a co-expression of epithelial markers and Vim was observed in tubular and solid anaplastic areas of the tumour. In contrast, spindle cells were negative to all epithelial markers and positive to all mesenchymal markers used.

Additionally, all parts of the tumour were negative to the specific myoepithelial markers cytokeratin 5/6 (CK5/6) and p63 (Table 1).

Tubular epithelial cells were strongly immunoreactive to the luminal epithelial marker E-cad (Fig. 3a), while polygonal and spindle cells were negative (Fig. 3b,c). Tubular epithelial cells and polygonal cells were positive for the general epithelial marker pan-cytokeratin [pan-CK] while spindle cells were negative (Fig. 3d–f). A positive reaction to Vim was observed in all areas of the tumour (Fig. 3g–i).HMGA2 elicits EMT by activating a series of transcription factors[24,25], while CD44 participates in the downregulation of E-cad commonly observed during EMT[12,28]. Immunohistochemically, there were no specific cross-reactivity of the HMGA2 selected antibody with feline tissue. On the other hand, tubular epithelial cells were negative for CD44 (Fig. 3j), while numerous CD44-positive polygonal and spindle tumour cells were observed (Fig. 3k,l).

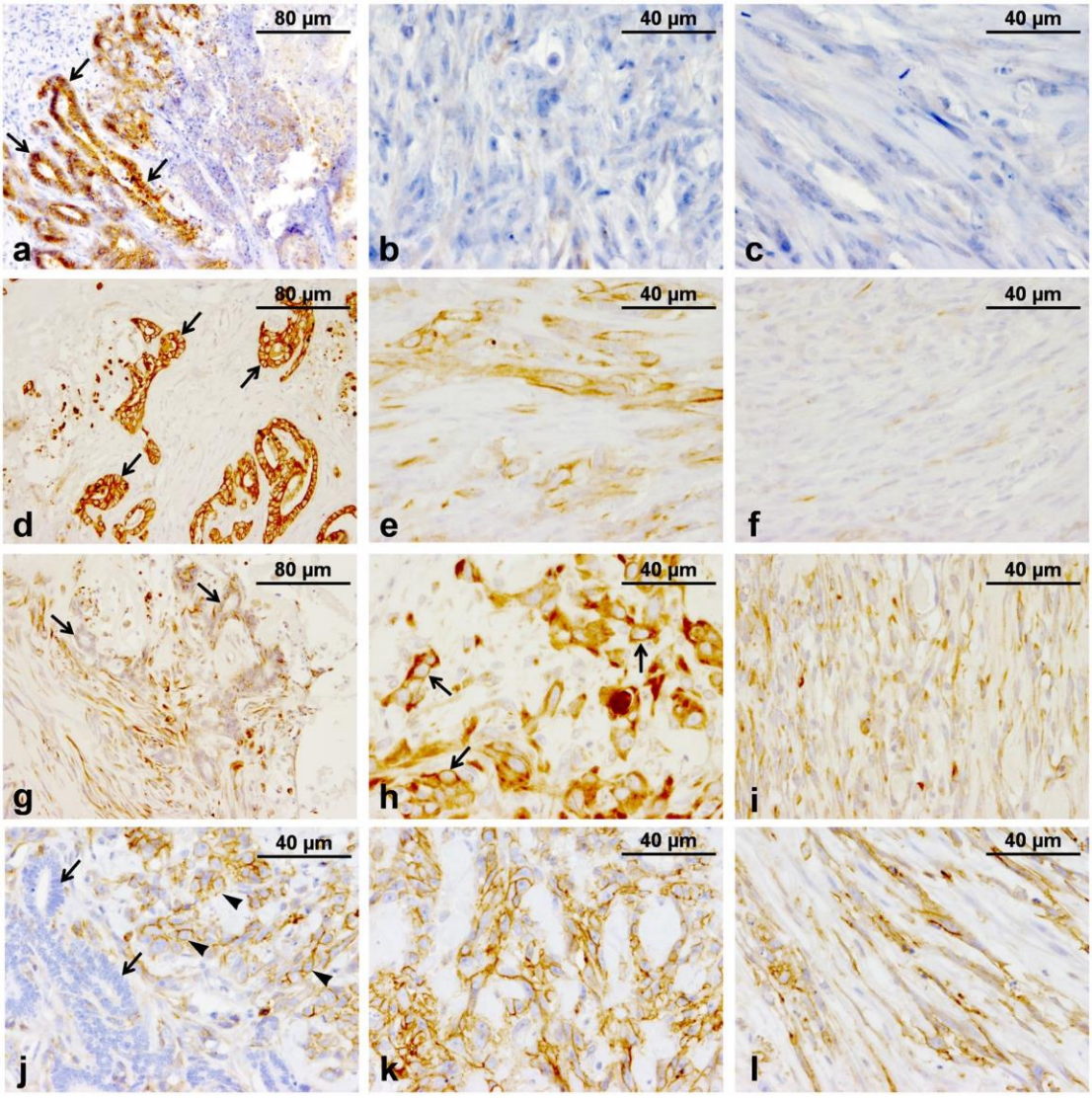

Figure 3. Immunohistochemical characteristics of the tumour. (**a**) E-cad; tubular epithelial cells strongly positive (arrows). (**b**) E-cad; polygonal cells in solid anaplastic areas of the tumour are negative. (**c**) E-cad; well-differentiated spindle cells negative. (**d**) pan-CK; intense cytoplasmic immunostaining by the neoplastic tubular cells (arrows). (**e**) pan-CK; polygonal cells moderately positive. (**f**) pan-CK; spindle cells negative. (**g**) Vim; moderate immunolabeling of neoplastic tubular epithelial cells (arrows). (**h**) Vim; intense cytoplasmic immunolabeling of the polygonal cells. (**i**) Vim; spindle cells moderately positive. (**j**) CD44; neoplastic tubular cells negative (arrows), polygonal cells moderately to intensely positive (arrowheads). (**k**) CD44; moderate to intense membrane staining of polygonal cells. (**l**) CD44; spindle cells moderately positive. Tubular epithelial cells were slightly positive to oestrogen and progesterone receptors (ER and PR) and negative to the human epidermal receptor-2 (HER-2). Polygonal cells were negative to ER and PR, but slightly positive to HER-2. Whereas, well-differentiated spindle cells were negative for all hormonal markers evaluated.

Marker	Tubuli-forming cells	Polygonal cells	Spindle cells
ER	17.5%	0	0
PR	27.6%	0	0
HER-2**	0	1+	0
COX-2*	0	0	0
p53	6.3%	3.3%	0
CLDN-2***	8	6	1
Ki67	47.3%	24.5%	22.4%

Table 2. Immunohistochemical characteristics of the tumour. *COX-2 scoring system[93], **HercepTest[94,95], ***CLDN2 scoring system[42].

The role of cyclooxigenase-2 (COX-2), p53, claudin 2 (CLDN-2), and ki67 as indicators of tumour aggressiveness and prognosis has been documented in FMCs[40–44]. Moreover, loss or reduced expression of claudins, in general, may contribute to the development of EMT[45–47]. In this case, the tumour was negative to COX-2. The expression of p53 was weak in tubular and polygonal cells, whereas well-differentiated spindle cells were negative. CLDN-2 was slightly positive in tubular and polygonal cells; spindle cells were negative. Additionally, a high Ki-67 proliferation index was observed in all areas of the tumour[44]. Results of the immunohistochemical characteristics of the tumour are detailed in Table 2.

Cell line phenotyping. TiHo-0906 cells at low and high passage reacted similarly to the markers employed; all pellets evaluated coexpressed epithelial and mesenchymal markers (Table 3). The immunohistochemical characteristics of the cell line resembled those of the polygonal epithelial cells present in the anaplastic areas of the tumour with exception of E-cad that was positive in most TiHo-0906 cells at low (Fig. 4a) and high passages (Fig. 4b). TiHo-0906 cells at low (Fig. 4c) and high passages (Fig. 4d) were positive for pan-CK, and Vim (Fig. 4e,f). Interestingly, some of the pellets evaluated in both low- and high-passaged cells were positive for the myoepithelial marker p63 (Fig. 4g, low-passaged cells), while the tumour was negative. An intense membrane staining for CD44 was observed on almost100% of the cells in all pellets evaluated (Fig. 4h,i, low and high passages respectively).

TiHo-0906 cells were slightly positive to the hormonal receptors (ER, PR), and HER-2. COX-2 labelling was negative in all of the pellets evaluated. p53 was moderately expressed in all of the pellets evaluated. CLDN-2 was weakly expressed in all pellets (score 1 to 3)[42]. The mean Ki-67 proliferation index of TiHo-0906 cells in pellets was 39.3% and 42.2% in early and high passages, respectively.

Marker	TiHo-0906 early passage			TiHo-0906 high passage		
	pellet 1	pellet 2	pellet 3	pellet 1	pellet 2	pellet 3
E-cad	+	+	+	+	+	+
CK8/18	+	+	+	+	+	+
pan-CK	+	+	+	+	+	+
CK14	+	+	+	+	+	+
CK5/6	–	–	–	–	–	–
p63	–	–	+	+	+	–
SMA	+	+	+	+	+	+
CALP	+	+	+	+	+	+
Vim	+	+	+	+	+	+
CD44	+	+	+	+	+	+

Table 3. Comparative expression profile of the cell line. +Positive, –Negative.

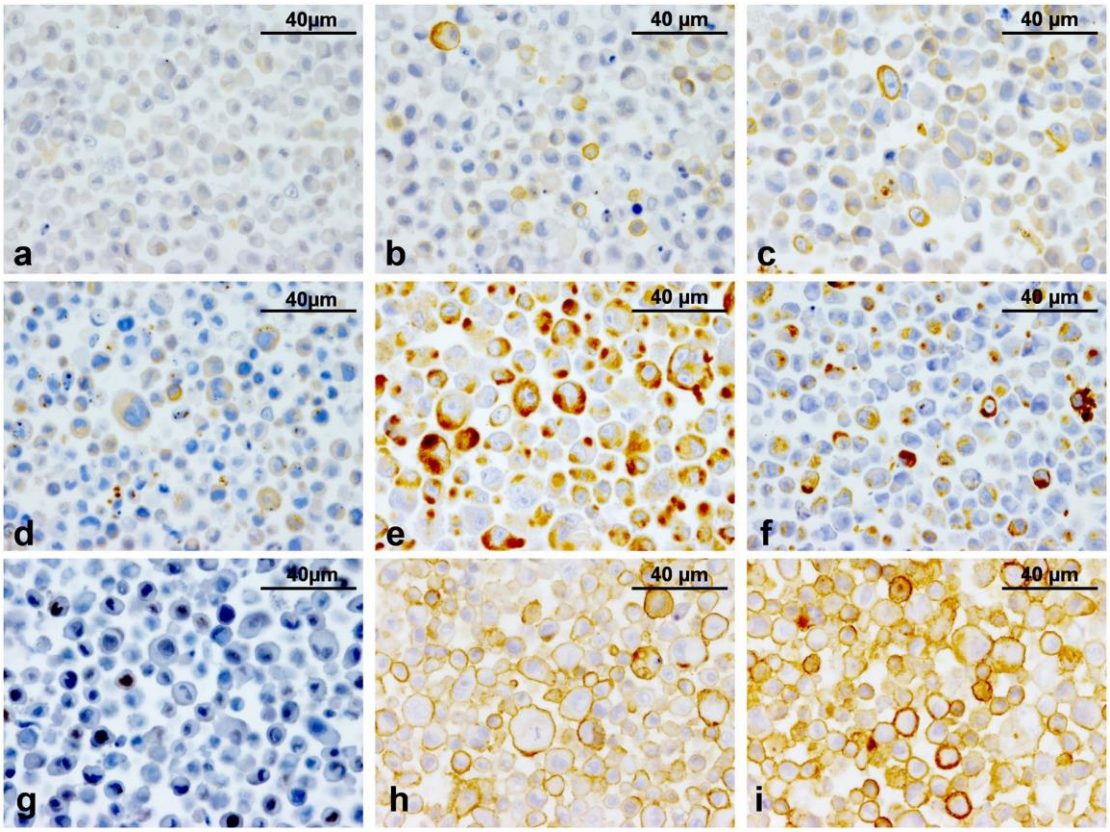

Figure 4. Immunohistochemical characteristics of the TiHo-0906 cell line. (**a**) E-cad, low passage (P8); most cells display a weak cytoplasmic and membranous labelling. (**b**) E-cad, high passage (P80); weak cytoplasmic and membranous labelling in most cells, some cells display a more intense reaction. (**c**) pan-CK, low passage (P8); moderate cytoplasmic labelling, some cells display a more intense reaction. (**d**) pan-CK, high passage (P80); moderate cytoplasmic labelling. (**e**) Vim, low passage (P8); strong cytoplasmic labelling and numerous positive cells. (**f**) Vim, high passage (P80); most of the cells are moderately positive, some cells are strongly positive. (**g**) p63, low passage (P8); moderate nuclear labelling in most of the cells, some nuclei are strongly positive. (**h**) CD44, low passage (P8); cellular membranes are moderately positive. (**i**) CD44, high passage (P80); moderate membranous labelling in most of the cells, some cells are strongly positive.

Copy number variation analysis. TiHo-0906 cells at low (P7) and high (P79) passages showed a high level of genomic instability when compared to the original tumour. The frequency of CNVs in TiHo-0906 cells increased during *in vitro* culturing. FCAs B2, B3, B4, and F2 in TiHo-0906 cells displayed most of the genomic regions with CNGs (Fig. 5).

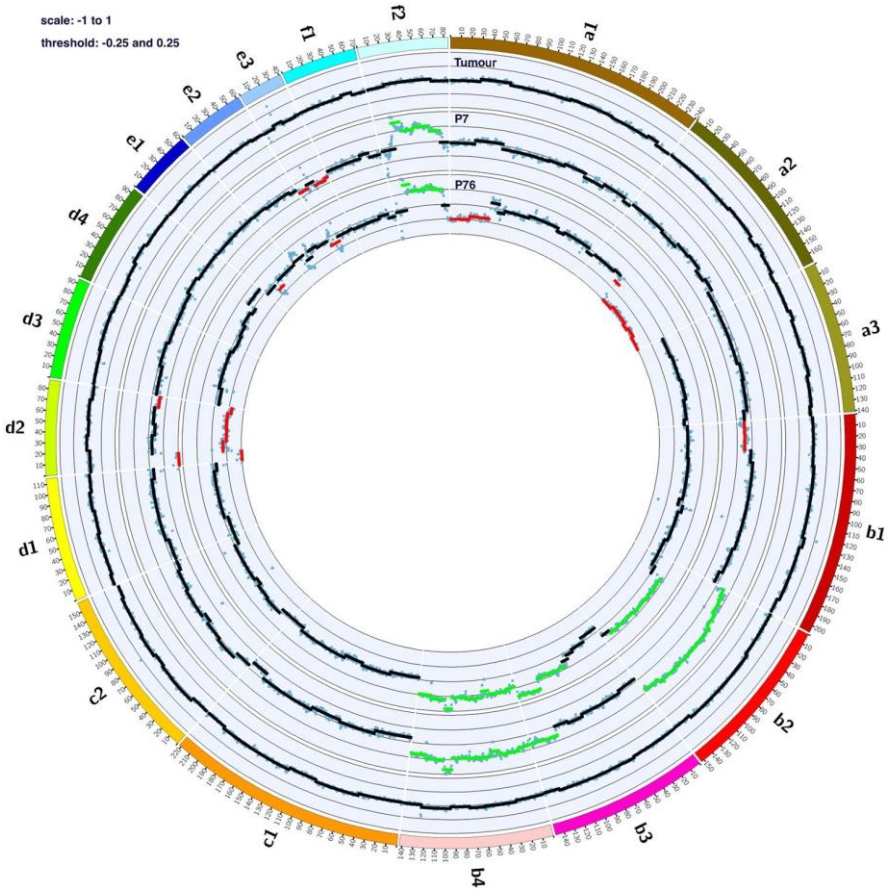

Figure 5. Comparative Circos plots of the original tumour and TiHo-0906 cells at low and high passages. Outer multicolour ring: chromosome location. Inner rings from the outside-in: original tumour, TiHo-0906 P7, and TiHo-0906 P76. Green lines indicate CNGs, and red lines indicate CNLs.

CNGs in chromosomes B2, B4 and F2 remained similar during subculturing. Interestingly, chromosomes B4 and F2 harbour some of the previously reported EMT-implicated genes associated with more frequent CNGs in different types of human cancer[36] (Table 4).

Gene	Feline chromosome	Location (bp)	TiHo-0906 P7	TiHo-0906 P76
EMT-associated CNGs[36]				
EGFR,***	A2	69,024,076–69,243,754		↓
TWIST1	A2	113,452,909–113,454,730		↓
*AKT1**	B3	148,724,327–148,745,203	↑	↑
VIM	B4	16,166,246–16,173,638	↑	↑
ZEB1	B4	28,693,675–28,892,926	↑	↑
KRAS	B4	60,631,473–60,670,232	↑	↑
ESRP1	F2	43,419,796–43,484,114	↑	↑
MTDH	F2	46,121,204–46,179,417	↑	↑
YWHAZ	F2	49,027,370–49,061,094	↑	↑
MYC,**,****	F2	70,514,069–70,519,003	↑	↑

Table 4. EMT-associated genes frequently affected by CNGs in multiple types of human cancer and their copy number status in TiHo-0906 cells. *Breast cancer-associated CNGs[33,34], **hMBCs-associated CNGs[7,32], ****Breast cancer cell lines-associated CNGs[35].

In general, the amount of CNLs also increased during cultivation. High-passaged TiHo-0906 cells showed losses on proximal chromosome A1, distal chromosome A2 and a focal deletion on chromosome E1 that were not observed in low-passaged cells. However, low-passaged TiHo-0906 cells showed a focal deletion of proximal chromosome B1 that was not observed in high-passaged cells. Additionally, the size of CNLs observed in chromosome E3 decreased during sub-cultivation. Some of the most important breast cancer-related genes in humans are located in the analysed corresponding feline regions[7,32,33] showing amplifications as well as deletions (details in Table 5).

Gene	Feline chromosome	Location (bp)	TiHo-0906 P7	TiHo-0906 P76
Breast cancer-associated CNGs[33,34]				
TERT	A1	239,584,995–239,606,213		↓
*CCND3***	B2	42,899,534–42,997,754		↑
FOXA1	B3	86,949,330–86,955,050		↑
MDM2	B4	93,710,547–93,739,225		↑
NF1	E1	19,031,895–19,383,941		↓
PPM1D	E1	25,189,431–25,236,039		↓
*EIF3****	F2	55,394,876–55,449,634	↑	↑
*PKHD1L1****	F2	56,539,146–56,697,161	↑	↑
*CSMD3****	F2	59,042,991–60,300,161	↑	↑
*ZHX2****	F2	68,234,407–68,397,794	↑	↑
*SAMD12****	F2	64,396,137–64,785,172	↑	↑
*EXT1****	F2	64,046,201–64,334,375	↑	↑
*MRPL13****	F2	66,202,612–66,254,545	↑	↑

*MTBP*****	F2	66,254,741–66,334,938	↑	↑
*SNTB1*****	F2	66,342,257–66,585,108	↑	↑
*RNF139*****	F2	69,585,566–69,597,426	↑	↑
*TATDN1*****	F2	69,586,490–69,643,856	↑	↑
Breast cancer-associated CNLs[33,34]				
BRCA2	A1	11,562,333–11,623,186		↓
RB1	A1	22,863,380–23,038,325		↓
MLL2/KMT2C	A2	166,021,109–166,309,274		↓
*CSMD1******	B1	2,777,407–4,810,740	↓	
*AGPAT5******	B1	6,723,000–6,783,055	↓	
Tumour *****	B1	22,910,796–23,201,016	↓	
*DLC1******	B1	25,013,341–25,575,894	↓	
*CLDN23******	B1	26,341,593–26,342,694	↓	
*MFHAS1******	B1	26,460,461–26,562,571	↓	
FOXO3	B2	98,320,907–98,445,633	↑	↑
GATA3	B4	7,378,473–7,400,352	↑	↑
*PTEN******	D2	7,565,534–7,659,710	↓	↓
hMBCs-associated CNGs[7,32]				
CCND2	B4	39,524,203–39,554,520	↑	↑
CDK4	B4	86,164,754–86,167,722	↑	↑
Additional important genes in regions displaying CNVs in TiHo-0906 cells				
FOXO1	A1	18,849,598–18,947,131		↓
AHR	A2	111,731,783–111,787,715		↓
MYB	B2	124,810,249–124,844,570	↑	↑
PFDN5	B4	81,683,255–81,686,020	↑	↑
HMGA2	B4	93,165,641–93,304,557	↑	↑
KSR1	E1	18,893,366–19,057,414		↓
RAC1	E3	5,019,032–5,042,577	↓	↓

Table 5. Breast cancer and specific hMBC-associated Genes frequently affected by CNVs and their copy number status in TiHo-0906 cells. **hMBCs-associated CNGs[7,32], ***hMBCs-associated CNLs[7,32], ****Breast cancer cell lines-associated CNGs[35], *****Breast cancer cell lines-associated CNLs[35].

Real-time PCR expression analyses of *HMGA2* and *CD44*. The levels of *HMGA2* and *CD44* in TiHo0906 cells were examined by absolute RT-PCR and compared to the corresponding reference tissues (feline testis, and healthy mammary feline tissue, respectively). The level of *HMGA2* expression in low and high passaged cells was higher than those of the reference tissue ($p = 0.001$, and $p < 0.0001$, respectively). Similarly, the *CD44* absolute expression in TiHo-0906 cells at low and high passages was significantly higher in comparison to the reference tissue ($p = 0.01$, and $p = 0.0015$, respectively). No significant differences in *HMGA2* and *CD44* expression were observed between low and high passages (Fig. 6).

Growth behaviour and migration activity. No statistical differences in BrdU incorporation and growth curves were found between low and high passages of the TiHo-0906 cell line (Fig. 7a,b). The doubling time for the cell line was 28.9 h at low passage and 27.4 h at high passage. Fourteen hours after the scratching, migrating cells completely covered the wound (400 µm) in early and high passages of the TiHo-0906 cell line (Fig. 7c–j). No significant differences regarding the time to wound closure were observed between low and high passages.

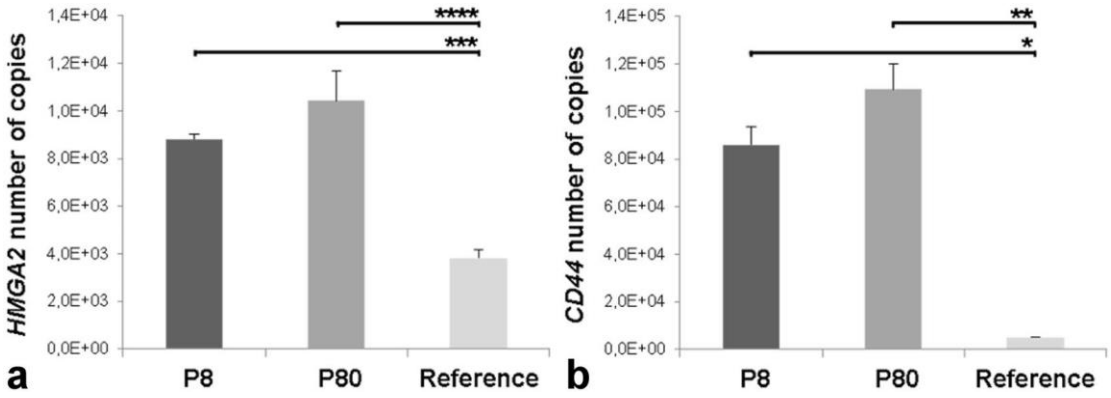

Figure 6. *HMGA2* and *CD44* qPCR-based expression. Comparative expression of (**a**) *HMGA2* and (**b**) *CD44* in TiHo-0906 cells at low (P8) and high (p80) passage versus selected reference tissues (feline testis, and healthy mammary feline tissue, respectively). Data are displayed as mean (SD); **p* < 0.05, ***p* < 0.01, ****p* < 0.001, and *****p* < 0.0001.

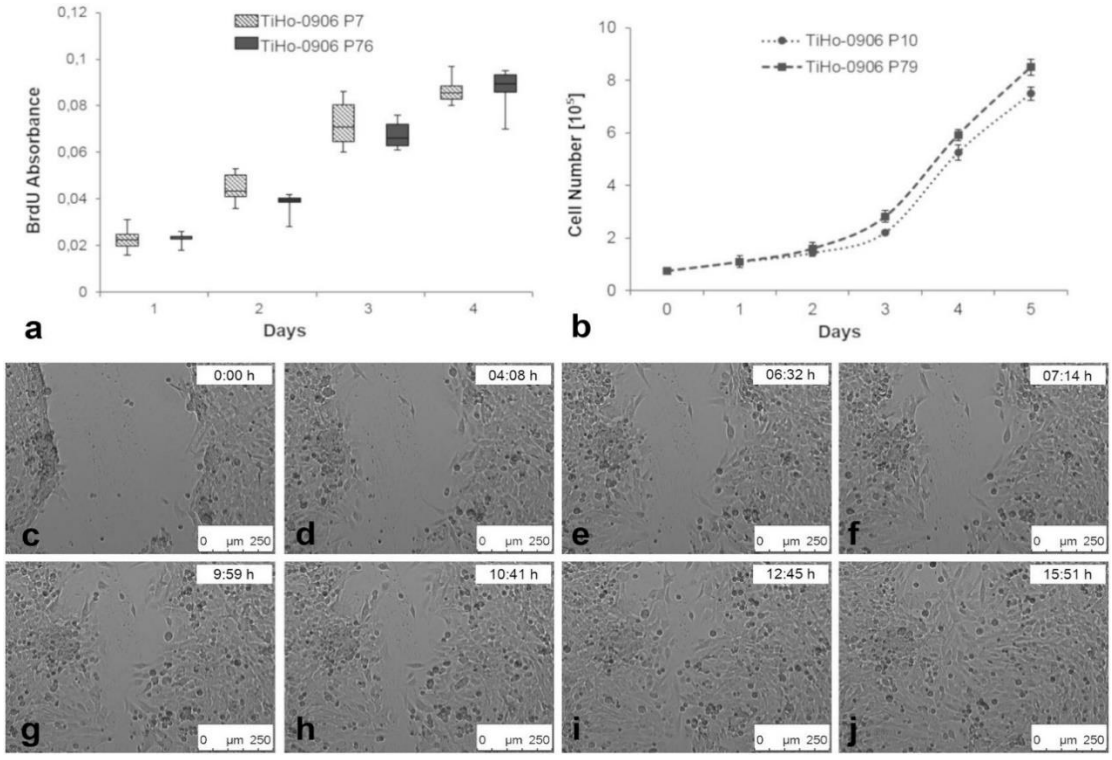

Figure 7. Cell proliferation, growth curves and scratch assay. (**a**) BrdU cell proliferation assay of TiHo-0906 at low and high passages, absorbance values expressed as Max V [delta 370–492]. (**b**) Growth curves of TiHo0906 at low and high passages, data are shown as mean (SD). (**c**–**j**) Scratch assay, TiHo-0906 P76 cell culture at inverted microscopy (10×).

Metabolic activity of TiHo-0906 cells after doxorubicin treatment. According to the MTS assay results, the metabolic activity of doxorubicin-treated TiHo-0906 cells at low and high passage starts to significantly decrease at 100 nM of doxorubicin ($p = 0.01$, and $p = 0.03$, respectively), for details see Fig. 8a. After incubation with different concentrations of doxorubicin, the metabolic activity of TiHo-0906 cells at low and high passages was not statistically different. However, the IC50 of cells at low passage was approximately 2-fold higher than the IC50 of cells at high passage (Fig. 8b,c).

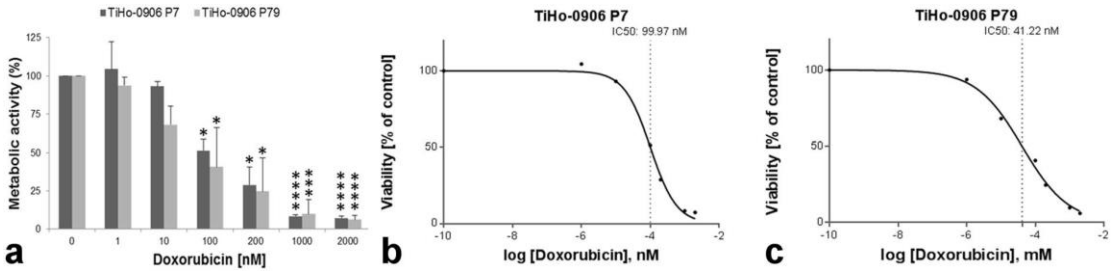

Figure 8. Influence of doxorubicin on metabolic activity of TiHo-0906 cells using MTS-test. (**a**) Doxorubicin resistance analysis of TiHo-0906 cells at low and high passage. Data are displayed as mean (SD) of metabolically active cells (%). Significance was calculated by comparing doxorubicin-treated versus untreated cells; $*p < 0.05$, $**p < 0.01$, $***p < 0.001$, and $****p < 0.0001$. Doxorubicin dose-response curves of (**b**) TiHo-0906 cells at low passage, IC50: 99.97 nM and (**c**) TiHo-0906 cells at high passage, IC50: 41.22 nM.

Effects of doxorubicin on apoptosis and cytotoxicity. After exposure to different concentrations of doxorubicin during 72 h. The amount of intact cells at low and high passage decreased from 91.1% (SD, 0.4%), and 86.5% (SD, 4.3%) in non-treated cells to 55.8% (SD, 3.1%), and 58.1% (SD, 2.1%) at the highest concentration of doxorubicin (2000 nM). In contrast, the amount of cell debris was consistently low in non-treated cells and increased proportionally to the concentration of doxorubicin, ranging from 8.2% (SD, 0.5%), and 13.5% (SD, 4.3%) in untreated cells at low and high passage to 43.3% (SD, 3.7%), and 41.9% (SD, 2.6%) at 2000 nM of doxorubicin, respectively. Response to doxorubicin—in terms of amount of intact cells and cellular debris—was not significantly different between low and high passages at any of the doxorubicin concentrations tested (Fig. 9a).

Intact cells were gated for viability on three different subpopulations as follows: viable, apoptotic, and dead cells. A significant dose-dependent reduction of viable cells at low and high passages starts after 72 h incubation with 50 nM of doxorubicin ($p < 0.0001$, and $p = 0.0003$, respectively). Viable cells at low and high passage decreased from 96.9% (SD, 0.4%), and 97.2% (SD, 0.2%) in non-treated cells to 54.6% (SD, 10.6%), and 30.9% (SD, 0.7%) at 2000 nM doxorubicin. The number of living cells was significantly higher in low-passaged cells at 50 nM, 100 nM, 200 nM, 500 nM and 2000 nM doxorubicin, more details are shown in Fig. 9b.

Doxorubicin induces dose-dependent apoptosis in TiHo-0906 cells at low and high passages, ranging from 5.2% (SD, 1.4%), and 4.6% (SD, 0.7%) at 1 nM doxorubicin to 45.1% (SD, 10.6%), and 65.9% (SD, 1.6%) at 2000 nM doxorubicin.

The amount of apoptotic cells was significantly higher in high-passaged cells at all doxorubicin concentrations up to 50 nM (Fig. 9c). Surprisingly, incubation with doxorubicin reduced the amount of viable cells while increasing that of apoptotic cells but was not able to significantly increase the amount of dead cells. Nonetheless, part of the cell debris excluded from viability gating could represent fragments of dead cells. Incubation with 50 nM doxorubicin induced the highest amount of dead cells observed (5.9%; SD, 1.6%). Comparing low and high passages, the amount of dead cells was only higher in cells at high passage incubated with 2000 nM doxorubicin (Fig. 9d).

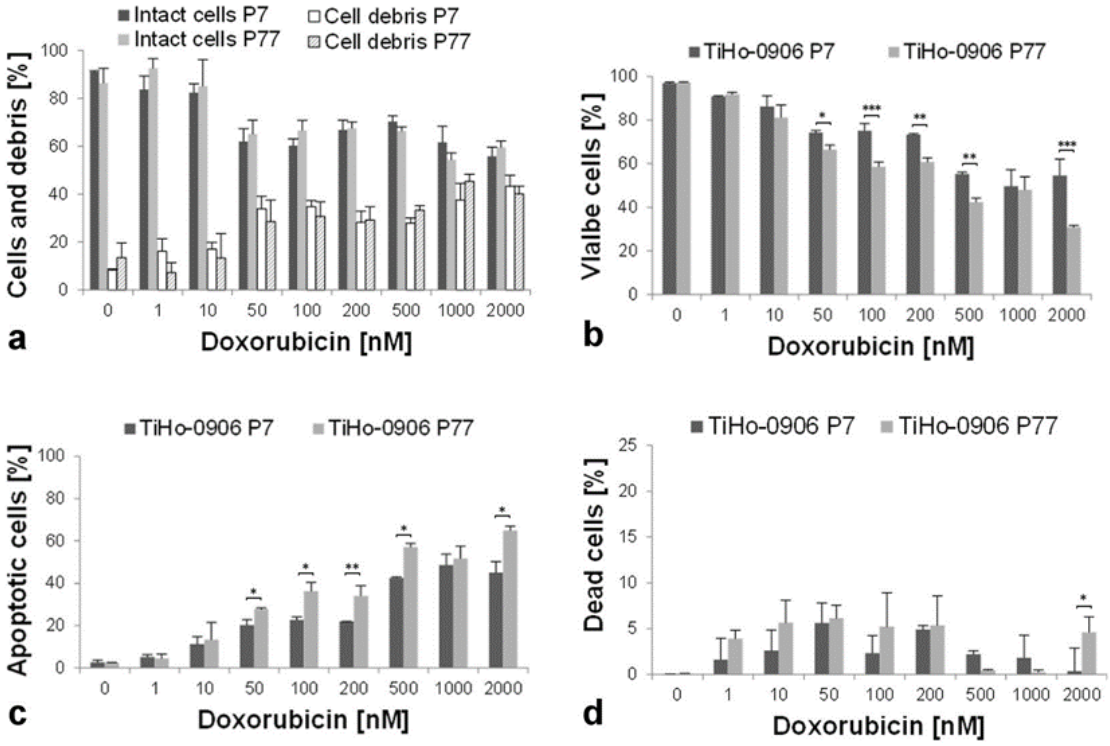

Figure 9. Flow cytometric assessment of doxorubicin effects on TiHo-0906 cells. (**a**) Percentage of intact cells (1st and 2nd column, low and high passage; respectively), and cell debris (3rd and 4th column, low and high passage; respectively) after incubation with doxorubicin. Cellular debris increases in proportion to the concentration of doxorubicin while intact cells decrease. Notice the higher amount of intact cells compared with cell debris at all doxorubicin concentrations tested. (**b**) In both passages tested viable cells decrease in a dose-dependent manner. Cells at low passage were more resistant to higher concentrations of doxorubicin (significance bars), except for 1000 nM. (**c**) The amount of apoptotic cells rises in parallel to the concentration of doxorubicin. Doxorubicin-induced Apoptosis was higher in cells at high passages in almost all concentrations tested (significance bars). (**d**) Incubation with doxorubicin was not able to give a significant increase of dead cells. Data are displayed as mean (SD); $*p < 0.05$, $**p < 0.01$, and $***p < 0.001$.

Discussion

Epithelial to mesenchymal transition can be observed *in vitro* and has been immunohistochemically portrayed in mammary cancer in dogs and humans[48–50]. The importance of EMT on FMCs has not been evaluated, and to the extent of our knowledge, EMT-associated genomic aberrations have not been documented in an FMC cell line. TiHo-0906 cells displayed a combined epithelial/mesenchymal phenotype and a high expression of EMT-related markers *HMGA2* (qPCR) and *CD44* (qPCR and immunohistochemistry). Moreover, the cell line was characterized by stable proliferation and migration activity during subculturing, and specific CNGs in FCAs B4 and F2 harbouring known EMT-associated genes as *VIM*, *ZEB1*, *KRAS*, *HMGA2*, *ESRP1*, *MTDH*, *YWHAZ*, and *MYC*[7,22,23,36,51–54]. The TiHo-0906 cell line represents a unique cellular model, probably derived from a poorly differentiated cellular subpopulation encompassed in the original tumour.

The cell line was derived from a tumour composed of malignant tubular-epithelial cells, malignant spindle cells, and small anaplastic areas with polygonal cells. Immunohistochemically, tubuli-forming areas showed a higher affinity for CKs while spindle areas were characterized by a mesenchymal profile. Interestingly, polygonal cells in anaplastic areas and TiHo-0906 cells co-expressed CKs and mesenchymal markers. In human breast cancer, this is associated with poor prognosis[27,55,56], in canine and human cellular models, with malignancy[38,55].

TiHo-0906 cells displayed an increasing genetic instability during sub-cultivation. Genomic aberrations observed in the cell line were not present in the tumour. This may be related to the fact that DNA isolated from the tumour represents a genomic mixture of all cellular subpopulations included in the sample[19], whereas the cultivated cells show clonal selection favouring a genomic shift. TiHo-0906 cells protein expression profile was more similar to that of the anaplastic polygonal cells in the tumour. This sub-population was, in fact, the least frequent of the three main cellular components of the tumour. However, considering that during the process of cell line establishment, cells with the higher rate of proliferation are likely to have a better survival chance in culture, the polygonal tumour cells may represent the cellular subpopulation with the faster growth rate and the higher amount of somatic aberrations. These findings also highlight the importance of cellular models as unique tools to study distinct aspects of the oncologic process specifically.

The tumour described in this study may represent a different histological subtype "FMCs with anaplastic and malignant spindle cells" from those included in the last WHO classification[2]. Matsuda *et al.*[57] reported a "tubulopapillary carcinoma" with spindle cells (CKs+, and SMA+) in a cat[57]. In contrast, the spindle-cell component in the tumour in this study was negative for CKs but positive for SMA. Paniago *et al.*[58] reported a "feline mammary carcinosarcoma" mainly composed of malignant pleomorphic cells, but no spindle cells were described[58]. Similar to the survival of the patient described in this study (three months), the animals reported by Matsuda *et al.*[57] and Paniago *et al.*[58] developed pulmonary metastasis and died three and two months after diagnosis, respectively[57,58].

Similar to the tumour described in this study, spindle-hMBCs are characterized by a dominant fibromatosis-like pattern with epithelial cells and limited regions of polygonal cells arranged in clumps or cords[59,60]. Immunohistochemically, spindle-hMBCs coexpress CKs (cytokeratin 8/18 [CK8/18], pan-CK, cytokeratin 14 [CK14], and CK5/6) and mesenchymal markers (SMA and Vim)[59,60]. Spindle cells in these tumours are malignant and display a variable reaction to CKs[61–63]. Therefore, a wide spectrum keratin panel (including pan-CK) may be useful for differentiating spindle-hMBCs from other spindle-cell lesions[60]. In the tumour described in this study, the spindle cells expressed SMA, CALP and Vim but lacked CKs including pan-CK, which according to the aforementioned would suggest a more likely mesenchymal phenotype. Since the tumour and derived cell line were enriched with EMT traits, and both, polygonal and spindle cells in the tumour expressed CD44, it appears reasonable to consider that both components may have arisen from EMT. However, we cannot completely rule out the presence of some non-neoplastic reactive mesenchymal cells (i.e. myofibroblasts) within the spindle component of the tumour. Considering the presence of both epithelial and mesenchymal components, carcinosarcoma would represent another possible differential diagnosis[64]. In dogs, mammary carcinosarcomas (commonly carcinoma and osteosarcoma) are described to express CK8/18 and Vim, but not CALP, p63 and CK14[64]. Although this expression profile has not been demonstrated in cats so far, a mammary gland carcinosarcoma is very unlikely in the present case on the basis of histological and immunohistochemical findings. Nonetheless, whether the spindle cells were originated from EMT or represented an additional neoplastic mesenchymal population remains at this point unanswered. In summary, the tumour described in this study shows some similarities with the spindle-hMBC, and it also resembles the FMC cases described by Matsuda *et al.* and Paniago *et al.*[57,58].

HMGA2 induces EMT[7,22–26,65,66]. In this study, we compared the absolute *HMGA2* qPCR-based expression of TiHo-0906 cells with a well-known reference tissue (testis) characterized by high expression of *HMGA2*[67]. The quantitative expression of *HMGA2* was significantly higher in TiHo-0906 cells when compared to the reference tissue. These findings are concordant with the CNGs observed in chromosome B4 harbouring *HMGA2*, which in combination with the characteristic fibroblastoid-shape and the highly migratory ability (demonstrated by *in vitro* scratching assay) also reveal a profoundly altered mesenchymal gene expression program; consistent with the combined epithelial/mesenchymal phenotype observed. hMBCs coexpress EMT- and CSCs-features[12]. Accordingly, these tumours may originate directly from epithelial cells that have undergone EMT and have therefore acquired CSCs properties, or from pre-existing CSCs expressing EMT-associated markers[8]. In FMC and human breast cancer cell lines, CSCs express high levels of CD133, CD44 and low (or none) CD24[30,68,69]. In this study, the immunohistochemical expression of CD24 and CD133 was not assessed due to the unavailability of the specific antibodies. However, the fact that only some TiHo-0906 cells expressed p63 when the original tumour was negative, may suggest the presence of some cells with stem cells features which may have acquired a myoepithelial phenotype during sub-cultivation as previously described in a human mammary gland derived cell line[70].

All cell types in the tumour expressed CD44, and there was a specific intense membrane staining for CD44 on almost all TiHo-0906 cells. The quantitative gene expression of *CD44* was also significantly higher in the cell line than in the reference tissue. These findings together with the comparative expression profile and *HMGA2* expression also suggest that the cell line was originated from the anaplastic polygonal cells in the tumour.

Several well-described breast cancer- and EMT-associated genes were affected by CNVs in the genome of the cell line. As reported by Zhao *et al.*[36] in a study exploring the relationship between EMT-implicated gene expression and CNVs in multiple cancer types in humans[36]; we observed that EMT-associated genes were more frequently affected by CNGs than by CNLs. As was mentioned before, most of the EMT-related genes affected by CNVs were located in amplified regions of FCAs B4 and F2. Affected regions of chromosome F2 harboured four of the most commonly EMT-associated genes reported by Zhao *et al.*[36]; this includes *ESRP1*, *MTDH*, *YWHAZ*, and *MYC*[36]. Among those, *ESRP1* regulates CD44 alternative splicing producing a more malignant isoform (CD44v), promoting invasiveness and distant metastasis in human breast CSCs[71]. TiHo-0906 cells overexpress CD44 and displayed CNGs in chromosome F2 harbouring *ESRP1* gene. Therefore, TiHo-0906 cell line might be a suitable model for the study of *ESRP1* and CD44 as possible therapeutic targets for FMC.

CNGs in chromosome F2 observed in the TiHo-0906 cells resemble one of the most common DNA aberrations reported in human breast cancer cell lines—CNGs at the long arm of human chromosome 8 (HSA 8q)—[35,72]. When comparing the human and feline karyotypes using fluorescence *in situ* hybridization (FISH), the entire HSA 8q is hybridized by the paint from FCA F2[73,74]. CNGs in chromosome F2 observed in the cell line also included some proposed breast cancer-related genes like *EIF3E*, *PKHD1L1*, *CSMD3*, *ZHX2*, *SAMD12*, *EXT1*, *MRPL13*, *MTBP*, *SNTB1*, *RNF139*, and *TATDN1*[35]. These findings highlight the importance of FCA F2 in FMC development and the close evolutionary relationship with the homologous disease in humans. Additionally, TiHo0906 cells at low and high passage also displayed CNGs in regions harbouring other known breast cancer-related genes like *FOXO3* and *MYB* (FCA B2), *AKT1* (FCA B3), and *GATA-3*, *CCND2*, *CDK4* and *PFDN5* (FCA B4).

CNLs were less common than CNGs. Most CNLs observed affected low or high passages of the cell line, but few of them affected both. For instance, CNLs in chromosome D2, and E3 harbouring *PTEN*, and *RAC1*, respectively; were preserved during prolonged subculturing. In contrast, CNLs in chromosome B1 were only observed in low-passaged cells. This chromosomic region harbours the *CSMD1*, *AGPAT5*, *TUSC3*, *DLC1*, *CLDN23*, and *MFHAS1* cancer-related genes. This aberration corresponds with the most common CNL in human breast cancer cell lines, located at the short arm of human chromosome 8 (HSA 8p)[35]. Using FISH, feline chromosome B1 labels the entire HSA 8p[73,74]. Additional CNLs affecting known breast cancer-, hMBCs-, and EMT-related genes were only detected after prolonged subculturing; including, FCA A1 containing *TERT*, *BRCA2*, *RB1*, and *FOXO1* genes; chromosome A2 harbouring *EGFR*, *TWIST*, *MLL2*, and *AHR*; chromosomes B2, B3, and B4 harbouring *CCND3*, *FOXA1*, and *MDM2*, respectively; and chromosome E1 harbouring *NF1*, *PPM1D*, and *KSR1*.

TiHo-0906 proliferation and migration activity remained comparable during subculturing. Growth curves and doubling times (28.9 h at low passage and 27.4 h at high passage) revealed a high proliferation similar to those reported for previously characterized FMC cell lines[39,75–77]. Migration activity was assessed by *in vitro* scratch assay revealing a shorter time to complete wound closure (approximately 14 h for both, early and high passages) than that previously reported in a recently characterised FMC cell line (approximately 24 h)[39].

After doxorubicin treatment, we observed a significant dose-dependent reduction of viable cells with active metabolism only after 72 h incubation with 100 nM of doxorubicin at low and high passages. These data may suggest a higher doxorubicin resistance of TiHo-0906 cells to that reported in an FMC cell line[78]. Nonetheless, methodological differences in viability assessment and exposure time to doxorubicin make comparison difficult. Resistance to doxorubicin, in terms of metabolic activity remained comparable during subculturing. However, flow cytometric assessment of doxorubicin effects on TiHo-0906 cells revealed a significant increase of apoptotic cells in high-passaged cells when compared to low-passaged cells at all doxorubicin concentrations up to 50 nM (except for 1000 nM). These findings are consistent with the observed two-fold reduction of the IC50 during sub-cultivation, suggesting a reduction in chemoresistance during prolonged subculturing. Similar findings have been reported for different cellular models in humans[79]. However, the specific mechanisms underlying this process are still not clear. To the best of our knowledge, resistance to doxorubicin has not been previously assessed by flow cytometry in FMC-derived cell lines. In this case, we observed a dose-dependent reduction of vital cells with simultaneous increasing of apoptotic cells.

Some immunohistochemical studies in veterinary medicine support the EMT hypothesis to explain the origin of the spindle-cell component on canine mammary metaplastic tumours[48,49]. There is also evidence suggesting a direct CSCs origin in cell lines derived from canine mammary spindle-cell tumours and sarcomas[80]. Although these two theories have been considered separately, a growing body of literature in human medicine suggests a link between them[8,13,14,50]. *In vitro* culture models are pivotal to understanding the role of EMT in the oncogenic process of FMC, determining the presence of possible subtypes and developing of new therapeutic approaches. However, the number of established FMC cell lines is still small[30,39,75–78,81–83].

In summary, the present study demonstrated that TiHo-0906 cells co-expressed epithelial and mesenchymal features, and some EMT markers like *HMGA2* and *CD44*. Additionally, TiHo-0906 cells are characterized by stable metabolic activity, proliferation rate, and ability to migrate during prolonged subculturing. Furthermore, our results indicate that specific CNVs observed in the cell line harbour a considerable amount of genes implicated in breast cancer development and EMT. CNGs in chromosomes B4 and F2 may be essential for EMT activation in the cat genome and closely resemble some of the typical genomic aberrations observed in human breast cancer. Nonetheless, further studies are necessary to determine the importance of these genomic aberrations in FMCs. The TiHo-0906 cell line represents a unique model consistently displaying EMT-associated traits at baseline.

Considering the poor prognosis of affected animals, further studies using *in vitro* models that closely resemble the uniqueness of the original tumours are of major value for the development of potential therapeutic approaches.

Methods

Primary tumour tissue. The TiHo-0906 cell line was obtained from the primary lesion of a 13-year-old female intact British Shorthair cat diagnosed with spontaneous FMC at clinical stage three according to McNeill *et al.*[84]. The cat was admitted to the Small Animal Clinic at the University of Veterinary Medicine Hannover and underwent unilateral chain mastectomy. No chemotherapy was performed and the cat was euthanised three months after surgery due to pulmonary metastasis. Tissue samples were obtained during the medically necessary surgery, after signed informed owner consent. Consequently, an ethical approval was not required (German Animal Welfare Act, § 7).

Cell culture establishment and maintenance. Immediately after surgery, a tumour tissue sample was placed in a tube with Hank's Balanced Salt Solution (Gibco) and kept overnight at 4 °C. The remainder of the surgical specimen was fixed in 10% neutral-buffered formalin and prepared for histopathological examination. The selected tumour tissue was minced into small pieces and digested with 4 mL 0.26% collagenase (SERVA) for 3 h at 37 °C with constant stirring. The digested cells were transferred into a sterile 25 cm^2 cell culture flask containing 5 mL medium 199 (Gibco) supplemented with 20% foetal bovine serum (FBS, Biochrom) and 2% penicillin/streptomycin (Biochrom). The culture was incubated at 37 °C in a humidified atmosphere of 5% CO_2 and split at confluency once or twice a week utilizing 1 mL TrypLE™ (Gibco) as dissociation reagent. Cryogenic preservation was performed once a week at 90% confluence. Cells were dispersed in TrypLE™ and resuspended in growth medium (medium 199 supplemented with 10% FBS, and 2% penicillin-streptomycin). The cell suspension was centrifuged at 1000 g for 10 min, the supernatant was discarded and the cell pellet was resuspended in 1 mL freezing medium (medium 199 supplemented with 20% FBS, 2% penicillin-streptomycin and 10% DMSO [AppliChem]) and transferred into cryogenic storage vials. Cryogenic vials were accommodated in a freezing container (Mr. Frosty, Nalgene), and transferred to a −80 °C freezer, after 24 h the vials were stored in a −150 °C freezer or in a liquid nitrogen storage vessel. TiHo-0906 was considered established when overcoming the passage 30th (P30).

All experiments described below were carried out in triplicate; those involving cells were performed using TiHo-0906 cells, or cell-pellets (5×10^6 cells) at low and high passage (P7–P10, and P76–P80, respectively). For pellets preparation, cells were detached with 1 mL TrypLE™, rinsed with PBS, counted with a PC-based Cellometer (Auto T4, Nexcelom Bioscience), and centrifuged at 1000 g for 10 min. For DNA and RNA isolation, pellets were stored at −80 °C. For cytology and immunohistochemistry, pellets were fixated in 10% neutral-buffered formalin and stored at room temperature.

Histopathology and cytology. After formalin fixation, paraffin sections (4 µm) of the original tumour were stained with H&E for histopathologic evaluation.

The samples were examined under light microscopy and the morphological diagnosis was performed following the WHO classification[2]. Histological grading of the tumour was performed according to the method described by Elston and Ellis 1991 and Castagnaro *et al.* 1998[85,86]. The cytomorphologic features of the cell line during long-term cultivation were examined microscopically based on H&E stained formalin-fixed, paraffin-embedded cell pellets at low (P7) and high (P80) passages.

Immunohistochemistry. Immunophenotyping by the avidin-biotin method was performed in the original tumour and cell pellets of TiHo-0906 (low [P7], and high [P80] passages) as described elsewhere[46] using the following markers (details see Table 6): E-cad, CK8/18, pan-CK, CK14, CK5/6, p63, SMA, CALP, Vim, HMGA2, CD44, ER, PR, HER-2, COX-2, p53, CLDN-2 and proliferation marker Ki-67. Positive and negative controls used for immunohistochemistry are listed in the Supplementary Table 1. For negative controls, the specific primary antibody was replaced by either an isotype control antibody or normal serum. For positive controls, only tissue samples were used that were sent to the department of pathology for diagnostic purposes not related to the present study. No animal was killed for the generation of positive controls.

Antibody	Type	Clone	Company	References
E-cad	mouse anti-human*	36/E-cad	BD Biosciences	96,97
CK8/18	mouse anti-human*	5D3	Novocastra	96,97
pan-CK	mouse anti-human*	AE1&AE3	Dako	96,97
CK14	rabbit anti-human**	—	Thermo Fischer Scientific	96,97
CK5/6	mouse anti-human*	D5/16B4	Dako	96,97
p63	mouse anti-human*	4A4	Biologo	96,97
SMA	mouse anti-human*	1A4	Dako	96,97
CALP	mouse anti-human*	CALP	Dako	96,97
Vim	mouse anti-human*	V9	Dako	96,97
HMGA2	rabbit anti-human**	HMGA2	Lifespan Biosciences	98
CD44	Rat anti-mouse CD44*	IM7	Bio-Rad Laboratories	30,82
ER	mouse anti-human*	6F11	AbD Serotec	96,97,99
PR	mouse anti-human*	10A9	Immunotech	96,97,99
HER-2	mouse anti-human*	CB11	Novocastra	94,95
COX-2	goat polyclonal IgG	—	Santa Cruz	93
p53	mouse anti-human*	DO-1	AbD Serotec	100
CLDN-2	mouse anti-human*	12H12	Thermo Fischer Scientific	42
Ki-67	mouse anti-human*	MIB-1	Dako	101

Table 6. Antibodies and evaluation methods used in this study. *Monoclonal Antibody, **Polyclonal Antibody.

Copy number variation analysis. Four 10-µm-thick sections were sliced from the tumour FFPE-block, using a microtome (pfm Slide 2003). Afterwards, the sections were deparaffinized and the DNA was isolated with the AllPrep DNA/RNA FFPE kit (QIAGEN) according to manufacturer's instructions. Before DNA isolation, 4×10^6 TiHo-0906 cells (P7 and P76) were homogenized using QIAshredder™ columns (QIAGEN). DNA isolation was performed with the AllPrep DNA/RNA Mini Kit (QIAGEN) following the manufacturer's protocol.

DNA yields and purity (260/280 ratio) were quantified with the Synergy 2 plate-reader (BioTek).

Starting from the DNA a sequencing library for each sample was prepared using the NEBNext® Ultra™ II DNA Library Preparation Kit for Illumina (New England Biolabs). Before library preparation, the DNA was sheared by ultrasound to an approximate size of 500 bp. An input of 500 ng DNA was used for each library. Sequencing was conducted on an Illumina NextSeq500 according to manufacturer's instructions.

The program CNV-seq (http://bmcbioinformatics.biomedcentral.com/articles/10.1186/1471-2105-10-80) was used for copy-number analyses; using feline healthy mammary tissue as normal reference control and a fixed window size of 1,000,000 bp. Control-tissue was collected from a recently euthanized intact female cat with no pathologies of the mammary gland. The raw results (log2ratios) were smoothed using a circular binary segmentation algorithm implemented in the program "Copynumber" (http://bioconductor.org/packages/release/bioc/html/copynumber).

Based on the results of the normal reference control, regions with log2-copy-number ratios of >0.25 or <−0.25 were scored as significantly aberrant. Additionally, some bins at telomeres were removed. All bins with smoothed log2-copy-number ratios of >0.25 were scored as amplified (CNGs) and all bins with <−0.25 were scored as deleted (CNLs).

Structural rearrangements (CNGs, and CNLs) observed were compared with those reported in human breast cancers[33,34], and were complemented by important EMT-related CNVs reported in multiple human cancer types[36], specific hMBCs-related CNVs[7,32], breast cancer cell lines-related CNVs[35], and additional cancer-associated genes reported on FMCs.

Real-time PCR expression analyses of *HMGA2* and *CD44*. HMGA2 expression is nearly undetectable in adult tissues except for meiotic and post-meiotic cells, in which its expression is high[67,87]. Consequently, we used feline testis as reference tissue. CD44 is overexpressed in metastatic mammary cancer tissues and CSCs, while its expression in the normal mammary gland is very low[88–90]. Accordingly, we used healthy mammary tissue as reference tissue. Testicular tissue was collected from a healthy tomcat during elective orchiectomy and mammary tissue from a recently euthanized (for medical reasons) intact female cat with no pathologies of the mammary gland.

Total RNA was isolated from TiHo-0906 cells (P8 and P80), fresh-frozen feline testicular tissue (*HMGA2* reference) and non-neoplastic feline mammary tissue (*CD44* reference) using the RNeasy Mini Kit (QIAGEN) according to manufacturer's protocol. The RNA yield and purity (260/280 ratio) were determined using a plate reader (Synergy 2, BioTek). The RNA was stored at −80 °C until use. *HMGA2* and *CD44* mRNA levels were measured using absolute quantification, relative to amplicon-specific standard curves. *HMGA2* standard curve sequence and amplification primers were based on a custom canine assay[91] and adjusted to the feline sequence. The feline *HMGA2* sequence was obtained by aligning the human exon 2, 3 and 4 sequences (NM_001300918.1) against cat chromosome B4.

The feline standard sequence was (5′–3′): *HMGA2* cat standard: AG AG TC CC TC C A AA GC AG CT CA AA AG AA AG CA GA AG CC AC TG GA GA AA AA CG GC CA AG AG GC AG AC CC AG GA AA TG GC CA. The primers were (5′–3′): *HMGA2* cat fw: AG TC CC TC CA AA GC AG CT CA AA AG and HMGA2 cat rv: G CC AT TT CC TG GG TC TG CC TC. *CD44* standard curve sequence and amplification primers were based on Ensembl-ID ENSFCAT00000005889.4, lying on the exon 3 and 4 border. *CD44* cat standard (5′–3′): TAC AT CG GT CA CA CA CC TG CC CA AT GC CT TT GA AG GA CC AA TT AC CA TA AC CA TT GT TA AC CG TG AT GG CA CC CG CTA TA. The primers were (5′–3′): *CD44* cat fw: CA TC GG TC AC AC AC CT GC CC and CD44 cat rv: TA GC GG GT GC CA TC AC GG TT.

Real-time PCR was carried out using the Mastercycler® ep realplex Real-Time PCR System (Eppendorf). The ® qPCR reactions were performed using the QuantiTect SYBR Green RT-PCR Kit (QIAGEN) in a total reaction volume of 20 µL and a primer concentration of 1 µL of 10 µM stock, for each primer. 100 ng of isolated total RNA were used per sample to measure mRNA copy numbers. The standard curves resulted from seven dilution steps, ranging from 10^2 to 10^8 copies. PCR conditions were as follows: 50 °C for 30 min cDNA synthesis, 95 °C for 15 min initial denaturation, 40 cycles at 94 °C for 15 s, 60 °C for 30 s and 72 °C for 30 s, completed by a melting curve analysis. All samples including the dilutions of the standard curve were measured in triplicate.

Growth behaviour and migration activity. TiHo-0906 cells proliferation was measured via Cell Proliferation ELISA, BrdU (colorimetric) Assay (Roche). TiHo-0906 cells (7.5×10^3 cells/well) at low (P7) and high (P76) passages were seeded in 96-well plates in octuplets and incubated at 37 °C in a humidified atmosphere of 5% CO_2. BrdU was added after 24 h, 48 h, 72 h and 86 h and incubated for 18 h each time. BrdU absorbance values at 370 nm (reference wavelength 492 nm) were recorded using a plate reader (Synergy 2, BioTek).

For calculating doubling time and growth curves, TiHo-0906 cells (P10 and P79) were seeded (7.5×10^5 cells/well) in 6-well plates in triplicates and incubated at 37 °C in a humidified atmosphere of 5% CO_2 for four days. Every 24 h, three replicative wells were dissociated with 1 mL TrypLE™ and the cells were counted using a PC-based Cellometer Auto-T4 (Nexcelcom Bioscience). The growth curves were established, and the doubling times were calculated using the "Doubling Time" online tool (http://doubling-time.com/compute.php).

TiHo-0906 cells migration ability was evaluated using the *in vitro* wound-scratching assay as previously reported[39]. Cells at low (P7) and high (P76) passages were cultured in 6 well culture plates in triplicates, once the cell confluence reached 100%, the growth medium was removed, the cell monolayer was gently scratched using a 200 µL pipette tip and rinsed with PBS, and the growth medium was replaced. Afterwards, cells were photographed every 10 min during 24 h using a live cell imaging microscope (DMI 6000 B, Leica Microsystems). Time to wound closure was defined as the time at which the wound was completely filled with cells.

Sensitivity to doxorubicin. The anti-proliferative effects of doxorubicin on TiHo-0906 cells were evaluated by assessing the cells metabolic activity with the CellTiter 96® MTS Proliferation Assay (Promega). Cells at low (P7) and high (P79) passages were seeded in 96-well plates (7.5×10^3 cells/well) and incubated for 18 h. The medium was aspirated and the cells were treated with different dilutions of doxorubicin (1 nM, 10 nM, 100 nM, 200 nM, 1000 nM, and 2000 nM [200 µL/well]). These concentrations of doxorubicin were below the range of the *in vivo* maximum plasma concentration in cats treated with clinically relevant dosages[92]. Each concentration was added in quadruplets, every plate contained a control of cells in growth medium and a negative control of the medium. After 72 h of incubation, the medium was changed, and 20 µL of the CellTiter 96® solution were added to each well. The plates were incubated at 37 °C in a humidified atmosphere of 5% CO_2 for 2 h and the absorbance values were recorded (reference wavelength 492 nm) and normalized to the medium negative control using a plate reader (Synergy 2, BioTek). The inhibitory activity of doxorubicin on TiHo-0906 cells at low and high passage was assessed by dose-response curves and IC50 using GraphPad Prism 3.0 (GraphPad Software Inc., San Diego, CA, USA), as calculated from the data on metabolic activity.

Apoptosis induced by doxorubicin. TiHo-0906 cells (P7 and P77) were seeded in 6-well plates (2×10^5 cells/well) and incubated for 18 h at 37 °C in a humidified atmosphere of 5% CO_2. Afterwards, the cells were exposed to different dilutions of doxorubicin (1 nM, 10 nM, 50 nM, 100 nM, 200 nM, 500 nM, 1000 nM, and 2000 nM [3 mL/well]) and then re-incubated for 72 h. After this period, media containing non-adherent and dead cells were collected. Adherent cells were dissociated with 1 mL TrypLE™ and centrifuged (1000 rpm for 6 min) together with the previously collected media. The supernatant was discarded, and cell pellets were resuspended in 500 µL of 1X Binding Buffer. Cell suspensions were incubated (10 min at room temperature in the dark) with 5 µL

Annexin V-FITC and 1 µL SYTOX Green Dye (Annexin V-FITC Detection Kit plus, PromoCell). Flow cytometry was performed using a MACSQuant® Analyzer 10 (Miltenyl Biotec). Dead cells treated with 1 mL 0.2% Triton™ X-100 (Sigma-Aldrich) and non-treated viable cells were used to set the gates. Annexin V-FITC and SYTOX Green Dye were measured in the FL-1 channel, and results were analysed with FlowJo Version 7.6.5 (FlowJo, Ashland, OR, USA). For data analysis, cell debris on the left-side of the plot were set as negative gate. Afterwards, intact cells were gated for viability on three different populations: viable, apoptotic, and dead.

Statistical analysis. All statistical analyses were performed using SAS software 7.1 (SAS Institute Inc., Cary, NC, USA); the significance threshold was set at $p \leq 0.05$. Data distribution was tested using Shapiro-Wilk test. Statistical analysis of BrdU cell proliferation test, growth curves, and real-time PCR expression analyses of *HMGA2* and *CD44* were performed using a 2-tailed Mann-Whitney-U test. Times to *in vitro* wound-scratch closure were analysed by two-tailed t-test. Results from MTS cell proliferation test and flow cytometry were evaluated using Wilcoxon's two-sample test.

References

1. Hayes, A. A. & Mooney, S. Feline mammary tumours. *Vet. Clin. North Am. Small Anim. Pract.* **15,** 513–20 (1985).
2. Misdorp, W., Else, R., Hellmen, E. & Lipscomb, T. *Histological classification of mammary tumours of the dog and cat*. (1999).
3. Zappulli, V. *et al.* Prognostic Evaluation of Feline Mammary Carcinomas: A Review of the Literature. *Vet. Pathol.* **52,** 46–60 (2015).
4. Wiese, D., Thaiwong, T., Yuzbasiyan-gurkan, V. & Kiupel, M. Feline mammary basal-like adenocarcinomas: a potential model for human triple-negative breast cancer (TNBC) with basal-like subtype. *BMC Cancer* **13,** 403 (2013).
5. Ellis, I. *et al.* In *Pathology and Genetics of Tumours of the Breast and Female Organs*. *WHO Classification of* Tumours. (eds Tavassoli, F. A. & Devilee, P.) 37–38 (IARCPress, 2003).
6. Mckinnon, E. & Xiao, P. Metaplastic Carcinoma of the Breast. *Arch Pathol Lab Med* **139,** 819–822 (2015).
7. Hennessy, B. T. *et al.* Characterization of a naturally occurring breast cancer subset enriched in epithelial-to-mesenchymal transition and stem cell characteristics. *Cancer Res.* **69,** 4116–4124 (2009).
8. May, C. D. *et al.* Epithelial-mesenchymal transition and cancer stem cells: a dangerously dynamic duo in breast cancer progression. *Breast Cancer Res.* **13,** 202 (2011).
9. Singh, A. & Settleman, J. EMT, cancer stem cells and drug resistance: an emerging axis of evil in the war on cancer. *Oncogene* **29,** 4741–4751 (2010).
10. Boyer, B., Vallés, A. M. & Edme, N. Induction and Regulation of Epithelial–Mesenchymal transitions. **60,** 1091–1099 (2000).
11. Radisky, E. S. & Radisky, D. C. Matrix Metalloproteinase-Induced Epithelial-Mesenchymal Transition in Breast Cancer. *J. Mammary Gland Biol. Neoplasia* **15,** 201–212 (2010).
12. Oon, M. L., Thike, A. A., Tan, S. Y. & Tan, P. H. Cancer stem cell and epithelial–mesenchymal transition markers predict worse outcome in metaplastic carcinoma of the breast. *Breast cancer Res. Treat. Treat* **150,** 31–41 (2015).
13. Morel, A.-P. *et al.* Generation of Breast Cancer Stem Cells through Epithelial-Mesenchymal Transition. *PLoS One* **3,** 1–7 (2008).
14. Mani, S. A. *et al.* The Epithelial-Mesenchymal Transition Generates Cells with Properties of Stem Cells. *Cell* **133,** 704–715 (2008).
15. Battula, V. L. *et al.* Epithelial-mesenchymal transition-derived cells exhibit multilineage differentiation potential similar to mesenchymal stem cells. *Stem Cells* **28,** 1435–1445 (2010).
16. Arumugam, T. *et al.* Epithelial to mesenchymal transition contributes to drug resistance in pancreatic cancer. *Cancer Res.* **69,** 5820–5828 (2009).
17. Cursons, J. *et al.* Stimulus-dependent differences in signalling regulate epithelial-mesenchymal plasticity and change the effects of drugs in breast cancer cell lines. *Cell Commun. Signal.* **13,** 26 (2015).
18. Hanahan, D. & Weinberg, R. A. The Hallmarks of Cancer. *Cell* **100,** 57–70 (2000).
19. Hanahan, D. & Weinberg, R. A. Hallmarks of cancer: the next generation. *Cell* **144,** 646–74 (2011).
20. Tsai, J. H. & Yang, J. Epithelial–mesenchymal plasticity in carcinoma metastasis. *Genes Dev.* **27,** 2192–2206 (2013).
21. Kalluri, R. & Weinberg, R. A. The basics of epithelial-mesenchymal transition. *J. Clin. Invest.* **119,** 1420–1428 (2009).
22. Watanabe, S. *et al.* HMGA2 maintains oncogenic RAS-induced epithelial-mesenchymal transition in human pancreatic cancer cells. *Am. J. Pathol.* **174,** 854–868 (2009).
23. Zha, L. *et al.* HMGA2 elicits EMT by activating the Wnt/β-catenin pathway in gastric cancer. *Dig. Dis. Sci.* **58,** 724–733 (2013).
24. Jiaqiang, D. O. N. G. *et al.* HMGA2–FOXL2 axis regulates metastases and epithelial-to-mesenchymal transition of chemoresistant gastric cancer. *Clin. Cancer Res.* **23,** 3461–3473 (2017).
25. Zhao, X.-P. *et al.* Overexpression of HMGA2 promotes tongue cancer metastasis through EMT pathway. *J. Transl. Med.* **14,** 26 (2016).
26. Morishita, A. *et al.* HMGA2 is a driver of tumour metastasis. *Cancer Res.* **73,** 4289–4299 (2013).
27. Vora, H. H. *et al.* Cytokeratin and vimentin expression in breast cancer. *Int. J. Biol. Markers* **24,** 38–46 (2009).
28. Cho, S. H. *et al.* CD44 enhances the epithelial-mesenchymal transition in association with colon cancer invasion. *Int. J. Oncol.* **41,** 211–218 (2012).
29. Ricardo, S. *et al.* Breast cancer stem cell markers CD44, CD24 and ALDH1: expression distribution within intrinsic molecular subtype. *J. Clin. Pathol.* **64,** 937–946 (2011).

30. Barbieri, F. *et al.* Isolation of stem-like cells from spontaneous feline mammary carcinomas: Phenotypic characterization and tumourigenic potential. *Exp. Cell Res.* **318,** 847–860 (2012).
31. Shlien, A. & Malkin, D. Copy number variations and cancer. *Genome Med.* **1,** 1–9 (2009).
32. Ross, J. S. *et al.* Genomic Profiling of Advanced-Stage, Metaplastic Breast Carcinoma by Next-Generation Sequencing Reveals Frequent, Targetable Genomic Abnormalities and Potential New Treatment Options. *Arch. Pathol. Lab. Med.* **139,** 642–649 (2015).
33. Ellis, M. J. *et al.* Whole-genome analysis informs breast cancer response to aromatase inhibition. *Nature* **486,** 353–360 (2012).
34. Nik-Zainal, S. *et al.* Mutational processes molding the genomes of 21 breast cancers. *Cell* **149,** 979–993 (2012).
35. Saito, S., Morita, K. & Hirano, T. High frequency of common DNA copy number abnormalities detected by bacterial artificial chromosome array comparative genomic hybridization in 24 breast cancer cell lines. *Hum. Cell* **22,** 1–10 (2009).
36. Zhao, M., Liu, Y. & Qu, H. Expression of epithelial-mesenchymal transition-related genes increases with copy number in multiple cancer types. *Oncotarget* **7,** 24688–99 (2016).
37. Lacroix, M. & Leclercq, G. Relevance of breast cancer cell lines as models for breast tumours: an update. *Breast Cancer Res. Treat.* **83,** 249–289 (2004).
38. Caceres, S. *et al.* Establishment and characterization of a new cell line of canine inflammatory mammary cancer: IPC-366. *PLoS One* **10,** e0122277 (2015).
39. Borges, A., Adega, F. & Chaves, R. Establishment and characterization of a new feline mammary cancer cell line, FkMTp. *Cytotechnology* **68,** 1529–43 (2016).
40. Sayasith, K., Sirois, J. & Doré, M. Molecular characterization of feline COX-2 and expression in feline mammary carcinomas. *Vet. Pathol.* **46,** 423–429 (2009).
41. Millanta, F., Citi, S., Della Santa, D., Porciani, M. & Poli, A. COX-2 expression in canine and feline invasive mammary carcinomas: correlation with clinicopathological features and prognostic molecular markers. *Breast Cancer Res. Treat.* **98,** 115–20 (2006).
42. Flores, A. R., Rêma, A., Carvalho, F., Faustino, A. & Dias Pereira, P. Reduced expression of claudin-2 is associated with high histological grade and metastasis of feline mammary carcinomas. *J. Comp. Pathol.* **150,** 169–74 (2014).
43. Hughes, K. & Dobson, J. M. Prognostic histopathological and molecular markers in feline mammary neoplasia. *Vet. J.* **194,** 19–26 (2012).
44. Castagnaro, M. *et al.* Ki-67 index as indicator of the post-surgical prognosis in feline mammary carcinomas. *Res. Vet. Sci.* **65,** 223–6 (1998).
45. Prat, A. *et al.* Phenotypic and molecular characterization of the claudin-low intrinsic subtype of breast cancer. *Breast Cancer Res.* **12,** R68 (2010).
46. Hammer, S. C. *et al.* Longitudinal claudin gene expression analyses in canine mammary tissues and thereof derived primary cultures and cell lines. *Int. J. Mol. Sci.* **17,** 1655 (2016).
47. Li, C. P. *et al.* CLDN14 is epigenetically silenced by EZH2-mediated $H_3K_{27}ME_3$ and is a novel prognostic biomarker in hepatocellular carcinoma. *Carcinogenesis* **37,** 557–566 (2016).
48. Beha, G. *et al.* Morphology of the Myoepithelial Cell: Immunohistochemical Characterization from Resting to Motile Phase. *Sci. World J.* **2012,** 1–8 (2012).
49. Gärtner, F., Geraldes, M., Cassali, G., Rema, A. & Schmitt, F. DNA Measurement and Immunohistochemical Characterization of Epithelial and Mesenchymal Cells in Canine Mixed Mammary Tumours: Putative Evidence for a Common Histogenesis. *Vet. J.* **158,** 39–47 (1999).
50. Sarrió, D. *et al.* Epithelial-mesenchymal transition in breast cancer relates to the basal-like phenotype. *Cancer Res.* **68,** 989–997 (2008).
51. Aigner, K. *et al.* The transcription factor ZEB1 (δEF1) promotes tumour cell dedifferentiation by repressing master regulators of epithelial polarity. *Oncogene* **26,** 6979–6988 (2007).
52. Taube, J. H. *et al.* Core epithelial-to-mesenchymal transition interactome gene-expression signature is associated with claudin-low and metaplastic breast cancer subtypes. *Proc. Natl. Acad. Sci. USA* **107,** 15449–54 (2010).
53. Wellner, U. *et al.* The EMT-activator ZEB1 promotes tumourigenicity by repressing stemness-inhibiting microRNAs. *Nat. Cell Biol.* **11,** 1487–95 (2009).
54. Lin, M. *et al.* Copy number gain and oncogenic activity of YWHAZ/14-3-3ζ in head and neck squamous cell carcinoma. *Int. J. Cancer* **125,** 603–611 (2009).
55. Heatley, M., Whiteside, C., Maxwell, P. & Toner, P. Vimentin expression in benign and malignant breast epithelium. *J. Clin. Pathol.* **46,** 441–445 (1993).

56. Korsching, E. *et al*. The origin of vimentin expression in invasive breast cancer: Epithelial- mesenchymal transition, myoepithelial histogenesis or histogenesis from progenitor cells with bilinear differentiation potential? *J. Pathol.* **206,** 451–457 (2005).
57. Matsuda, K. *et al*. Tubulopapillary Carcinoma with Spindle Cell Metaplasia of the Mammary Gland in a Cat. *J. Vet. Med. Sci.* **70,** 479–481 (20 08).
58. Paniago, J. D. G. *et al*. Mammary carcinosarcoma in cat: a case report. *Arq. Bras. Med. Vet. Zootec* **62,** 812–815 (2010).
59. Gobbi, H., Simpson, J. F., Borowsky, A., Jensen, R. A. & Page, D. L. Metaplastic breast tumours with a dominant fibromatosis-like phenotype have a high risk of local recurrence. *Cancer* **85,** 2170–2182 (1999).
60. Adem, C., Reynolds, C., Adlakha, H., Roche, P. & Nascimento, A. Wide spectrum screening keratin as a marker of metaplastic spindle cell carcinoma of the breast: an immunohistochemical study of 24 patients. *Histopathology* **40,** 556–562 (2002).
61. Sneige, N. *et al*. Low-Grade (Fibromatosis-Like) Spindle Cell Carcinoma of the Breast. *Am. J. Surg. Pathol.* **25,** 1009–1016 (2001).
62. Moten, A. S., Jayarajan, S. N. & Willis, A. I. Spindle cell carcinoma of the breast: a comprehensive analysis. *Am. J. Surg.* **211,** 716–721 (2016).
63. Carter, M., Hornick, J., Lester, S. & Fletcher, C. Spindle cell (sarcomatoid) carcinoma of the breast: a clinicopathologic and immunohistochemical analysis of 29 cases. *Am. J. Surg. Pathol.* **30,** 300–9 (2006).
64. Goldschmidt, M. H., Peña, L. & Zappulli, V. In *Tumours in* Domestic *Animals* (ed. Meuten, D. J.) 748 (John Wiley & Sons, Inc, 2016).
65. Luo, Y., Li, W. & Liao, H. HMGA2 induces epithelial-to-mesenchymal transition in human hepatocellular carcinoma cells. *Oncol. Lett.* **5,** 1353–1356 (2013).
66. Sun, M. *et al*. HMGA2/TET1/HOXA9 signaling pathway regulates breast cancer growth and metastasis. *Proc. Natl. Acad. Sci.* **110,** 9920–9925 (2013).
67. Chieffi, P. *et al*. HMGA1 and HMGA2 protein expression in mouse spermatogenesis. *Oncogene* **21,** 3644–3650 (2002).
68. Al-Hajj, M., Wicha, M. S., Benito-Hernandez, Adalberto Morrison, S. J. & Clarke, M. F. Prospective identification of tumourigenic breast cancer cells. *Proc. Natl. Acad. Sci. USA* **100,** 3893–98 (2003).
69. Pang, L. Y. *et al*. Feline mammary carcinoma stem cells are tumourigenic, radioresistant, chemoresistant and defective in activation of the ATM/p53 DNA damage pathway. *Vet. J.* **196,** 414–423 (2013).
70. Chua, H. L. *et al*. NF-κB represses E-cadherin expression and enhances epithelial to mesenchymal transition of mammary epithelial cells: Potential involvement of ZEB-1 and ZEB-2. *Oncogene* **26,** 711–724 (2007).
71. Hu, J., Li, G., Zhang, P., Zhuang, X. & Hu, G. A CD44v+ subpopulation of breast cancer stem-like cells with enhanced lung metastasis capacity. *Cell Death Dis.* **8,** e2679 (2017).
72. Jonsson, G. *et al*. High-resolution genomic profiles of breast cancer cell lines assessed by tiling BAC array comparative genomic hybridization. *Genes. Chromosomes Cancer* **46,** 543–558 (2007).
73. Wienberg, J. *et al*. Conservation of human vs. feline genome organization revealed by reciprocal chromosome painting. *Cytogenet. Cell Genet.* **77,** 211–7 (1997).
74. Yang, F. *et al*. Reciprocal chromosome painting illuminates the history of genome evolution of the domestic cat, dog and human. *Chromosom. Res.* **8,** 393–404 (2000).
75. Minke, J. M. *et al*. Isolation of two distinct epithelial cell lines from a single feline mammary carcinoma with different tumourigenic potential in nude mice and expressing different levels of epidermal growth factor receptors. *Cancer Res.* **51,** 4028–37 (1991).
76. Muleya, J. S. *et al*. Establishment and characterization of a new cell line derived from feline mammary tumour. *J. Vet. Med. Sci.* **60,** 931–5 (1998).
77. Uyama, R. *et al*. Establishment and characterization of eight feline mammary adenocarcinoma cell lines. *J. Vet. Med. Sci.* **67,** 1273–6 (2005).
78. Penzo, C., Ross, M., Muirhead, R., Else, R. & Argyle, D. J. Effect of recombinant feline interferon-ω alone and in combination with chemotherapeutic agents on putative tumour-initiating cells and daughter cells derived from canine and feline mammary tumours. *Vet. Comp. Oncol.* **7,** 222–229 (2009).
79. Kruczynski, A. & Kiss, R. Evidence of a direct relationship between the increase in the *in vitro* passage number of human nonsmall-cell-lung cancer primocultures and their chemosensitivity. *Anticancer Res.* **13,** 507–13 (1993).
80. Hellmén, E., Moller, M., Blankenstein, M. A., Andersson, L. & Westermark, B. Expression of different phenotypes in cell lines from canine mammary spindle-cell tumours and osteosarcomas indicating a pluripotent mammary stem cell origin. *Breast Cancer Res. Treat.* **61,** 197–210 (2000).

81. Elshire, H. D. Some studies on the feline mammary adenocarcinoma as a model of human breast cancer. Ph.D. Dissertation. (University of Southern California, 1984).
82. Michishita, M. *et al*. Flow cytometric analysis for detection of tumour-initiating cells in feline mammary carcinoma cell lines. *Vet. Immunol. Immunopathol.* **156**, 73–81 (2013).
83. Norval, M., Maingay, J. & Else, R. W. Characteristics of a feline mammary carcinoma cell line. *Res. Vet. Sci.* **39**, 157–64 (1985).
84. McNeill, C. J. *et al*. Evaluation of adjuvant doxorubicin-based chemotherapy for the treatment of feline mammary carcinoma. *J. Vet. Intern. Med.* **23**, 123–9 (2009).
85. Elston, C. & Ellis, I. Pathological prognostic factors in breast cancer. I. The value of histological grade in breast cancer: experience from a large study with long-term follow-up. *Histopathology* **19**, 403–410 (1991).
86. Castagnaro, M. *et al*. Tumour grading and the one-year post-surgical prognosis in feline mammary carcinomas. *J. Comp. Pathol.* **119**, 263–75 (1998).
87. Cleynen, I. & Van de Ven, W. J. M. The HMGA proteins: A myriad of functions (Review). *Int. J. Oncol.* **32**, 289–305 (2008).
88. Iida, N. & Bourguignon, L. Y. New CD44 splice variants associated with human breast cancers. *J. Cell. Physiol.* **162**, 127–33 (1995).
89. Matsumura, Y. & Tarin, D. Significance of CD44 gene products for cancer diagnosis and disease evaluation. *Lancet* **340**, 1053–8 (1992).
90. Hebbard, L. *et al*. CD44 expression and regulation during mammary gland development and function. *J. Cell Sci.* **113**(Pt 14), 2619–30 (2000).
91. Winkler, S. *et al*. HMGA2 expression in a canine model of prostate cancer. *Cancer Genet. Cytogenet.* **177**, 98–102 (2007).
92. Hahn, K., Frazier, D., Cox, S. & Legendre, A. Effect of infusion regime on doxorubicin pharmacokinetics in the cat. *J. Am. Anim. Hosp. Assoc.* **33**, 427–433 (1997).
93. Clemente, M. *et al*. Different role of COX-2 and angiogenesis in canine inflammatory and non-inflammatory mammary cancer. *Vet. J.* **197**, 427–32 (2013).
94. Santos, S. *et al*. ERBB2 in cat mammary neoplasias disclosed a positive correlation between RNA and protein low expression levels: A model for erbB-2 negative human breast cancer. *PLoS One* **8**, e83673 (2013).
95. Soares, M., Correia, J., Rodrigues, P., Simões, M. & Matos, A. De. Feline HER2 Protein Expression Levels and Gene Status in Feline Mammary Carcinoma: Optimization of Immunohistochemistry (IHC) and *In Situ* Hybridization (ISH) Techniques. *Microsc. Microanal.* **19**, 876–882 (2013).
96. Beha, G. *et al*. Molecular portrait-based correlation between primary canine mammary tumour and its lymph node metastasis: possible prognostic-predictive models and/or stronghold for specific treatments? *BMC Vet. Res.* **8**, 219 (2012).
97. Brunetti, B. *et al*. Molecular Phenotype in Mammary Tumours of Queens: Correlation between Primary Tumour and Lymph Node Metastasis. *J. Comp. Path.* **148**, 206–13 (2013).
98. Willenbrock, S. *et al*. Generation and characterisation of a canine EGFP-HMGA2 prostate cancer *in vitro* model. *PLoS One* **9**, 1–12 (2014).
99. Millanta, F. *et al*. Comparison of steroid receptor expression in normal, dysplastic, and neoplastic canine and feline mammary tissues. *Res. Vet. Sci.* **79**, 225–32 (2005).
100. Morris, J. S. *et al*. Immunohistochemical expression of TopBP1 in feline mammary neoplasia in relation to histological grade, Ki67, ERalpha and p53. *Vet. J.* **175**, 218–26 (2008).
101. Hennecke, S. *et al*. Prevalence of the prefoldin subunit 5 gene deletion in canine mammary tumours. *PLoS One* **10**, 1–10 (2015).

Acknowledgments. The authors wish to thank Kerstin Rohn, Regina Carlson, Heike Thiemeyer, Eva Packeiser, Annika Mohr, Camila Penter, Florenza Lüder Ripoli, Tatjana Harting, Susanne C. Hammer, Alexandra Anders, and Claudia Windhövel, for their excellent technical assistance, valuable comments, and suggestions.

Author contributions. José Luis Granados-Soler, Ingo Nolte, Hugo Murua Escobar, and Marion Hewicker-Trautwein performed the primary study design; Ingo Nolte, Hugo Murua Escobar, Daniela Betz, and Marion Hewicker-Trautwein performed the manuscript revision, and final approval; Johannes Junginger and Marion Hewicker-Trautwein performed the histopathology and immunohistochemistry; Kirsten Bornemann-Kolatzki, Julia Beck and

Bertram Brenig performed the DNA sequencing and CNVs; Jan Torben Schille performed the qPCR experiments, José Luis Granados-Soler performed the cell cultivation, growth curves, scratching assay, proliferation assay, flow cytometry, DNA, and RNA isolation, qPCR and CNVs data analysis, analysed the data and wrote the paper.

Supplementary information. Accompanies this paper at https://doi.org/10.1038/s41598-018-31682-1

Competing interests. The authors declare no competing interests.

Publisher's note. Springer Nature remains neutral with regard to jurisdictional claims in published maps and institutional affiliations.

Author comments. The authors slightly adapt the original format in which this article was published to include it in this thesis, all contents and graphics remain exactly as in the original published version.

"Genomic and transcriptomic analysis of FMCs"

Neoplastic and healthy mammary tissue samples from 33 cats diagnosed with FMCs and treated by surgery at the Small Animals Clinic, University of Veterinary Medicine Hannover Foundation were included for the genomic and transcriptomic analyses performed Table 2. Thirty-one cats were retrospectively included and two were prospectively enrolled.

Clinical relevant information was collected from medical records. In cases in which all information was not available, owners were contacted telephonically, per post or per email. FFPE samples were retrieved from the archives of the Institute for Pathology, University of Veterinary Medicine Hannover Foundation. Frozen tissue samples were obtained from the frozen-tissue bank of the Small Animal Clinic.

Breed	Age (years)	Reproductive status	Tumour size [49]	Lymph node invasion	Clinical Stage [49]	Diagnosis	HMG [47,48]
DSH	16	I	T2	Y	3	TC	II
DSH	10	S	T2	Y	3	TC	II
Norwegian Forest	14	I	T3	N	3	TC	III
DSH	20	S	T3	Y	3	TC	II
British shorthair	13	I	T3	Y	3	TC	III
DSH	13	S	T3	N	3	TC	I
Norwegian forest	12	S	T1	Y	3	SC	III
DSH	8	I	T2	Y	3	SC	II
DSH	11	S	T1	Y	3	TC	I
DSH	14	I	T1	N	1	TC	II
DSH	13	S	T1	N	1	TC	I
Abyssinian	9	S	T2	N	2	TC	II
DSH	16	S	T2	N	2	TC	I
DSH	11	S	T1	N	1	CC	I
Siamese	15	I	T2	Y	3	SC	II
DSH	17	I	T3	Y	3	CC	III
Chartreux	14	S	T3	Y	3	SC	III
Chartreux	13	I	T3	Y	3	CC	I
DSH	10	I	T3	Y	3	CC	III

DSH	8	I	T1	N	1	TC	III
DSH	14	I	T1	N	1	TC	II
DSH	6	S	T1	N	1	IPC	III
DSH	13	S	T1	N	1	IPC	I
DSH	11	S	T1	N	1	TC	I
Persian	11	I	T1	N	1	IPC	I
DSH	13	I	T1	N	1	IPC	II
DSH	16	S	T2	Y	3	TC	II
DSH	13	S	T2	Y	3	TC	II
DSH	15	I	T2	N	2	TC	III
DSH	13	S	T2	Y	3	TC	I
Norwegian Forest	17	S	T3	Y	3	TC	I
DSH	7	I	T3	N	3	TC	I
Maine coon	9	I	T3	N	3	TC	I

DSH, Domestic Shorthair; S, spayed; I, intact; T1, < 2 cm; T2, 2-3 cm; T3, > 3 cm; N, no; Y, yes; TC, tubulopapillary carcinomas; IPC, intraductal papillary carcinomas; SC, solid carcinomas; and CC, comedocarcinomas.

Table 2. Characteristics of animals selected for genomic and transcriptomic analysis.

DNA and RNA isolation, nucleic acids sequencing, immunostaining and data analyses procedures are described in the following manuscripts entitled "**Analysis of Somatic Copy-Number Variations and Feline Mammary Carcinoma Survival**" and "**High-Resolution Transcriptome Profiling of Feline Mammary Carcinomas**".

Analysis of somatic copy-number variations and feline mammary carcinoma survival

José Luis Granados-Soler[1,5], Kirsten Bornemann-Kolatzki[3], Julia Beck[3], Bertram Brenig[4], Ekkehard Schütz[3], Daniela Betz[1], Johannes Junginger[2], Marion Hewicker-Trautwein[2], Hugo Murua Escobar[5&], Ingo Nolte[1&*]

Feline mammary carcinomas (FMCs) are characterised by early metastasis. As the disease-free survival (DFS) and overall survival (OS) are short, prognostic determination is crucial to guide treatment. Somatic copy-number variations (CNVs) are used to identify and analyse critical genomic regions in different mammalian cancer types. Next-generation sequencing (NGS) allows rapid high-resolution characterisation of potentially clinical relevant CNVs. Thirty-three female cats with FMCs were surgically treated and followed up for a two-year post-operative period. CNVs analysis by NGS was performed on DNA isolated from formalin-fixed paraffin-embedded (FFPE) and fresh-frozen tumour (FT) samples. The analysed tumours represented tubulopapillary carcinomas (group TC; n = 25) and solid carcinomas and comedocarcinomas (group SC; n = 8). Detected CNVs and correlation to epidemiological, clinical, and histological variables on DFS and OS were statistically analysed. Cats in the group SC had the lower DFS and OS, and the higher amount of CNVs. In the univariate and multivariate analysis, histological malignancy grade (HMG), copy number losses (CNL) in feline chromosome (FCA) B1 as well as copy number gains (CNGs) in FCAs B4 and F2 negatively influenced DFS and OS. CNLs in FCA B1 included important tumour-repressors such as *CSMD1*, *MTUS1*, *MSR1* and *TUSC3*. CNGs in regions of FCA B4 and F2 were enriched in epithelial to mesenchymal transition (EMT) related genes and metastasis-promoting transcription factors including *GATA3*, *VIM*, *ZEB1*, *MYC* and *PTK2*. These data evidence an association between CNVs in FCAs B1, B4 and F2, and poor prognosis in FMCs.

[1]Small Animal Clinic, University of Veterinary Medicine Hannover Foundation, Hannover, Germany. [2]Department of Pathology, University of Veterinary Medicine Hannover Foundation, Hannover, Germany. [3]Chronix Biomedical, Göttingen, Germany. [4]Institute of Veterinary Medicine, University of Göttingen, Göttingen, Germany. [5]Haematology, Oncology and Palliative Medicine, Clinic III, University of Rostock, Rostock, Germany. [&]These authors equally contributed to this manuscript. *Corresponding author, E-mail: Ingo.Nolte@tiho-hannover.de

Introduction

FMCs are generally malignant hormone-independent adenocarcinomas[1–4]. Animals affected usually have a reduced survival due to the high probability of postoperative local recurrence and early metastatic spreading[2,5–7]. The median OS in untreated cats after tumour detection varies from four months to three years depending on tumour size and clinical staging[6–10]. Thus, early diagnosis, prognostic determination, and appropriate treatment selection are of major importance. In the clinical practice, the histological classification[11] and clinical staging[12] are currently the most widely used methods to guide treatment. However, according to a literature review by Zappulli *et al.* (2015) the most reliable prognostic parameters for FMCs are the HMG, and lymph node status at diagnosis[2]. The expression of molecular markers (i.e., HER2, ER, PR and Ki67) —commonly used in human medicine— are less reliable in veterinary medicine, probably due to the lack of protocols standardization, molecular tool cross-reactivity and consensus on data analysis[2]. In addition to those parameters, genomic analysis can provide further prognostic relevant information and may help to understand the molecular pathogenesis of the neoplastic change.

In recent years, there has been exponential progress in molecular analysis with profound implications for our understanding of mammary cancer biology[13]. Thereby somatic CNVs (CNGs and CNLs) characterising structural aberrations affecting neoplastic cells genomes have been used to analyse mammary cancers[14]. In fact, comparative genome hybridisations (CGH) and mass parallel sequencing CNV analyses have been successfully used in human mammary cancer research and diagnostics[15–18]. Therefore, somatic CNVs may directly contribute to understand global gene expression deregulation as well as genomic rearrangements leading to expression of fusion transcripts with transforming potential in FMCs development and progression[19–21]. Furthermore, specific CNVs can be used to identify genomic regions commonly affected in patients with poor prognosis[19,22] and poor response to therapy[22–24] contributing to an individual characterization of specific cancer subtypes[25,26]. To the best of our knowledge, there are no studies in FMCs correlating the frequency and localization of these structural aberrations with clinical parameters and survival. This study explores the influence of somatic CNVs in FMCs survival.

Results

Animals. Thirty-three female cats were included in the study; thirty-one were retrospectively included and two were prospectively enrolled. The age at diagnosis ranged from 6 to 20 years (mean [SD]: 12.4 [3.0] years). Sixteen (48.5%) cats were spayed and the remaining 17 (51.5%) were intact at the time point of diagnosis but were spayed at the time of mastectomy. At diagnosis, 15 cats (45.4%) showed lymph node metastasis (inguinal or axillary) as confirmed by histopathology. None of the animals included revealed distant metastases at the time point of diagnosis. Thirteen tumours (39.4%) were histologically graded as HMG I, 11 (33.3%) as HMG II, and nine (27.3%) as HMG III. Histopathologically, twenty-five cats had tubulopapillary carcinomas, among which four cats had intraductal papillary carcinomas (group TC), whereas eight cats showed solid carcinomas (n = 4) or comedocarcinomas (n =4), both grouped as SC. A detailed description of animals included in each group is depicted in Table 1.

Breed	Age (years)	Reproductive status	Tumour size[12]	Lymph node invasion	Clinical stage[12]	HMG[27,28]
group TC						
Domestic shorthair	13	S	T1	N	1	I
Domestic shorthair	11	I	T1	Y	3	I
Domestic shorthair	14	I	T1	N	1	II
Domestic shorthair	8	S	T1	N	1	I
Domestic shorthair	14	S	T1	N	1	II
Domestic shorthair	11	S	T1	N	1	I
Domestic shorthair*	6	S	T1	N	1	I
Persian*	11	I	T1	N	1	I
Domestic shorthair*	13	S	T1	N	1	I
Domestic shorthair*	13	I	T1	N	1	II
Domestic shorthair	16	I	T2	Y	3	II
Domestic shorthair	11	S	T2	N	2	II
Domestic shorthair	10	S	T2	Y	3	II
Domestic shorthair	13	S	T2	Y	3	II
Abyssinian	9	I	T2	N	2	II
Domestic shorthair	15	I	T2	N	2	III
Domestic shorthair	16	I	T2	N	2	III
Domestic shorthair	13	S	T2	Y	3	I
Norwegian Forest	17	S	T3	Y	3	I
Norwegian Forest	14	I	T3	N	3	III
Domestic shorthair	20	S	T3	Y	3	II
British shorthair	13	I	T3	Y	3	III
Domestic shorthair	13	S	T3	N	3	I
Domestic shorthair	7	I	T3	N	3	I
Maine coon	9	I	T3	N	3	I
group SC						
Norwegian forest**	12	S	T1	Y	3	III
Domestic shorthair***	11	S	T1	N	1	III
Siamese**	15	I	T2	Y	3	I
Domestic shorthair**	8	I	T2	Y	3	II
Domestic shorthair ***	17	I	T3	Y	3	III
Chartreux**	14	I	T3	Y	3	III
Chartreux***	13	I	T3	Y	3	II
Domestic shorthair***	10	S	T3	Y	3	III

TC, tubulopapillary carcinomas; SC, solid carcinomas and comedocarcinomas; S, spayed; I, intact; T1 < 2 cm; T2: 2-3 cm; T3 > 3 cm; N, no; Y, yes. * Intraductal papillary carcinoma, **Solid carcinoma, ***comedocarcinoma.

Table 1. Characteristics of cats included in this study.

Tissue samples DNA quantification. Thirty-three neoplastic mammary samples were included: 23 FFPE samples (group TC, n = 16; group SC, n = 7), and 10 FT samples (group TC, n = 9; group SC, n = 1). The DNA yields from FT samples (n = 10) were more consistent when compared to those of FFPE samples, ranging from 1466.2 to 16538.7 ng (mean [SD]: 7727.8 [4915.7] ng). In contrast, DNA yields from FFPE samples (n = 23) varied greatly and included some outliers, DNA values ranged from 2406.8 to 52201.7 ng (mean [SD]: 16746.7 [12991.5] ng). However, a 260/280 ratio of ~1.8 was observed in all samples evaluated.

Somatic CNVs analysis. Four FFPE samples (stored for over 15 years) of the group TC failed library preparation due to low DNA quality, and in three FT samples of the same group no CNVs were detected, these seven samples were later excluded from CNV-survival analysis (group TC, n = 18; group SC, n = 8). In total 140 genomic regions were found affected by CNVs (Supplementary table 1) with sizes ranging between 2 Mb to 72 Mb (mean [SD]: 19.8 [13.3] Mb); 25 regions were exclusively affected by CNGs, eight by CNLs, while the remaining 107 were affected by CNGs or CNLs in different patients. In general, the distribution of genomic regions affected by CNVs was similar between both groups; CNGs and CNLs affected extensive genomic regions of all chromosomes studied (Fig. 1a and 1b). However, the percentage of aberrant genomic windows (or bins) affected by CNVs in the in the group SC (n = 8, 33.2 to 71.7%; mean [SD]: 52.9 [13.9] %) was significantly higher (p = 0.003) than that of the group TC (n = 18, 1.1 to 74%; mean [SD]: 24.4 [22.5] %); Fig. 1c. The percentage of bins affected by CNLs in the group SC was significantly higher than those affected by CNGs in the same group (p < 0.0001); in contrast, the amount of CNLs and CNGs was not statistically different in the group TC (p = 0.09); (Fig. 1c).Six out of 18 patients in the group TC showed a high-CNVs percentage. In the group SC seven out of eight patients displayed a high-CNVs percentage. The percentage of aberrant bins affected by CNGs (Fig. 1d) was similar when comparing both groups (p = 0.3) while the percentage of those affected by CNLs (Fig. 1e) was significantly higher in the group SC when compared to the group TC (p = 0.009).

Follow-up and censoring. At the end of the study period (24 months), twelve cats (48%) in the group TC (n = 25) had developed local recurrence and nine of them (36%) developed subsequent distant metastasis (eight, pulmonary/pleural; one, intestinal). One cat in this group developed pulmonary/pleural metastasis without previous local recurrence, and twelve cats (40%) did not develop any kind of recurrence; cats without recurrence (n = 12) at the end of the study period were excluded from DFS analysis. In the group SC (n = 8), five cats (63%) developed local recurrence, and all animals developed pulmonary/pleural metastasis before completing the study period. Consequently, none of the animals allocated in the group SC was censored from DFS analysis.

In the group TC, eight cats (32%) were still alive at the time of censorship; however, two of those animals developed local recurrence (21 and 24 months after surgery). In twelve cases included in this group the cause of death was related to the progression of the neoplastic disease, while five cats died due to non-tumour related causes (two, anaesthetic complications during mastectomy; one, euthanized during mastectomy due to concomitant intestinal primary tumour and liver metastasis; one, severe cardiac disease [15 months after surgery]; and one, renal failure [16 months after surgery]).

In this group, all animals that were alive at the end of the study period (n = 8) and those who died due to non-tumour related causes (n = 5) were excluded from OS analysis. In the group SC (n = 8), all animals died due to the progression of the neoplastic disease before the end of the study period. Accordingly, none of the animals allocated in the group SC was censored from OS analysis.

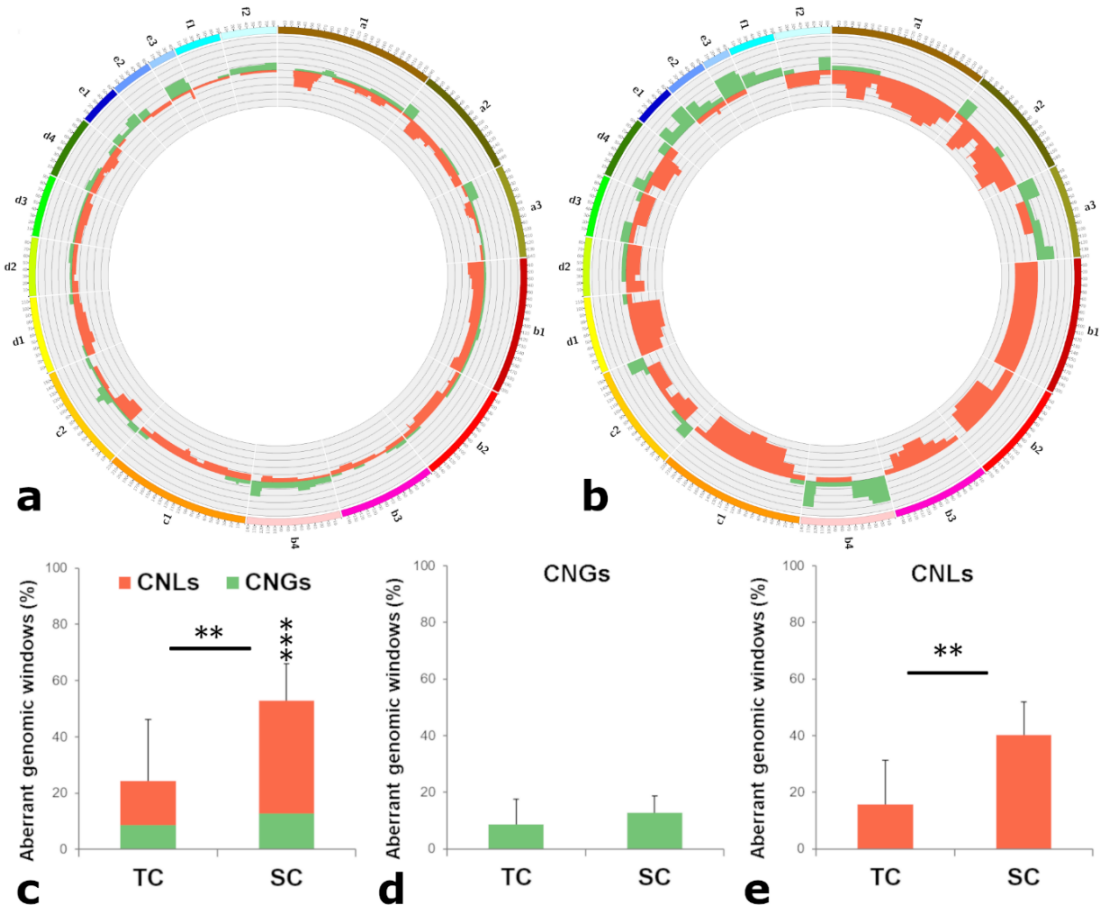

Figure 1. Copy-number variations. Comparative circos plots of (**a**) TC group (n=18) and (**b**) SC group (n=8). Outer multicolour ring illustrates chromosome location, green and orange regions in the central ring pinpoint CNGs and CNLs, respectively. Bar graphs show percentage of affected genomic windows by (c) CNVs, (d) CNGs and (e) CNLs. TC; tubulopapillary carcinoma, SC; solid carcinoma and comedocarcinomas. Data are displayed as mean (SD); * $p < 0.05$, ** $p < 0.01$, and *** $p < 0.001$

DFS and OS univariate analysis. After censorship, 21 cats (TC = 13, and SC = 8) were included in the DFS analysis and twenty cats (TC = 12, and SC = 8) were included in the OS analysis. A significant difference in lymph node status was detected when comparing both groups after censorship (DFS [p = 0.04], and OS [p = 0.05]), all additional epidemiological, clinical and histopathological characteristics of patients and tumours allocated in both groups were not statistically different ($p > 0.05$).

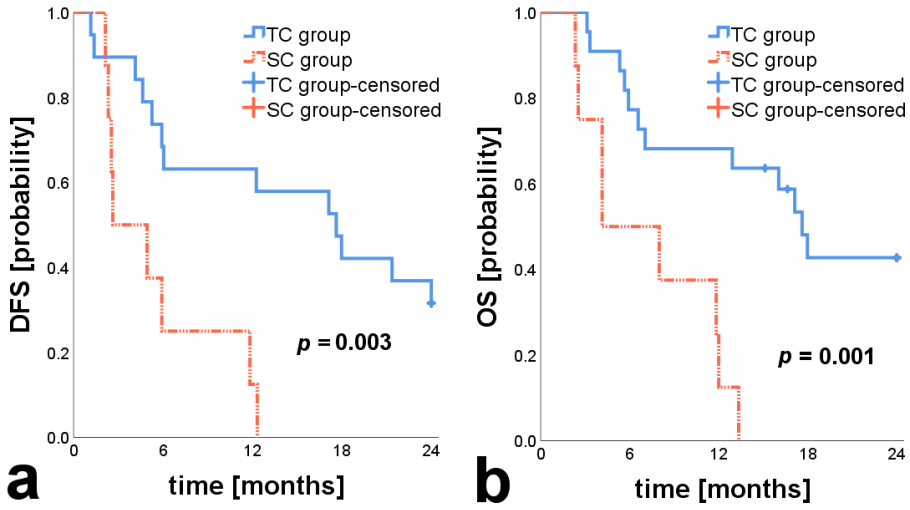

Figure 2. Survival curves DFS and OS. Kaplan-Meier curves of (a) DFS and (b) OS for cats with tubulopapillary carcinomas [TC], and solid carcinomas and comedocarcinomas [SC].

The DFS (Fig. 2a) and OS (Fig. 2b) of cats in group TC were significantly higher (p = 0.003 and p = 0.001; respectively) than those of cats allocated in the group SC (Table 2). In the univariate analysis, HMG (p < 0.0001) and lymph node metastasis (p = 0.001) were significantly associated with reduced DFS. On the other hand, OS was negatively influenced by HMG (p < 0.0001), lymph node metastasis (p = 0.001), tumour size (p = 0.04) and clinical stage (p = 0.01). Additionally, the DFS and OS of cats with tumours displaying high-CNVs, high-CNGs, and high-CNLs were significantly shorter than those of cats with tumours displaying low-CNVs, low-CNGs, and low-CNLs; respectively, details in Table 2.

Genomic regions commonly affected by CNVs. One genomic region was found commonly affected by CNGs in 14 of the analysed cases affecting FCA E3 (1–36 Mb). Further five regions were found commonly affected by CNLs (A1 30–59 Mb [n = 16], A1 59–66 MB [n = 17], B1 1–23 Mb [n = 14], B1 23–31 Mb [n = 13], and C2 21–50 Mb [n = 14]. Chromosomal regions commonly affected by CNLs harboured the feline orthologue of multiple human breast cancer-related genes previously reported as commonly deleted including *MYCBP2*, *TUSC3*, *MFHAS1*, *WRN* and *NRG1*[15,23,24,26,29,30]; details in Table 2. Among the six common CNVs identified, only CNGs in FCA E3 1–36 and CNLs in FCA B1 1–23 and B1 23–31 Mb were significantly correlated with reduced DFS and OS (Table 3).

After functional annotation clustering analysis, genes in regions commonly affected by CNGs and CNLs significantly clustered to specific biological processes related to epithelial to mesenchymal transition (EMT) elicitation. Amplifications in FCA E3 1–36 Mb included genes implicated in actin cytoskeleton organization, and cellular proliferation and motion such as *SBDS*, *ITGAM*, *PDGFA* and *RAC1* (Table 4). On the other hand, regions commonly deleted (FCAs A1 30–59 Mb, A1 59–66 MB, B1 1–23 Mb, B1 23–31 Mb, and C2 21–50 Mb) included genes involved in cell morphogenesis such as *MYCBP2*, *SLITRK5*, *SLITRK6* and *PCM1*, and cell-cell adhesion and cell adhesion including *LMO7*, *CLDN23*, and *PCDH20* (Table 4).

Variable	DFS months (mean ± sem)	*p*-value*	OS months (mean ± sem)	*p*-value*
Histological category				
group TC	14.9 ± 2.1 (n = 13)	0.003	13.5 ± 1.2 (n = 12)	0.001
group SC	5.6 ± 1.5 (n = 8)		7.2 ± 1.6 (n = 8)	
CNVs distribution				
low-CNVs	17.2 ± 2.1 (n = 9)	0.01	18.7 ± 1.6	0.01
high-CNVs	6.6 ± 1.8 (n =10)		10.6 ± 2.2	
low-CNGs	16.7 ± 2.3 (n = 9)	0.02	18.6 ± 1.6	0.01
high-CNGs	7.2 ± 1.9 (n = 10)		10.7 ± 2.2	
low-CNLs	16.1 ± 1.7 (n = 8)	0.008	19.4 ± 1.5	0.001
high-CNLs	7.3 ± 1.6 (n = 11)		9.7 ± 1.9	
TC, tubulopapillary carcinomas; SC, solid carcinomas and comedocarcinomas. *Log Rank (Mantel-Cox); test of equality of survival distributions				

Table 2. DFS and OS of cats according to histological category (group TC, and SC) and high- or low-CNVs; high- or low-CNGs; and high- or low-CNLs.

FCA (Mb)	HSA	DFS Log-Rank p value	OS Log-Rank p value	Relevant genes
Common CNGs				
E3 1–36	7 and 16	**0.02**	**0.05**	*FAM20C*, *PDGFA*, *PRKAR1B*, *SUN1*, *GET4*, *ADAP1*, *GPER1*, *MAFK*, *MAD1L1*, *NUDT1*, *EIF3B*, *LFNG*, *GNA12*, *CARD11*, *SDK1*, *FOXK1*, *FBXL18*, *ACTB*, *FSCN1*, *RAC1*, *PMS2*, *BRI3*, *TRRAP*, *SMURF1*, *KPNA7*, *ARPC1B*, *BUD31*, *CUX1*, *CPSF4*, *AKAP9*, *HIP1*, *ELN*, *SBDS*, *ITGAM*, *FUS*, *EIF3C*, *SBK1*, *IL21R*, *PRKCB1I*, *PALB2*, *CDR2*, *MYH11*, *ERCC4*, *SNX29*, *TNFRSF17*, *RMI2*, *PRM3*, *TNP2*, *SOCS1*, *DEXI*, *CIITA*, *EMP2*
Common CNLs				
A1 30–59	13	0.9	0.8	*PCDH17*, *DIAPH3*, *TDRD3*, *PCDH20*, *PCDH9*, *KLHL1*, *DACH1*, *PIBF1*, *KLF5*, *KLF12*, *TBC1D4*, *UCHL3*, *COMMD6*, *LMO7*, *KCTD12*, *FBXL3*, *MYCBP2***, *SCEL*, *EDNRB*, *POU4F1*, *RNF219 SPRY2*, *SLITRK6*
A1 59–66	13	0.4	0.7	*SLITRK5*, *GPC5*, *GPC6*
B1 1–23†	8 and 4	**0.05**	**0.01**	*FBXO25***, *CSMD1***, *ANGPT2*, *AGPAT5***, *VEGFC*, *IRF2*, *PCM1***, *MTUS1***, *PDGFRL***, *MSR1***,*TUSC3***
B1 23–31	8	**0.05**	**0.01**	*DLC1***, *CLDN23***, *MFHAS1***, *ERI1***, *GSR***, *WRN***, *NRG1***
C2 21–50	3	0.4	0.5	*COL8A1***, *NIT2***, *LNP1***, *ADGRG7*, *TFG**
FCA, feline chromosome; HSA, homologue human chromosomes; DFS, disease free survival; OS, overall survival; TC, tubulopapillary carcinoma group; SC, solid carcinoma and comedocarcinoma group. *Group size after censorship, **breast cancer-associated CNLs[15,23,24,26,29,30], †significant variable in multivariate analysis. Significant *p* values are highlighted in bold				

Table 3. Common CNVs detected in this study.

Biological process	Genes	*p* value	Annotation cluster
Genes in common CNGs*			
regulation of organelle organization†	*SBDS*, *ARPC1B*, *ELN*, *ERCC4*, *PDGFA*, *RAC1*	4.20E-04	1 (enrichment score: 2.09)
regulation of cytoskeleton† organization	*SBDS*, *ARPC1B*, *ELN*, *PDGFA*, *RAC1*	6.70E-04	
regulation of actin cytoskeleton organization†	*ARPC1B*, *ELN*, *PDGFA*, *RAC1*	2.30E-03	
cell proliferation†	*SBDS*, *ELN*, *EMP2*, *FSCN1*, *ITGAM*, *PDGFA*, *RAC1*, *TNFRSF17*	2.60E-04	2 (enrichment score: 1.99)
regulation of actin cytoskeleton‡	*ARPC1B*, *ACTB*,*GNA12*, *ITGAM*, *PDGFA*, *RAC1*	9.20E-04	
cell motion†	*SBDS*, *ARPC1B*, *ACTB*, *ITGAM*, *RAC1*, *TNP2*	1.20E-02	
Genes in common CNLs**			
cell projection organization†	*KLF5*, *MYCBP2*, *POU4F1*, *SLITRK5*, *SLITRK6*, *KLHL1*, *PCM1*	2.70E-04	1 (enrichment score: 2.12)
cell part morphogenesis†	*MYCBP2*, *POU4F1*, *SLITRK5*, *SLITRK6*, *PCM1*	3.70E-03	
cell-cell adhesion†	*LMO7*, *CLDN23*, *PCDH17*, *PCDH20*, *PCDH9*	4.90E-03	2 (enrichment score: 1.45)
cell adhesion†	*LMO7*, *CLDN23*, *COL8A1*, *DLC1*, *PCDH17*, *PCDH20*, *PCDH9*	7.30E-03	
*CNGs in FCA E3 1–36 Mb, **CNLs in FCAs A1 30–59 Mb, A1 59–66 MB, B1 1–23 Mb, B1 23–31 Mb, and C2 21–50 Mb. †GOTERM, ‡KEGG-PATHWAY			

Table 4. Genes in genomic regions affected by common CNGs and CNLS that significantly cluster for specific biological processes related to EMT elicitation. Functional annotation clustering analysed with DAVID Bioinformatics.

CNVs related to reduced DFS and OS. In order to identify cancer-related genes associated with early recurrence, we compared the DFS and OS of animals displaying each one of the 140 specific genomic aberrations identified with those of animals lacking the same mutations. The DFS and/or OS of cats with tumours displaying specific genomic aberrations listed in Table 5 (CNGs) and Table 6 (CNLs) were significantly shorter compared with that of cats with tumours lacking the same mutations. Amplified chromosomic regions significantly correlated with poor outcome (reduced DFS and OS) encompassed genes previously reported as commonly amplified in human breast cancer[15,24,26,29,30] including *ALK*, *MYCN*, *GATA3*, *VIM*, *ZEB1*, *MYC* and *PTK2* (Table 6); among those *VIM* and *ZEB1* are EMT-implicated genes which higher expression correlates with CNGs in multiple human cancers [17]. Additionally, the cancer gene census validated *ALK* and *MYC* amplifications as common in different human cancers[31]. On the other hand, genomic regions affected by CNLs that negatively influenced DFS and OS harboured frequently deleted human breast cancer-related genes[15,23,24,26,29,30] such as *LPL*, *DUSP26* and *PTK2B*, and genes previously validated as common somatic deletions by the cancer gene census in different human cancers[31] such as *PTEN*, *PAX5* and *TSC1*.

FCA (Mb)	HSA	Animals affected	DFS Log-Rank *p* value	OS Log-Rank *p* value	Relevant genes
A3 119–144	2	5	**0.05**	**0.01**	*ALK*[**,***], *SLC5A6*, *DNMT3A*, *NCOA1*, *WDCP*, *KLHL29*, *MYCN*[**], *ODC1*, *HPCAL1*
B4 1–29[‡]	10	5	**0.01**	**0.04**	*DIP2C*, *KLF6*, *KIN*, *TAF3*[**], *GATA3*[**], *CCDC3*, *MCM10*, *PHYH*, *SEPHS1*, *VIM*[**,****], *MLLT10*, *ABI1*, *ZEB1*[**,****]
B4 29–34	10	9	**0.01**	0.10	*KIF5B*
B4 34–40	12	8	**0.05**	0.3	*ERC1*, *KDM5A*
C2 1–21[†]	21	6	**0.002**	**0.01**	*PRMT2*, *S100B*, *PCNT*, *YBEY*, *MCM3AP*, *FTCD*, *COL6A2*, *SLC19A1*, *COL18A1*, *ITGB2*, *PTTG1IP*, *SUMO3*, *TRPM2*, *AIRE*, *DNMT3L*, *TRAPPC10*, *CSTB*, *PDXK*, *RRP1B*, *SIK1*, *U2AF1*, *PDE9A*, *SLC37A1*, *TMPRSS3*, *TFF1*, *TFF2*, *TFF3*, *ABCG1*, *TMPRSS2*, *PCP4*, *HMGN1*, *ETS2*, *ERG*, *DYRK1A*, *SIM2*, *CLDN14*, *CHAF1B*, *CBR3*, *SETD4*, *RUNX1*, *RCAN1*, *SLC5A3*, *KCNE2*, *IFNGR2*, *IFNAR1*, *IL10RB*, *IFNAR2*, *OLIG2*, *HUNK*, *SOD1*, *TIAM1*, *CLDN8*, *CLDN17*, *GRIK1*, *BACH1*, *CCT8*, *USP16*, *ADAMTS5*
C2 138–159[†]	3	6	**0.0001**	**<0.0001**	*MYD88*, *CTNNB1*, *MLH1*
D4 1–17	9	6	**0.009**	**0.006**	*OMD*, *SYK*, *PDCD1LG2*, *CD274*, *JAK2*, *GLIS3*, *RFX3*, *DMRT1*, *DOCK8*, *FOXD4*[**]
F2 1–17	8	4	**0.05**	**0.003**	*PRKDC*, *MCM4*, *UBE2V2*, *SNTG1*, *EFCAB1*, *RB1CC1*, *NPBWR1*, *TCEA1*, *RP1*, *LYN*, *MOS*, *PLAG1*, *CHCHD7*, *SDR16C5*, *PENK*, *IMPAD1*
F2 63–84[‡]	8	7	**0.02**	**<0.0001**	*RAD21*, *SLC30A8*, *EXT1*[**], *SAMD12*[**], *TNFRSF11B*, *MAL2*, *NOV*[**], *TAF2*, *DCC1*, *MRPL13*[**], *MTBP*[**], *SNTB1*[**], *HAS2*, *ZHX2*[**], *FBXO32*, *RNF139*[**], *TATDN1*[**], *MTSS1*, *SQLE*, *TRIB1*, *MYC*[**,***,****], *GSDMC*, *ASAP1*, *ADCY8*, *OC90*, *HHLA1*, *KCNQ3*, *LRRC6*, *PHF20L1*, *TG*, *SLA*, *WISP1*[**], *NDRG1*[**], *ST3GAL1*, *KHDRBS3*, *PTK2*[****], *CHRAC1*[**], *AGO2*, *TSNARE1*, *JRK*, *EEF1D*[**], *SCRIB*[****], *PARP10*, *MAF1*, *BOP1*[**], *HSF1*[**], *RECQL4*[**]

FCA, feline chromosome; HSA, homologue human chromosomes; DFS, disease free survival; OS, overall survival; TC, tubulopapillary carcinoma group; SC, solid carcinoma and comedocarcinoma group. [*]Group size after censorship, [**]Breast cancer-associated CNGs[15,24,26,29,30], [***]amplification validated by the cancer gene census in human cancers[31], [****]EMT-related genes commonly affected by CNGs in multiple cancer types[17], [†]genomic regions exclusively affected by CNGs, [‡]significant variable in multivariate analysis, significant *p* values are highlighted in bold

Table 5. CNGs associated with poor DFS and OS the univariate analysis.

FCA (Mb)	HSA	Animals affected	DFS Log-Rank *p* value	OS Log-Rank *p* value	Relevant genes
B1 31–51	8	11	0.07	**0.04**	*FUT10*, *MAK16***, *DPYSL2***, *CDCA2***, *KCTD9***, *GNRH1***, *DOCK5***, *NKX3-1***, *LOXL2***, *CHMP7***, *RHOBTB2***, *EGR3*, *HR***, *XPO7***, *DOK2***, *LZTS1***, *ATP6V1B2***, *LPL***, *NAT1***, *HOOK3*, *DKK4*, *POLB***, *IKBKB***, *KAT6A***, *ANK1***, *BRF2***, *FGFR1***, *NSD3*, *LSM1*, *STAR*, *EIF4EBP1*, *RAB11FIP1*, *PROSC*, *ERLIN2*, *ZNF703*, *UNC5D***, *DUSP26***, *RNF122***, *PTK2B***
B1 184–207	4	11	**0.006**	**0.01**	*SLC34A2*, *SLIT2*, *LCORL*, *FGFBP1*, *CPEB2*, *BOD1L1*, *NKX3-2*, *SLC2A9***, *STX18***, STK32B, *WFS1***, *PPP2R2C***, *SORCS2***, *HTRA3***, *HTT*, *GRK4*, *NSD2*, *FGFR3*
C1 91–104†	1	9	**0.006**	**0.01**	*RBM15***, *TRIM33*, *NRAS*, *ATP1A1*, *TENT5C*, *NOTCH2*, *PDE4DIP*
D2 1–20	10 1	7	**0.002**	**<0.0001**	*PTEN***,***, *FAS*, *RYR2***, *MTR*, *NID1*, *EGLN1***, *CAPN9*, *COG2*, *ACTA1***, *RAB4A***
D4 57–69†	9	10	0.07	**0.008**	*FANCG*, *PAX5****, *XPA*, *NR4A3*
D4 77–98	9	5	**0.007**	**0.001**	*CNTRL*, *SET*, *FNBP1*, *ABL1***, *NUP214*, *TSC1***,***, *RALGDS*, *BRD3*, *NOTCH1*

FCA, feline chromosome; HSA, homologue human chromosomes; DFS, disease free survival; OS, overall survival; TC, tubulopapillary carcinoma group; SC, solid carcinoma and comedocarcinoma group. *Group size after censorship, **breast cancer-associated CNLs[15,23,24,26,29,30], ***deletion validated by the cancer gene census in human cancers[31], †genomic regions exclusively affected by CNLs, significant *p* values are highlighted in bold

Table 6. CNLs associated with poor DFS and OS in univariate analysis.

After functional annotation clustering, regions affected by CNGs negatively influencing DFS and/or OS were enriched in genes that significantly clustered for different biological processes involved in transcription regulation; such as, *GATA3*, *HMGN1*, *ETS2*, *MYC*, *MYCN* and *ZEB1*. On the other hand, genes in CNLs correlated with poor DFS and OS were involved in different biological processes related to apoptosis evasion including *NOTCH1*, *NOTCH2*, *WFS1* and *DLC1*, and pathways in cancer; including *NRAS*, *GNRH1* and *PTEN* (Table 7).

Biological process	Genes	*p*-value	Annotation cluster
Genes in CNGs correlated with poor DFS and OS*			
structure-specific DNA binding†	*KIN*, *KLF6*, *PMS2*, *RECQL4*, *CTNNB1*, *ERCC4*, *MCM4*, *MLH1*, *MYC*, *ZEB1*	9.20E-05	1 (enrichment score: 3.16)
double-stranded DNA binding†	*KIN*, *KLF6*, *PMS2*, *RECQL4*, *CTNNB1*, *MLH1*, *MYC*, *ZEB1*	2.20E-04	

transcription regulator activity†	*BACH1*, *DNMT3L*, *GATA3*, *GLIS3*, *KLF6*, *MAF1*, *AIRE*, *CTNNB1*, *DMRT1*, *FOXD4*, *HSF1*, *HMGN1*, *KDM5A*, *MLLT10*, *NCOA1*, *OLIG2*, *PLAG1*, *RCAN1*, *RFX3*, *RUNX1*, *SIK1*, *SIM2*, *TCEA1*, *USP16*, *ERG*, *ETS2*, *MYC*, *MYCN*, *ZEB1*, *ZHX2*	2.20E-04	2 (enrichment score: 2.85)
transcription factor activity†	*BACH1*, *DNMT3L*, *GATA3*, *GLIS3*, *KLF6*, *MAF1*, *AIRE*, *CTNNB1*, *DMRT1*, *FOXD4*, *HSF1*, *HMGN1*, *KDM5A*, *MLLT10*, *NCOA1*, *OLIG2*, *PLAG1*, *RCAN1*, *RFX3*, *RUNX1*, *SIK1*, *SIM2*, *TCEA1*, *USP16*, *ERG*, *ETS2*, *MYC*, *MYCN*, *ZEB1*, *ZHX2*	4.30E-04	
Genes in CNLs correlated with poor DFS and OS**			
negative regulation of apoptosis†	*FAS*, *NKX3-2*, *NOTCH1*, *NOTCH2*, *WFS1*, *GNRH1*, *HTT*, *IKBKB*, *NRG1*, *NRAS*, *PTEN*, *POLB*	1.00E-05	1 (enrichment score: 3.33)
regulation of apoptosis†	*FAS*, *NKX3-2*, *NOTCH1*, *NOTCH2*, *WFS1*, *ABL1*, *DLC1*, *GNRH1*, *HTT*, *IKBKB*, *NRG1*, *NRAS*, *PTEN*, *POLB*, *RYR2*, *WRN*, *XPA*	2.50E-05	
pathways in cancer‡	*FAS*, *NKX3-2*, *ABL1*, *EGLN1*, *FGFR1*, *FGFR3*, *IKBKB*, *NRAS*, *PTEN*, *RALGDS*, *VEGFC*	1.60E-04	2 (enrichment score: 2.3)
*CNGs in FCAs A3 119–144, B4 1–29, B4 29–34, B4 34–40, C2 1–21, C2 138–159, D4 1–17, E3 1–36, F2 1–17 and F2 63–84, **CNLs in FCAs B1 1–23, B1 23–31, B1 31–51, B1 184–207, C1 91–104, D2 1–20, D4 57–69 and D4 77–98. †GOTERM, ‡KEGG-PATHWAY			

Table 7. Genes in genomic regions affected by CNGs and CNLS that negatively influenced DFS and OS. Functional annotation clustering analysed with DAVID Bioinformatics.

Multivariate analysis. In the multivariate analysis, HMG (p = 0.003), CNLs in FCA B1 1–23 Mb (p = 0.05), and CNGs in FCAs B4 1–29 Mb (p = 0.01) and F2 63–84 Mb (p = 0.005) remained significantly associated with poor DFS (Table 8). On the other hand, HMG (p = 0.0003), high-CNLs (p = 0.04), CNLs in FCA B1 1–23 Mb (p = 0.01) and CNGs in FCAs B4 1–29 Mb (p = 0.04) and F2 63–84 Mb (p = 0.001) remained significantly associated with reduced OS (Table 8). FCA B1 1–23 Mb included different genes previously reported as frequently deleted in human breast cancer such as *CSMD1*, *MTUS1*, and *TUSC3*. On the other hand, CNGs in FCAs B4 1–29 Mb and F2 63–84 Mb were characterized by harbouring different breast-cancer related genes previously reported as commonly amplified including transcription factors such as *GATA3*, *ZEB1* and *MYC*[15,24,26,29,30].

Variable	DFS (n = 21)		OS (n =20)	
	HR (95% CI)	*p* value	HR (95% CI)	*p* value
HMG	3.4 (1.5–7.6)	0.003	7.6 (2.7–21.3)	0.0003
CNLs B1 1–23M	3.1 (1.1–9.6)	0.05	6.3 (1.5–26.9)	0.01
CNGs B4 1-29M	4.4 (1.4–13.8)	0.01	3.4 (1.1–11.3)	0.04
CNGs F2 63–84M	6.8 (1.8–25.8)	0.005	21.8 (3.6–129.6)	0.001
high-CNLs	NS	NS	4.7 (1.1–20.7)	0.04
NS; non-significant variable				

Table 8. Significant variables in multivariate analysis.

Discussion

Somatic CNVs can be used to identify genomic regions involved in cancer development and progression[14,18,32]. To the best of our knowledge, this study represents the first analysis of CNVs and their association with survival in FMCs. Cats were grouped based on tumour morphology and biological behaviour in two groups (solid carcinomas and comedocarcinomas [SC], and tubulopapillary carcinomas [TC]). In line with previous studies[33,34], patients allocated in the group SC had significantly lower DFS and OS compared to group TC. Additionally, solid carcinomas and comedocarcinomas had a significantly higher amount of genomic aberrations (CNVs; p = 0.003), which provide evidence for a higher genomic instability compared with tubulopapillary carcinomas. Similarly, a higher amount of genomic aberrations (CNGs and CNLs) is associated with recurrence and worse prognosis in human breast cancer[16,35].To evaluate the influence of specific CNVs (CNGs and CNLs) in FMC survival, the tumours were classified into high- or low-CNVs, high- or low-CNGs, and high- or low-CNLs according to whether the percentage of affected bins was greater or lower than their respective median value. In the univariate analysis, a higher amount of CNVs, CNGs and CNLs was significantly correlated with reduced DFS and OS. In the multivariate analysis, only a higher amount of CNLs remained significantly associated with reduced OS. CNLs were more frequent than CNGs in the group SC. In contrast, the amount of CNGs and CNLs was not significantly different in the group TC. Additionally, the percentage of bins affected by CNLs in the group SC was significantly higher than that of the group TC. Accordingly, a higher frequency of CNLs may be associated with a worse outcome in the group SC, and may be implicated in the development of distinct malignancy-related characteristics in solid carcinomas and comedocarcinomas.

We identified 140 genomic regions affected by CNVs (Supplementary table 1). Considering that the recurrence of specific CNVs (both CNGs and CNLs) may indicate that such genomic regions are likely to harbour cancer-related genes[36]; we first characterized the most common CNVs detected (CNGs in FCA E3 1–36 Mb [n = 12] and CNLs in FCAs A1 30–59 Mb [n = 14], A1 59–66 Mb [n = 15], B1 1–23 Mb [n = 13], B1 23–31 [n = 12] and C2 21–50 Mb [n = 12]). The proximal amplified region of FCA E3 (1–36 Mb) encompasses up to 50 cancer-related genes including different genes implicated in actin cytoskeleton organization and cellular motion such as *SBDS*, *ITGAM, PDGFA, RAC1.* Conversely, common deleted regions (FCAs A1 30–59 Mb, A1 59–66 Mb, B1 1–23 Mb, B1 23–31 Mb, and C2 21–50 Mb) included genes implicated in cell-cell adhesion and components of tight junction strands such as *LMO7, CLDN23, PCDH17, PCDH20* and *PCDH9*. The acquisition of migratory properties including reorganization of the actin cytoskeleton and loss of the cell-cell adhesion is associated with EMT-elicitation[37,38]. CNLs in the proximal region of FCA B1 (1–23 Mb, n = 14; 23–31 Mb, n = 12; and 31–51 Mb, n = 11) correspond with a frequently deleted genomic region (HSA 8p) in different types of human cancer including breast cancer, this regions harbour multiple established or putative tumour-suppressor genes including *CSMD1*, *MSR1*, *MTUS1*, *TUSC3, DLC1, NRG1* and *LZTS1*[19,22,23,39–41].

Among all common CNVs identified in this study, only CNGs in FCA E3 1–36 Mb, and CNLs in FCAs B1 1–23 Mb and B1 23–31 Mb negatively influenced both DFS and OS in the univariate analysis. In the multivariate analysis, only common CNLs in FCA B1 1–23 Mb remained significantly associated with poor DFS and OS. FCA B1 1–23 Mb genomic region harbours breast cancer-related genes commonly affected by CNLs[15,24,30] such as *FBXO25*, *CSMD1*, *ANGPT2*, *AGPAT5*, *PCM1*, *MTUS1*, *PDGFRL*, and *TUSC3*. *TUSC3* deletion is associated with poor prognosis and may be a useful biomarker and therapeutic target in different types of human cancer [42–46]. *TUSC3* (tumour suppressor candidate 3) encodes an endoplasmic reticulum protein involved in N-glycosylation; loss of *TUSC3* may lead to protein maturation disturbances by improper glycosylation resulting in malignant cell transformation[43,46]. In this study, *TUSC3* was deleted in 13 patients and its deletion was correlated with poor DFS and OS in the univariate and multivariate analyses; due to its functional significance in protein maturation and in the development of multiple tumour types; *TUSC3* deletion may be also a good biomarker and poor prognosis indicator in FMCs. Recombinant Ad-*TUSC3* gene therapy, mutant-specific *TUSC3* rescue drugs and targeting the negative regulators of *TUSC3* have been proposed as molecularly-tailored therapeutic options to restore *TUSC3* protein function in patients carrying this specific genomic aberration[43,45,46].

Less frequent CNGs (Table 5) and CNLs (Table 6) were also significantly correlated with poor DFS and/or OS in the univariate analysis. Among these, genomic regions affected by CNGs (A3 119–144, B4 1–29, B4 29–34, B4 34–40, C2 1–21, C2 138–159, D4 1–17, F2 1–17 and F2 63–84) were enriched in transcription factors including *GATA3, HMGN1, ZEB1, MYC* and *MYCN,* which regulate cell cycle progression, apoptosis and cellular transformation. *ZEB1* is a well-known EMT-inducing and metastasis-promoting transcription factor[47–50], while *MYC* and *MYCN* are implicated in the downregulation of E-cadherin through the activation of miR-9[51]. Additionally, *MYCN* amplification correlates with poor prognosis in different tumours in humans, especially neuroblastoma[51–53]. We also observed two gene amplifications previously validated by the gene cancer census in multiple human cancers (*ALK* and *MYC*)[31]. *ALK* amplifications and mutations are correlated with poor prognosis in different types of human cancers[54–56]; however, treatment with specific ALK-inhibitors like crizotinib and alectinib have been reported to increase survival of human patients with non-small cell lung cancer carrying specific mutations and amplifications of *ALK* gene[57,58]. In this study, amplifications of *ALK* were identified in five patients and were correlated with poor prognosis, these patients may be part of a distinct molecular subgroup that could benefit from individualized therapy with specific ALK-inhibitors.

Among all CNGs related to poor outcome in the univariate analysis, DFS and OS remained significantly influenced by CNGs in FCAs B4 1–29 Mb and F2 63–84 Mb in the multivariate analysis. FCA B4 1–29 Mb genomic region harbours different breast cancer-related genes commonly affected by CNGs[15,24,30] including *KIN*, *TAF3*, *CCDC3*, *MCM10*, *GATA3*, *PHYH* and *SEPHS1*. Additionally, this genomic region also harbours previously reported EMT-associated genes commonly affected by CNGs in different types of human cancer such as *VIM* and *ZEB1*[17].

FCA F2 63–84 Mb genomic region harbours more than 30 breast cancer-related genes commonly affected by CNGs in human breast cancer[15,24,30], among those *MYC*, *SCRIB*, *NDRG1* and *PTK2* have been described as EMT-related genes commonly affected by CNGs in multiple human cancer types[17]. The influence of FCAs B4 and F2 amplifications on EMT elicitation in an FMC-derived cell line was previously described for our group[59]. In this study, CNGs in FCA B4 1–29 Mb and F2 63–84 Mb were correlated with reduced DFS and OS in the univariate and multivariate analyses. Moreover, CNGs affecting additional regions of FCAs B4 (29–34 Mb [n = 10] and 34–40 [n = 12]) and F2 (1–17Mb [n = 8]) negatively influenced DFS and OS in the univariate analysis (Tables 5 and 6). These results now provides evidence about the influence of FCAs F2 and B4 CNGs on FMC survival, and may also highlight the importance of EMT on FMC early recurrence and reduced survival.

Genomic regions affected by CNLs that negatively influenced DFS and OS (B1 1–23, B1 23—31, B1 31–51, B1 184–207, C1 91–104, D2 1–20, D4 57–69 and D4 77–98) harboured frequently deleted human breast cancer-related genes[15,23,24,26,29,30] such as *LPL*, *DUSP26* and *PTK2B* (Table 7), and genes previously validated as common somatic deletions by the cancer gene census in different human cancers[31] such as *PTEN*, *PAX5* and *TSC1*. Additionally, genes in CNLs correlated with poor DFS and OS were involved in different biological processes related to apoptosis evasion including *NOTCH1, WFS1* and *DLC1,* and pathways in cancer; including *NRAS*, *GNRH1* and *PTEN.*

In line with previous studies HMG was significantly correlated with poor outcome[2,28]. Among all epidemiological, clinical, and histopathological independent variables evaluated only HMG was significantly associated with poor DFS and OS in the univariate and multivariate analysis highlighting the importance and clinical utility of HMG as prognostic factor in FMCs. Despite the differences in DNA quality isolated from FFPE and FT samples, the feasibility of FFPE tissues for NGS analyses has been proved, showing a higher concordance in results achieved from paired samples (FT/FFPE) which may diminishes over storage time[60]. In this study, the DNA yields and 260/280 ratios of the two different origins of samples (FFPE and FT) were similar. However, the fact that the DNA isolated from four FFPE specimens stored for over 15 years was not suitable for library preparation may be associated with the effect of storage time and fixation process on DNA quality.

This study may be biased because of a small sample size. In proportional hazards regression, the recommended number of events per variable (EPV) is 10 [61]. Due to the small number of patients included in this study, several independent variables were characterized with a lower EPV value. Therefore, the results of this study need to be validated in a larger series. Additionally, the wide confidence intervals observed may also be related to small or sparse data biases[62]. A longer study period would be advisable considering those cases which developed late-recurrence in the group TC. In summary, this study provides evidences about the importance of specific CNVs as useful prognostic markers in FMCs. Cats with solid carcinomas and comedocarcinomas had shorter survival than cats with tubulopapillary carcinomas. Moreover, solid carcinomas and comedocarcinomas are characterized by a higher amount of CNLs. CNLs on specific regions of FCA B1, and CNGs in FCAs B4 and F2 negatively influenced both DFS and OS.

CNLs in FCA B1 included important tumour-repressors and resemble the HSA 8p deletion which is strongly linked to poor prognosis in breast cancer. On the other hand, amplified regions of FCA B4 and F2 were enriched in EMT-related genes and metastasis-promoting transcription factors. Further efforts are necessary to sequence a larger series of FMC genomes, characterize somatic CNVs significantly associated with reduced survival, identify the cancer-related gene targets located on these aberrant genomic regions, and define their importance as therapeutic targets on FMCs.

Methods

Animals. Thirty-three female cats surgically treated for FMC at the Small Animal Clinic of the University of Veterinary Medicine Hannover from 2000 to 2016 were enrolled in this study. Clinical history and reproductive status were obtained. Only cats, for which thoracic radiographs to investigate the presence of metastases at diagnosis and during the follow-up period were available, were included in this study. Patients were clinically staged using the modified World Health Organization (WHO) system [12]. Due to the previously reported reduced survival of cats with solid carcinomas (8 months) compared to tubulopapillary carcinomas (36 months)[2,33]; patients were grouped based on biological behaviour and morphology of the tumours into two categories (TC and SC). The group TC included tubulopapillary carcinomas, and the group SC comprised both solid carcinomas and comedocarcinomas. All cats underwent unilateral chain mastectomy, including resection of involved lymph nodes. The patients were followed up for a two-year post-operative period or until death. Long-term follow-up was obtained by clinical records analysis and telephone interviews with the owners.

Tissue samples. FFPE and/or FT tumour samples were collected for histopathological examination and DNA isolation. The FFPE specimens were retrospectively retrieved from the archives of the Department of Pathology, University of Veterinary Medicine Hannover. The FT samples included were retrieved from the frozen tissue bank of the Small Animal Clinic, University of Veterinary Medicine Hannover. FFPE and FT samples were collected for diagnostic purposes during the medically necessary surgery after owner's written approval. Consequently, this study was not an animal experiment according to the German Animal Welfare Act and an ethical approval was not required.

Histopathological examination. Paraffin sections (4 µm) of the tumour samples were stained with haematoxylin eosin (H&E) for histopathologic evaluation. The samples were examined under light microscopy and the morphological diagnosis was performed following the WHO classification [11]. Histological grading of the tumours was performed according to the method described by Elston and Ellis (1991), and Castagnaro *et al.* (1998)[27,28]. Complete surgical excision and lymph node metastasis were histopathologically confirmed in all cases.

DNA Isolation. FFPE samples: four 10-µm-thick sections were sliced using a microtome (pfm Slide 2003, pfm medical ag). Afterwards, the sections were deparaffinized and the nucleic acids were isolated with the AllPrep DNA/RNA FFPE kit (QIAGEN) following the manufacturer's instructions.

FT samples: the frozen tissue was previously homogenized using a TissueLyser (II—5 mm stainless steel bead, QIAGEN GmbH, Hilden, Germany). DNA was isolated using the AllPrep DNA/RNA Mini Kit (QIAGEN) following the manufacturer's instructions. The DNA yields were determined with the Synergy 2 microplate reader (BioTek) and the purity of each sample was determined by calculating the 260/280 ratio. Samples were stored at -80°C until use.

Copy-number variation analysis. DNA sequencing and CNVs analysis was performed according to the methodology described by Granados-Soler *et al.* (2018)[59]. Based on the results of the normal reference control (feline healthy mammary tissue), regions with log2-copy-number ratios of > 0.2 or < -0.2 were scored as significantly aberrant. All aberrant bins with smoothed log2-copy-number ratios of > 0.2 were scored as amplified (CNGs) and all bins with < -0.2 were scored as deleted (CNLs). Structural rearrangements detected were compared with those previously reported in human breast cancers[15,23,24,26,29,30], amplifications and deletions validated by the cancer gene census in human cancers[31], and were complemented by EMT-related genes reported in multiple human cancer types[17], specific FMCs and human breast cancer cell lines-related somatic CNVs[15,59], and additional cancer-associated genes previously reported on FMCs. Additionally, to determine enriched biological terms, lists of the genes harboured in genomic regions most commonly affected by CNVs, and those correlated with poor outcome (reduced DFS and/or OS) were uploaded to the DAVID Bioinformatics server (http://david.abcc.ncifcrf.gov), which was employed for functional annotation clustering[63,64].

Statistical analysis. The statistical software SPSS (IBM SPSS Statistics for Windows, Version 23.0. Armonk, NY, USA) was employed to perform all statistical analysis. For all the statistical analyses, a $p \leq 0.05$ was considered significant. Epidemiological, clinical, and histopathological variables included were age, breed, reproductive status, tumour size, lymph node metastasis (confirmed by histopathology), distant metastasis, modified WHO clinical stage[12], and HMG[27,28]. CNVs, CNGs, and CNLs were categorized into high or low according to whether the percentage of affected bins was lower or greater than their respective median value. Presence or absence of CNVs (CNGs and/or CNLs) at specific genomic regions was included as a categorical variable. Local recurrence, distant metastases, and death were considered as follow-up variables. Descriptive statistics of patients allocated in histological categories TC and SC regarding all epidemiological, clinical, histopathological and follow-up variables were performed. DFS, and OS were defined as months from surgery to tumour recurrence (local or distant), and to death, respectively. Cats were censored from DFS analysis at death without recurrence. Animals alive at the end of the study period (24 months) and animals which died due to non-tumour related causes were censored from OS analysis. After censorship, differences between groups regarding all epidemiological, clinical, and histopathological characteristics were assessed using Chi-Square Independence Test. Univariate Kaplan-Meier log rank analyses were applied to determine whether histologic diagnosis (TC or SC), CNVs status (high- or low-CNVs, high- or low-CNGs, and high- or low-CNLs), presence or absence of CNVs (CNGs and CNLs) affecting specific genomic regions and all additional epidemiological, clinical, and histopathological variables were associated with DFS and OS.

A multivariate Forward Stepwise Cox proportional hazards regression analysis over histological diagnosis strata (TC and SC) was applied to evaluate the influence of independent variables on dependent follow-up variables (DFS and OS), the variable entry and retention criteria were set at 0.25 and 0.1, respectively[65].

References

1. Wiese, D., Thaiwong, T., Yuzbasiyan-gurkan, V. & Kiupel, M. Feline mammary basal-like adenocarcinomas: a potential model for human triple-negative breast cancer (TNBC) with basal-like subtype. *BMC Cancer* **13,** 403 (2013).
2. Zappulli, V. *et al.* Prognostic Evaluation of Feline Mammary Carcinomas: A Review of the Literature. *Vet. Pathol.* **52,** 46–60 (2015).
3. Hayes, H., Milne, K. & Mandell, C. Epidemiological features of feline mammary carcinoma. *Vet. Rec.* **108,** 476–479 (1981).
4. Misdorp, W. & Weijer, K. Animal model of human disease: breast cancer. *Am. J. Pathol.* **98,** 573–6 (1980).
5. Hughes, K. & Dobson, J. M. Prognostic histopathological and molecular markers in feline mammary neoplasia. *Vet. J.* **194,** 19–26 (2012).
6. Hahn, K. A., Bravo, L. & Avenell, J. S. Feline breast carcinoma as a pathologic and therapeutic model for human breast cancer. *In Vivo* **8,** 825–8 (1994).
7. Hahn, K. A. & Adams, W. H. Feline mammary neoplasia: biological behavior, diagnosis, and treatment. *Feline Pr.* **25,** 5–11 (1977).
8. Giménez, F. & Hecht, S. Early detection, aggressive therapy Optimizing the management of feline mammary masses. *J. Feline Med. Surg.* **12,** 214–224 (2010).
9. Hayden, D. W. & Nielsen, S. W. Feline mammary tumours. *J. Small Anim. Pract.* **12,** 687–98 (1971).
10. Morris, J. Mammary tumours in the cat: size matters, so early intervention saves lives. *J. Feline Med. Surg.* **15,** 391–400 (2013).
11. Misdorp, W., Else, R., Hellmen, E. & Lipscomb, T. *Histological classification of mammary tumors of the dog and cat*. (1999).
12. McNeill, C. J. *et al.* Evaluation of adjuvant doxorubicin-based chemotherapy for the treatment of feline mammary carcinoma. *J. Vet. Intern. Med.* **23,** 123–9 (2009).
13. Vuong, D., Simpson, P. T., Green, B., Cummings, M. C. & Lakhani, S. R. Molecular classification of breast cancer. *Virchows Arch* **465,** 1–14 (2014).
14. Shlien, A. & Malkin, D. Copy number variations and cancer. *Genome Med.* **1,** 1–9 (2009).
15. Saito, S., Morita, K. & Hirano, T. High frequency of common DNA copy number abnormalities detected by bacterial artificial chromosome array comparative genomic hybridization in 24 breast cancer cell lines. *Hum. Cell* **22,** 1–10 (2009).
16. Bergamaschi, A. *et al.* Distinct patterns of DNA copy number alteration are associated with different clinicopathological features and gene-expression subtypes of breast cancer. *Genes, Chromosom. Cancer* **45,** 1033–1040 (2006).
17. Zhao, M., Liu, Y. & Qu, H. Expression of epithelial-mesenchymal transition-related genes increases with copy number in multiple cancer types. *Oncotarget* **7,** 24688–99 (2016).
18. Zack, T. I. *et al.* Pan-cancer patterns of somatic copy number alteration. *Nat. Genet.* **45,** 1134–1140 (2013).
19. Lebok, P. *et al.* 8P Deletion Is Strongly Linked To Poor Prognosis in Breast Cancer. *Cancer Biol. Ther.* **16,** 1080–1087 (2015).
20. Iddawela, M. *et al.* Integrative analysis of copy number and gene expression in breast cancer using formalin-fixed paraffin-embedded core biopsy tissue: A feasibility study. *BMC Genomics* **18,** 1–13 (2017).
21. Stephens, P. J. *et al.* Complex landscapes of somatic rearrangement in human breast cancer genomes. *Nature* **462,** 1005–1010 (2009).
22. Moelans, C. B., Maldegem, C. M. G. Van & Wall, E. Van Der. Copy number changes at 8p11-12 predict adverse clinical outcome and chemo- and radiotherapy response in breast cancer. *Oncotarget* **9,** 17078–17092 (2018).
23. Cai, Y. *et al.* Loss of Chromosome 8p Governs Tumor Progression and Drug Response by Altering Lipid Metabolism. *Cancer Cell* **29,** 751–766 (2016).
24. Ellis, M. J. *et al.* Whole-genome analysis informs breast cancer response to aromatase inhibition. *Nature* **486,** 353–360 (2012).
25. Knight, J. F. *et al.* KIBRA (WWC1) Is a Metastasis Suppressor Gene Affected by Chromosome 5q Loss in Triple-Negative Breast Cancer. *Cell Rep.* **22,** 3191–3205 (2018).

26. Ross, J. S. *et al.* Genomic Profiling of Advanced-Stage, Metaplastic Breast Carcinoma by Next-Generation Sequencing Reveals Frequent, Targetable Genomic Abnormalities and Potential New Treatment Options. *Arch. Pathol. Lab. Med.* **139,** 642–649 (2015).
27. Elston, C. & Ellis, I. Pathological prognostic factors in breast cancer. I. The value of histological grade in breast cancer: experience from a large study with long-term follow-up. *Histopathology* **19,** 403–410 (1991).
28. Castagnaro, M. *et al.* Tumour grading and the one-year post-surgical prognosis in feline mammary carcinomas. *J. Comp. Pathol.* **119,** 263–75 (1998).
29. Nik-Zainal, S. *et al.* Mutational processes molding the genomes of 21 breast cancers. *Cell* **149,** 979–993 (2012).
30. Haverty, P. M. *et al.* High-resolution genomic and expression analyses of copy number alterations in breast tumors. *Genes, Chromosom. Cancer* **47,** 530–542 (2008).
31. Forbes, S. A. *et al.* COSMIC: Exploring the world's knowledge of somatic mutations in human cancer. *Nucleic Acids Res.* **43,** D805–D811 (2015).
32. Beroukhim, R. *et al.* The landscape of somatic copy-number alteration across human cancers. *Nature* **463,** 899–905 (2010).
33. Seixas, F., Palmeira, C., Pires, M. A., Bento, M. J. & Lopes, C. Grade is an independent prognostic factor for feline mammary carcinomas: a clinicopathological and survival analysis. *Vet. J.* **187,** 65–71 (2011).
34. Mills, S. W. *et al.* Prognostic Value of Histologic Grading for Feline Mammary Carcinoma: A Retrospective Survival Analysis. *Vet. Pathol.* **52,** 238–249 (2014).
35. Isola, J. J. *et al.* Genetic aberrations detected by comparative genomic hybridization predict outcome in node-negative breast cancer. *Am. J. Pathol.* **147,** 905–11 (1995).
36. Korkola, J. & Gray, J. W. Breast cancer genomes - form and function. *Curr. Opin. Genet. Dev.* **20,** 4–14 (2010).
37. Hennessy, B. T. *et al.* Characterization of a naturally occurring breast cancer subset enriched in epithelial-to-mesenchymal transition and stem cell characteristics. *Cancer Res.* **69,** 4116–4124 (2009).
38. Boyer, B., Vallés, A. M. & Edme, N. Induction and Regulation of Epithelial–Mesenchymal transitions. **60,** 1091–1099 (2000).
39. Sabatier, R. *et al.* Claudin-low breast cancers: clinical, pathological, molecular and prognostic characterization. *Mol. Cancer* **13,** 228 (2014).
40. Menotti-Raymond, M. *et al.* An autosomal genetic linkage map of the domestic cat, Felis silvestris catus. *Genomics* **93,** 305–313 (2009).
41. Yuan, B. Z. *et al.* DLC-1 gene inhibits human breast cancer cell growth and in vivo tumorigenicity. *Oncogene* **22,** 445–450 (2003).
42. Conway, K. *et al.* Racial variation in breast tumor promoter methylation in the carolina breast cancer study. *Cancer Epidemiol. Biomarkers Prev.* **24,** 921–930 (2015).
43. Yuan, J. *et al.* Tumor suppressor candidate 3: A novel grading tool and predictor of clinical malignancy in human gliomas. *Oncol. Lett.* **15,** 5655–5661 (2018).
44. Vaňhara, P. *et al.* Loss of the oligosaccharyl transferase subunit TUSC3 promotes proliferation and migration of ovarian cancer cells. *Int. J. Oncol.* **42,** 1383–1389 (2013).
45. Horak, P. *et al.* TUSC3 Loss Alters the ER Stress Response and Accelerates Prostate Cancer Growth in vivo. *Sci. Rep.* **4,** 1–9 (2014).
46. Yu, X. *et al.* TUSC3: a novel tumour suppressor gene and its functional implications. *J. Cell. Mol. Med.* **21,** 1711–1718 (2017).
47. Schmalhofer, O., Brabletz, S. & Brabletz, T. E-cadherin, β-catenin, and ZEB1 in malignant progression of cancer. *Cancer Metastasis Rev.* **28,** 151–166 (2009).
48. Wellner, U. *et al.* The EMT-activator ZEB1 promotes tumorigenicity by repressing stemness-inhibiting microRNAs. *Nat. Cell Biol.* **11,** 1487–95 (2009).
49. Aigner, K. *et al.* The transcription factor ZEB1 (δEF1) promotes tumour cell dedifferentiation by repressing master regulators of epithelial polarity. *Oncogene* **26,** 6979–6988 (2007).
50. Zheng, X. *et al.* Epithelial-to-mesenchymal transition is dispensable for metastasis but induces chemoresistance in pancreatic cancer. *Nature* **527,** 525–530 (2015).
51. Ma, L. *et al.* miR-9 , a MYC / MYCN-activated microRNA , regulates E-cadherin and cancer metastasis. *Nat. Cell Biol.* **12,** (2010).
52. Kooi, I. E. *et al.* A meta-analysis of retinoblastoma copy numbers refines the list of possible driver genes involved in tumor progression. *PLoS One* **11,** 1–20 (2016).
53. Jansson, M. D. & Lund, A. H. MicroRNA and cancer. *Mol. Oncol.* **6,** 590–610 (2012).

54. Ji, J. H. *et al.* Identification of Driving ALK Fusion Genes and Genomic Landscape of Medullary Thyroid Cancer. *PLoS Genet.* **11,** 1–12 (2015).
55. Singh, R. R. *et al.* Clinical massively parallel next-generation sequencing analysis of 409 cancer-related genes for mutations and copy number variations in solid tumours. *Br. J. Cancer* **111,** 2014–2023 (2014).
56. Meißner, T. *et al.* Metastatic triple-negative breast cancer patient with TP53 tumor mutation experienced 11 months progression-free survival on bortezomib monotherapy without adverse events after ending standard treatments with grade 3 adverse events. *Cold Spring Harb. Mol. case Stud.* **3,** 1–23 (2017).
57. Gadgeel, S. M. *et al.* Safety and activity of alectinib against systemic disease and brain metastases in patients with crizotinib-resistant ALK-rearranged non-small-cell lung cancer (AF-002JG): Results from the dose-finding portion of a phase 1/2 study. *Lancet Oncol.* **15,** 1119–1128 (2014).
58. Vijayvergia, N. & Mehra, R. Clinical challenges in targeting anaplastic lymphoma kinase in advanced non-small cell lung cancer. *Cancer Chemother. Pharmacol.* **74,** 437–446 (2014).
59. Granados-Soler, J. L. *et al.* TiHo-0906: a new feline mammary cancer cell line with molecular, morphological, and immunocytological characteristics of epithelial to mesenchymal transition. *Sci. Rep.* **8,** 13231 (2018).
60. Hedegaard, J. *et al.* Next-generation sequencing of RNA and DNA isolated from paired fresh-frozen and formalin-fixed paraffin-embedded samples of human cancer and normal tissue. *PLoS One* **9,** (2014).
61. Peduzzi, P., Concato, J., Feinstein, A. R. & Holford, T. R. Importance of events per independent variable in proportional hazards regression analysis II. Accuracy and precision of regression estimates. *J. Clin. Epidemiol.* **48,** 1503–1510 (1995).
62. Greenland, S., Mansournia, M. A. & Altman, D. G. Sparse data bias: A problem hiding in plain sight. *BMJ* **353,** 1–6 (2016).
63. Huang, D. W., Sherman, B. T. & Lempicki, R. A. Systematic and integrative analysis of large gene lists using DAVID bioinformatics resources. *Nat. Protoc.* **4,** 44 (2008).
64. Huang, D. W., Sherman, B. T. & Lempicki, R. A. Bioinformatics enrichment tools: Paths toward the comprehensive functional analysis of large gene lists. *Nucleic Acids Res.* **37,** 1–13 (2009).
65. Bursac, Z., Gauss, C. H., Williams, D. K. & Hosmer, D. W. Purposeful selection of variables in logistic regression. *Source Code Biol. Med.* **3,** 1–8 (2008).

Acknowledgments. The authors wish to thank Heike Thiemeyer, Eva Packeiser, Kerstin Rohn and Jan Torben Schille for their excellent technical assistance, valuable comments and suggestions.

Author Contributions. José Luis Granados-Soler, Ingo Nolte, Hugo Murua Escobar, and Marion Hewicker-Trautwein performed the primary study design; Ingo Nolte, Hugo Murua Escobar, Bertram Brenig, Johannes Junginger, Daniela Betz, and Marion Hewicker-Trautwein performed the manuscript revision and final approval; Kirsten Bornemann-Kolatzki, Julia Beck, Ekkehard Schütz and Bertram Brenig performed the DNA sequencing and CNVs; José Luis Granados-Soler retrieved the data, performed the DNA isolation, and CNVs data analysis, analysed the data and wrote the paper.

Competing Interest. The author(s) declare no competing interests.

High-resolution transcriptome analysis of feline mammary carcinomas and derived cell lines

José Luis Granados-Soler [1,5], Kirsten Bornemann-Kolatzki[3], Julia Beck[3], Bertram Brenig[4], Ekkehard Schütz[3], Daniela Betz[1], Johannes Junginger[2], Marion Hewicker-Trautwein[2], Hugo Murua Escobar[5&], Ingo Nolte[1&*]

Feline mammary carcinomas (FMCs) heterogeneity has been realised through histopathology and immunohistochemistry. Nonetheless, the actual extent of diversity can be appreciated only through detailed molecular approaches. Next-generation sequencing (NGS) allows characterisation of differentially-expressed genes (DEGs) modulating the FMCs dysregulation. This study aimed to identify DEGs, dysregulated molecular pathways, and possible biomarkers and therapeutic targets in FMCs and derived cell lines. Transcriptomic analysis was performed on RNA isolated from tumour and healthy mammary samples (paraffin-embedded and frozen-tissue) from 33 female cats with FMCs, and two FMCs-derived cell lines. Additionally, the immunoexpression of epithelial, mesenchymal, and hormonal markers was assessed. At the transcriptomic level, immunohistochemical groups were not separated. However, common DEGs in human triple-negative and claudin-low breast cancers were identified (e.g. *FOXM1*, *MYBL2*, and *HSPB7*). Upregulated genes influenced cell-growth and death regulation (e.g. *CDK1*, *ESPL1*, *CHEK1*, *MCM3*, and *CCNB1*). Downregulated genes were involved in pathways that prevent tumour spreading including tight-junction components (e.g. *CLDN4*, *CLDN5*, *CLDN8* and *CLDN23*) and cell adhesion molecules (e.g. *CD40*, *CDH1*, *ICAM2*, *ITGAM* and *ITGB2*). DEGs participating in the PI3K-Akt (e.g. *FLT4*, *PDGFD* and *BRCA1*) and p513 (e.g. *CCNB2*, *CDK1* and *RRM2*) signalling pathways were identified. Cellular models shared many similarities with original tumours; however, alterations correlated with endocrine regulation, circadian rhythm and metabolic pathways showed important differences. NGS can be used to identify pivotal biological processes in FMCs. Furthermore, transcriptomic profile comparison of FMCs and cell lines provide information about which aspects of the neoplastic change can be modelled in vitro and also denote important constraints.

[1]Small Animal Clinic, University of Veterinary Medicine Hannover Foundation, Hannover, Germany. [2]Department of Pathology, University of Veterinary Medicine Hannover Foundation, Hannover, Germany. [3]Chronix Biomedical, Göttingen, Germany. [4]Institute of Veterinary Medicine, University of Göttingen, Göttingen, Germany. [5]Haematology, Oncology and Palliative Medicine, Clinic III, University of Rostock, Rostock, Germany. [&]These authors equally contributed to this manuscript. *Corresponding author, E-mail: Ingo.Nolte@tiho-hannover.de

Introduction

Mammary cancer is a major health problem in human and veterinary medicine. In recent years, there has been substantial progress in the molecular portraying of human breast cancer, leading to a more detailed classification—beyond the histological diagnosis[1–7]. In veterinary medicine, the heterogeneity of the feline and canine mammary cancers—and cells composing the tumour microenvironment—have been realised through the conventional histopathological examination and immunohistochemical profiling. Nonetheless, the actual extent of diversity among mammary cancer in dogs and cats can be appreciated only through molecular analyses in order to realise true individualised therapy.

Feline mammary carcinomas (FMCs) are locally invasive tumours, characterized by early lymph node/lymphovascular invasion and distant metastasis[8–10]. Cats affected usually have a reduced survival, and a poor response to treatment[11–13]. As previously reported in human breast cancer[1,4,6,14–18], FMCs may represent a heterogeneous group of diseases with distinctive molecular traits influencing therapeutic response, disease-free survival (DFS), and overall survival (OS). The current standard therapy for FMCs is the complete excision of the tumour by removing one or preferably both mammary chains and associated lymph nodes[19,20]. Some clinical studies have investigated the benefit of different chemotherapeutic regimens with variable results[12,13,21,22]. However, due to the lack of information about which subset of patients would specifically benefit from the proposed therapies[12,13,21–23] most of them are not commonly used in the clinical practice. Immortalised cell lines are useful to study specific characteristics of the neoplastic process and for the testing of novel treatment modalities under controlled conditions[3,24–27]. Only few cell lines derived from primary FMCs or metastatic lesions have been established and initially characterised[26–32]. However, in most of the cases the molecular characteristics of derived cell lines were not compared with those of the original tumours.

A detailed analysis and evaluation of differentially expressed genes between FMCs, derived cell lines and healthy mammary tissues is necessary to identify specific molecular pathways and biological processes commonly dysregulated in FMCs and, moreover, to determine which aspects from the original tumours can be reliably modelled *in vitro*. NGS allows rapid high-resolution characterisation of differentially expressed genes participating in multiple processes modulating the neoplastic change and cancer progression[6,7,25,33–35]. The aim of this study was to compare the transcriptomic characteristics of FMC tissues, derived FMC cell lines and healthy mammary tissues in order to identify deregulated genes, possible therapeutic targets, and enriched biological processes and molecular pathways characterising the FMCs dysregulation.

Results

Animals and samples. Tumour and healthy mammary tissue samples from 33 female cats diagnosed with FMCs were included. In those cases, in which FFPE and FT neoplastic samples were available (n = 8), FT samples were preferred for RNA sequencing, in the remaining cases (n = 25) FFPE samples were selected for RNA isolation and sequencing.

After microscopic evaluation, healthy tissue was identified in 12 cases, in which healthy tissue was separated by macrodissection using a 4-mm-diameter punch biopsy instrument. Thus FFPE samples (n = 37) included 25 neoplastic samples and 12 healthy mammary tissue samples. FT samples (n = 9) included 8 neoplastic and one healthy mammary tissue sample. Additionally, three samples from two different previously stablished neoplastic cell lines were included (TiHo-0906 passage 7 and 77[27], and TiHo-1605 passage 8). Cell lines included were derived from two of the patients enrolled in this study. A detailed description of animals and samples included is depicted in Table 1

Breed	Age (years)	Tumour size [13]	Lymph node invasion	Clinical Stage [13]	Type of sample	Diagnosis	HMG [36,37]
DSH	16	T2	Y	3	FT	TC	II
DSH	10	T2	Y	3	FT	TC	II
Norwegian Forest	14	T3	N	3	FT	TC	III
DSH	20	T3	Y	3	FT	TC	II
British shorthair	13	T3	Y	3	FT***	TC	III
DSH	13	T3	N	3	FT	TC	I
Norwegian forest	12	T1	Y	3	FT	SC	III
DSH	8	T2	Y	3	FT**,****	SC	II
DSH	11	T1	Y	3	FFPE*	TC	I
DSH	14	T1	N	1	FFPE*	TC	II
DSH	13	T1	N	1	FFPE*	TC	I
Abyssinian	9	T2	N	2	FFPE*	TC	II
DSH	16	T2	N	2	FFPE*	TC	I
DSH	11	T1	N	1	FFPE	CC	I
Siamese	15	T2	Y	3	FFPE	SC	II
DSH	17	T3	Y	3	FFPE*	CC	III
Chartreux	14	T3	Y	3	FFPE*	SC	III
Chartreux	13	T3	Y	3	FFPE*	CC	I
DSH	10	T3	Y	3	FFPE*	CC	III
DSH	8	T1	N	1	FFPE*,†	TC	III
DSH	14	T1	N	1	FFPE*,†	TC	II
DSH	6	T1	N	1	FFPE*,†	IPC	III
DSH	13	T1	N	1	FFPE†	IPC	I
DSH	11	T1	N	1	FFPE†	TC	I
Persian	11	T1	N	1	FFPE†	IPC	I
DSH	13	T1	N	1	FFPE†	IPC	II
DSH	16	T2	Y	3	FFPE†	TC	II
DSH	13	T2	Y	3	FFPE†	TC	II
DSH	15	T2	N	2	FFPE†	TC	III
DSH	13	T2	Y	3	FFPE†	TC	I
Norwegian Forest	17	T3	Y	3	FFPE†	TC	I

DSH	7	T_3	N	3	FFPE†	TC	I
Maine coon	9	T_3	N	3	FFPE†	TC	I
DSH, Domestic Shorthair; T_1, < 2 cm; T_2, 2-3 cm; T_3, > 3 cm; N, no; Y, yes; TC, tubulopapillary carcinomas; IPC, intraductal papillary carcinomas; SC, solid carcinomas; and CC, comedocarcinomas. *FFPE control, **FT control, ***TiHo-0906 cell line derived, ****TiHo-1605 cell line derived, †neoplastic FFPE sample not suitable for sequencing due to low RNA quality							

Table 1. Characteristics of cats and samples included in this study.

Histopathological examination and Immunohistochemistry. Histopathologically, twenty-one cats had tubulopapillary carcinomas (TC); four cats, intraductal papillary carcinomas (IPC); four cats, solid carcinomas (SC); and four cats, comedocarcinomas (CC). Thirteen tumours were histologically graded as HMG I, 11 as HMG II, and nine as HMG III. All tumours were positive to the epithelial markers E-cad, CK 8/18 and Pan-CK. A variable expression of the mesenchymal markers (CALP, SMA and Vim) and basal marker P63 was observed in all tumours; however, in TCs and IPCs positive cells were always detected at a basal location and interlobular regions. In contrast, SCs and CCs showed a diffuse pattern of expression with a variable grade of intensity. Luminal expression of Vim was detected in eight cases with TCs and two with IPCs.

RNA isolation and sequencing. The amount of RNA isolated from FFPE samples (n = 37; 25 neoplastic and 12 healthy) varied broadly, ranging from 96.4 to 36744.8 ng (mean [SD]: 10487 [11426.9] ng). RNA yields from FT samples (n = 9) ranged from 1691.7 to 19973.2 ng (mean [SD]: 8927.9 [5157.1] ng). On the other hand, RNA yields from cell line samples (n = 3) were in general more consistent, ranging from 89456.2 to 92350.2 ng (mean [SD]: 91004.7 [1190.2] ng). Despite the differences in RNA amount, a 260/280 ratio of ~2 was observed in all samples.

RNA integrity number (RIN) values for FFPE samples (n = 37; 25 neoplastic and 12 healthy) were low, ranging from 1.3 to 2.5 (mean [SD]: 2.1 [0.3]), samples with the lowest RIN values were excluded from library preparation and sequencing. Since it was impossible to obtain high quality RNA from FFPE samples, those with the higher RIN values (n = 23; 11 neoplastic and 12 healthy) were selected, and libraries were prepared using 5-fold of the usual input amount, the remaining samples (14 FFPE neoplastic samples) were excluded from RNA sequencing (Details in Table 1). Afterward, library material was sequenced. All RIN values for frozen tissue (6.5–9, mean [SD]: 7.9 [0.8]) and cell line samples (9–9.4, mean [SD]: 9.2 [0.2]) were good and within the recommended range of 6–9. After mapping to the feline genome, read count for annotated genes were obtained using the Gage-R package. Subsequently read counts for all protein-coding genes were analysed using the Edge-R package.

Multi-dimensional scaling plots. Analyses started with the generation of multi-dimensional scaling (MDS) plots (Fig. 1). Three well differentiated neoplastic clusters were observed (FT = 8, FFPE = 8, and cell lines = 3). One cluster included only healthy samples (FFPE = 4 and FT = 1); however, the FT healthy sample included in this cluster was a little bit apart from the FFPE healthy samples.

We identified a mixed cluster containing FFPE neoplastic and healthy samples all samples included in this cluster were excluded from differential gene expression analyses. The diversity of histologic features of FMCs included in this study was not reflected at the MDS plot.

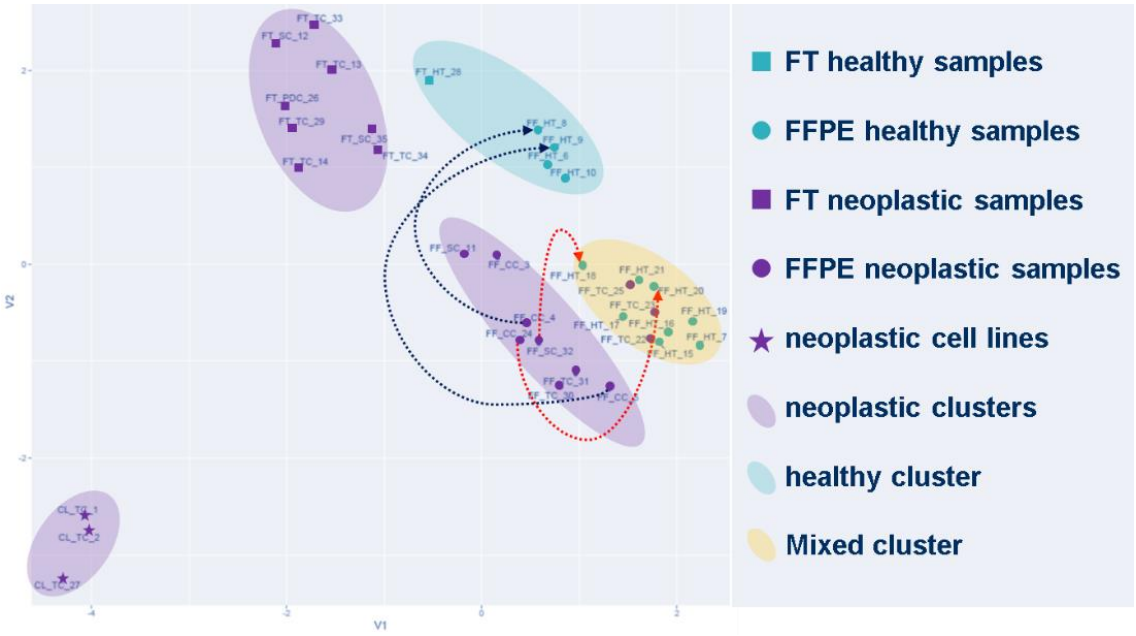

Figure 1. MDS analysis of the expression profiles of healthy and neoplastic feline mammary samples. Dashed arrows indicate FFPE sample pairs (neoplastic and healthy tissue from the same animal). FFPE healthy samples in the yellow mixed cluster have their respective neoplastic counterpart very close (red dashed arrows). Healthy FFPE samples in the green cluster are far from their respective neoplastic counterpart (blue dashed arrows). Cell line samples (stars) cluster together and apart from all other samples.

Expression changes of individual genes between neoplastic and healthy mammary tissues. DEG comparisons for different histological diagnoses were skipped, because no separation/clustering was observed in the MDS plot. An additive model was fitted that adjusts for any differences between the FFPE and FT samples. We identified 3416 DEGs ($p < 0.05$) between neoplastic and healthy samples (FFPE and FF). Among those 881 genes (321 up- and 560 downregulated) showed a False Discovery Rate (FDR) < 0.05; the top 10 up- and downregulated genes are listed in Table 2. Among DEGs (FDR < 0.05) we detected eight upregulated (*ASPM*, *KIF4A*, *IQGAP3*, *FOXM1*, *NEK2*, *NUF2*, *KIF2C* and *MYBL2*) and nine downregulated (*AQP7*, *PCK1*, *GPD1*, *ADIPOQ*, *LEP*, *PLIN1*, *ATP1A2*, *CD300LG* and *HSPB7*) genes of the previously reported top-25 over- and under-expressed genes in human TNBC (hTNBC)[38] (Table 2).

Gene name	Gene Symbol	FDR
Top 10 upregulated genes		
BRCA1, DNA repair associated	*BRCA1*	5.02E-04
cell division cycle 25C	*CDC25C*	5.69E-04
citron rho-interacting serine/threonine kinase	*CIT*	7.68E-04
epithelial cell transforming 2	*ECT2*	1.45E-03
cytoskeleton associated protein 2	*CKAP2*	1.65E-03
abnormal spindle microtubule assembly	*ASPM*	1.83E-03
sperm associated antigen 5	*SPAG5*	2.08E-03
Rac GTPase activating protein 1	*RACGAP1*	2.31E-03
TPX2, microtubule nucleation factor	*TPX2*	2.68E-03
CTP synthase 1	*CTPS1*	2.77E-03
Top 10 downregulated genes		
tenascin XB	*TNXB*	1.46E-04
latent transforming growth factor beta binding protein 4	*LTBP4*	2.23E-04
four and a half LIM domains 1	*FHL1*	2.23E-04
scavenger receptor class A member 5	*SCARA5*	2.75E-04
Gelsolin	*GSN*	5.02E-04
protein phosphatase 1 regulatory subunit 15A	*PPP1R15A*	5.69E-04
leiomodin 1	*LMOD1*	5.69E-04
cell death inducing DFFA like effector a	*CIDEA*	5.69E-04
SAM and SH_3 domain containing 1	*SASH1*	7.35E-04
C1q and TNF related 2	*C1QTNF2*	7.68E-04
FDR, False Discovery Rate		

Table 2. Top 10 up- and downregulated genes between neoplastic and healthy mammary tissues.

Clustering analysis of differentially expressed genes between neoplastic and healthy mammary tissues. Differentially expressed genes (FDR <0.05) were analysed with the DAVID online tool to identify possible enriched KEGG pathways (Kyoto Encyclopaedia of Genes and Genomes). We identified important cancer-related genes (e.g. *LAMA3, FLT4, PDGFD and BRCA1)* participating in the intracellular cell cycle regulator signalling pathway PI3K-Akt. Additionally, we detected various genes (e.g. *CD36 CPT1A* and *PCK1*) participating in different pathways linked to cellular lipid metabolism endocrine regulation (PPAR signalling pathway) and maintenance of glucose homeostasis (glucagon signalling and insulin resistance pathways). Moreover, additional genes (e.g. *LAMB2*, *LAMA3*, *CD34* and *CLDN5*) related to focal and cell adhesion were detected. To determine the role of up- and downregulated genes in specific KEGG pathways, an independent analysis including only up- or downregulated genes was performed. Upregulated genes were mainly involved in cell cycle regulation and p53 signalling pathways (e.g. *CDK1, CHEK1, CCNB1* and *CCNB2*). Additional upregulated genes enriched pathways also related to DNA replication and repair (e.g. *DNA2, POLA1, MCM3* and *MCM4*), and nucleotide metabolism (e.g. *DCK* and *TK1*).

On the other hand, downregulated genes enriched different pathways related to environmental adaptation (e.g. *CRY2 and NR1D1*), cellular interaction (e.g. *VEGFC, JUN, FLT4, PDGFD, CLDN5* and *ACTN3*), endocrine regulation (e.g. *CD36 CPT1A* and *PCK1*), and signal transduction (e.g. *BMP4, DCN, ID3*, and *SMAD1*), details in Table 3.

Biological process	KEGG pathway	Count	Genes	*p*-value	FDR
All differentially expressed genes					
Signal transduction	PI3K-Akt signalling pathway	9	*LAMB2, LAMA3, FLT4, FGF10, PDGFD, BRCA1, GHR, PCK1, KDR*	0.02	21.8
Endocrine regulation	PPAR signalling pathway	4	*CD36, FABP4, CPT1A, PCK1*	0.03	31.6
	Insulin signalling pathway	5	*PYGM, SOCS2, TRIP10, LIPE, PCK1*	0.01	42.1
	Glucagon signalling pathway	5	*CD36, PYGM, PGAM2, CPT1A, PCK1*	0.01	56.1
	Insulin resistance	4	*CD36, PYGM, CPT1A, PCK1*	0.01	69.9
Cellular interaction	Focal adhesion	6	*LAMB2, LAMA3, FLT4, JUN, PDGFD, KDR*	0.01	48.3
	Cell adhesion molecules (CAMs)	5	*CD34, CLDN5, PECAM1, ESAM, JAM2*	0.01	55.1
Cancer	Pathways in cancer	8	*BMP4, FOS, FZD10, LAMB2, LAMA3, MSH2, JUN, FGF10*	0.02	70.9
Upregulated genes					
Cell growth and death	Cell cycle	17	*E2F1, ANAPC1, E2F2, CDK1, E2F3, TTK, ESPL1, CHEK1, CDC25C, MCM3, MCM4, CDC25A, CCNB1, CDC45, CCNB2, BUB1, BUB1B*	9.34E-13	9.36E-10
	p53 signalling pathway	5	*CCNB1, CDK1, CCNB2, RRM2, CHEK1*	0.009	9.2
DNA replication and repair	DNA replication	4	*DNA2, POLA1, MCM3, MCM4*	0.009	9.2
	Pyrimidine metabolism	6	*RRM2, DCK, POLA1, CMPK1, TK1, TYMS*	0.02	25.8
Downregulated genes					
Environmental adaptation	Circadian rhythm	5	*CRY2, NR1D1, PER2, PER1, ARNTL*	5.94E-04	0.6
Cellular interaction	Focal adhesion	14	*LAMA2, VEGFC, CAV1, LAMA3, TNXB, LAMB2, MYL2, JUN, FLT4, MYLPF, ACTN3, PDGFD, ZYX, KDR*	0.01	13.3
	Tight junction	9	*PPP2R1B, EPB41L3, MYL2, MYH2, CLDN5, MYH11, MYLPF, ACTN3, JAM2*	0.05	53.6
Endocrine regulation	PPAR signalling pathway	7	*CD36, PLIN1, FABP4, AQP7, ADIPOQ, CPT1A, PCK1*	0.02	23.4
	Adipocytokine signalling pathway	6	*LEP, CD36, ACACB, ADIPOQ, CPT1A, PCK1*	0.06	53
Signal transduction	TGF-beta signalling pathway	7	*BMP4, PPP2R1B, ID1, RPS6KB2, DCN, ID3, SMAD1*	0.06	51.2
KEGG, Kyoto Encyclopaedia of Genes and Genomes; FDR, False Discovery Rate					

Table 3. KEGG pathway analysis for differentially expressed genes between neoplastic and healthy mammary samples. Data analysed with DAVID Bioinformatics.

Clustering analysis of differentially expressed genes between cell lines and healthy mammary tissues. We identified 9596 genes differentially expressed ($p < 0.05$) between cell lines and healthy samples (FFPE and FF). Among those 8304 showed an FDR < 0.05, and 6114 genes (2356 up- and 3758 downregulated) FDR < 0.01. Differentially expressed upregulated genes (FDR < 0.01) were primarily related to cell cycle regulation (e.g. *TGFB2*, *MYC*, *CCND1*, *CHEK1*, *TP53* and *CDK4*) carbohydrate (e.g. *MDH1* and *ENO1)*, amino acid (e.g. *BCAT1*) and lipid metabolism (e.g. *SCD* and *TECR*). Additionally, we identified different upregulated genes participating in DNA replication and repair (e.g. *RFC3*, *AK2* and *NUDT5*), and pathways related to specific types of human cancers such as *COL4A2*, *COL4A1*, *THBS1*, *MMP1*, *WNT11* and *AKT1*; details in Supplementary table 1. On the other hand, downregulated genes were mainly involved in signal transduction (e.g. *EGFR*, *PDGFRA*, *PTK2B*, *AKT3*, *SOCS2* and *KRAS*), immune response (e.g. *VWF*, *VEGFC*, *KIT* and *STAT3*), cellular interaction (e.g. COL1A2 DOCK1 EGF), tight junction components (e.g. CLDN4, CLDN5 CLDN7, CLDN8), and motility (e.g. *FGFR1*, *APC* and *ITGB2*); Details in Supplementary table 2.

Discussion

In this study, the transcriptome characteristics of FMCs and derived cell lines are described for the first time. In agreement with previous studies in human[5,15,39] and canine mammary cancers[40], important cancer-related genes such as *LAMA3*, *FLT4*, *PDGFD* and *BRCA1* participating in the PI3K-Akt signalling pathway were differentially expressed between FMCs and healthy mammary tissues. Previous studies in FMCs[9,41] have demonstrated a significant correlation between distinctive immunohistochemical expression levels of important members of this pathway (e.g. AKT and PTEN) and tumour malignancy and poor histological differentiation. Our results now provide evidence about the importance of different possible therapeutic targets participating in this pathway. Similarities between the expression profiles of FMCs and those previously reported in hTNBCs were observed in this study, including the identification of eight commonly upregulated genes (i.e. *ASPM*, *KIF4A*, *IQGAP3*, *FOXM1*, *NEK2*, *NUF2*, *KIF2C* and *MYBL2*), and nine commonly downregulated genes (i.e. *AQP7*, *PCK1*, *GPD1*, *ADIPOQ*, *LEP*, *PLIN1*, *ATP1A2*, *CD300LG* and *HSPB7*) in hTNBCs[38].

Upregulated genes in FMC tissues including *CDK1*, *CCNB2*, *RRM2* and *CHEK1* were mainly involved in processes related to cell growth and death regulation, highlighting the importance of the p53 signalling pathway in FMCs elicitation. This characteristic expression pattern was furthermore observed in the derived FMC cell lines analysed, where additional upregulated genes (e.g. *TGFB2*, *MYC*, *CCND1*, *CHEK1*, *TP53* and *CDK4*) participating in cell cycle regulation and p53 signalling pathway were detected. Similarly, additional pathways related to DNA replication and repair were significantly upregulated in FMC tissues and derived cell lines including previously reported upregulated genes in human breast cancer (e.g. *MCM2*, *RRM1*, *RRM2* and *TYMS*)[42–45]. Genes such as *RRM1*, *RRM2* and *TYMS* participate in the reprogramming of metabolic pathways associated to nucleotide synthesis and their upregulation have been correlated with tumour progression in a variety of human cancers including breast cancer[45–47].

Interestingly, the upregulation of *RRM2* have been observed in isolated circulating tumour cells (CTCs) from woman with metastatic breast cancer suggesting a potential role as biomarker[48]. Furthermore, therapeutic strategies like the mediated siRNA silencing of *RRM2* by systemic delivery of a nanoparticles suppresses head and neck tumour growth[47] and *RRM2* knockdown in head and neck squamous cell carcinoma (HNSCC) and non-small cell lung cancer (NSCLC) cell lines induces apoptosis[45]. Cell lines included in this study may be suitable models for the *in vitro* testing of this therapeutic strategy in FMCs.

Additional metabolic pathways (e.g. Glycolysis—Gluconeogenesis, Oxidative phosphorrylation, etc.) were only upregulated in derived cell lines. Metabolic phenotypes observed in cell lines may be influenced as an adaptive response to culture environment and do not necessarily reflect the original tumour metabolic profile[49]. However, considering the small sample size and the influence of RNA quality of the neoplastic tissues included in this study (especially FFPE samples) differences between FMCs and derived cell lines transcriptomic characteristics must be carefully interpreted. On the other hand, pathways related to endocrine regulation of neoplastic progression (e.g. PPAR signalling pathway, insulin signalling pathway, etc.) that were significantly enriched with differentially expressed genes in the FMC tissues were not significantly altered in the cell lines.

FMC tissues included in this study showed a significant downregulation of the circadian rhythm KEGG pathway—characteristic that was not observed in the cell lines analysed. Similar findings were recently detected in lymphomas[25]. Recent studies support the theory that genetic disruption of key components (e.g. *CRY2, PER2*) of the clock mechanism in combination with specific metabolic alterations may increase tumourigenesis do to alterations in the cell cycle[50–52]. However, the specific mechanisms underlying this process in distinct types of cancer are still unravelled.

Pathways involved in maintenance of tissue architectural structure (e.g. focal adhesion and tight junction) were enriched with downregulated genes in both, FMC tissues and derived cell lines. Different studies using several approaches have associated this characteristic with an inability to prevent tumour dissemination[25,53,54], and with epithelial to mesenchymal transition (EMT)[27,55,56] in different types of human and animal tumours. Additional related pathways (i.e. cell adhesion molecules (CAMs), cytokine-cytokine receptor interaction, ECM-receptor interaction, Gap junction and regulation of actin cytoskeleton) were significantly downregulated in the cell lines evaluated. Furthermore, the transcriptomic profile of FMC tissues and cell lines included in this study revealed a significant downregulation of various members of the claudin family including *CLDN4, CLDN5 CLDN7* and *CLDN8*. Similar findings were previously reported by immunohistochemical profiling of FMC tissues[10,54,57] and CNV analysis of a FMC-derived cell line (TiHo-0906, also included in this study)[27], our results now provide new evidences confirming the similarities between FMCs and claudin-low human breast cancer.

A considerable amount of FFPE samples were excluded from DEG analyses due to lack of similarity between biological replicates and RNA quality. It is unclear whether the macrodissection technique employed was not useful to completely separate healthy from tumour tissue during sampling, or of those areas of microscopically confirmed healthy tissue have already undergone molecular neoplastic changes not reflected in their morphology. Transcriptomic studies using a small sample size often lack reproducibility, validation of the present findings using independent external data and preferably only FF samples would be advisable in order to increase statistical power.

Our results confirm that massive parallel RNA sequencing can be reliably used to identify pivotal biological processes in FMCs, and moreover to determine important target genes susceptible of therapeutic intervention. Furthermore, transcriptomic profile comparison of FMC tissues with derived cell lines provide important information about which aspects of the neoplastic change can be reliably modelled *in vitro* and also denote important constraints.

Methods

Animals and samples. In this study, tumour and healthy mammary tissue samples (FFPE and/or FT) from female cats treated for FMC by surgery at the Small Animal Clinic of the University of Veterinary Medicine Hannover between 2000 and 2016 were included. Cats, ranging in age from 6 to 20 years were diagnosed and surgically treated by uni- or bi-lateral chain mastectomy. FFPE samples were retrieved from the archives of the Institute for Pathology, and FT samples from the frozen-tissue bank of the Small Animal Clinic, University of Veterinary Medicine Hannover. All samples were collected during medically necessary mastectomy after owner's written consent. Therefore, this study was not considered an animal experiment according to the German Animal Welfare Act and an ethical approval was not required.

Histopathological examination and Immunohistochemistry. Tumour FFPE samples were sliced into 4 µm-thick sections and stained with haematoxylin eosin (H&E) for histopathologic evaluation and histological grading. The histopathological diagnosis was conducted following the WHO classification [58], the HMG was calculated as described elsewhere [36,37]. H&E-stained sections from all available FFPE blocks of patients included in this study were examined under light microscopy to determine the presence of healthy mammary tissue that could be used as control for transcriptomic analyses.

The immunoexpression of E-cad, CK8/18, pan-CK, CK14, CK5/6, p63, SMA, CALP, Vim, CD44, ER, PR, HER-2, COX-2, p53, CLDN-2 and proliferation marker Ki-67 was evaluated by the avidin-biotin complex technique as previously described[59] (details in Table 4). No animal was killed for the generation of positive controls, all tissue specimens used as positive controls for this study were sent to the department of pathology for diagnosis. Negative controls included normal serum and isotype control antibodies (details in Supplementary table 3).

Antibody	Type	Clone	Company
E-cad	mouse anti-human*	36/E-cad	BD Biosciences
CK8/18	mouse anti-human*	5D3	Novocastra
pan-CK	mouse anti-human*	AE1&AE3	Dako
CK14	rabbit anti-human**	—	Thermo Fischer Scientific
CK5/6	mouse anti-human*	D5/16B4	Dako
p63	mouse anti-human*	4A4	Biologo
SMA	mouse anti-human*	1A4	Dako
CALP	mouse anti-human*	CALP	Dako
Vim	mouse anti-human*	V9	Dako
CD44	Rat anti-mouse CD44*	IM7	Bio-Rad Laboratories
ER	mouse anti-human*	6F11	AbD Serotec
PR	mouse anti-human*	10A9	Immunotech
HER-2	mouse anti-human*	CB11	Novocastra
COX-2	goat polyclonal IgG	—	Santa Cruz
p53	mouse anti-human*	DO-1	AbD Serotec
CLDN-2	mouse anti-human*	12H12	Thermo Fischer Scientific
Ki-67	mouse anti-human*	MIB-1	Dako

Table 4. Antibodies used in this study. *Monoclonal Antibody, **Polyclonal Antibody.

RNA isolation and sequencing. FFPE samples were sliced into four 10-µm-thick sections with a microtome (pfm Slide 2003, pfm medical ag). FFPE sections were deparaffinised and RNA was isolated with the AllPrep DNA/RNA FFPE kit (QIAGEN) following the manufacturer's instructions. In cases in which healthy and neoplastic mammary tissue were present in the same FFPE block, healthy tissue was separated by macrodissection using a 4-mm-diameter punch biopsy instrument. To increase the amount of sample material, grossly macrodissected 4-mm-diameter sections were sliced up to 20 times into 10-µm-thick sections. Samples were deparaffinised and RNA was subsequently isolated as described above. Afterwards, H&E-stained tissue sections from FFPE blocks—where healthy tissue was macrodissected—were microscopically evaluated to confirm the presence of healthy tissue in the macrodissected regions.

One 10-mg-tissue-section was dissected from each FT sample using a sterile scalpel blade and placed into a tube. Afterwards, tissue sections were homogenized with a TissueLyser (II—5 mm stainless steel bead, QIAGEN) and RNA was subsequently isolated using the AllPrep DNA/RNA Mini Kit (QIAGEN) following the manufacturer's instructions. RNA samples were stored at -80°C until use. In those cases, in which FFPE and FT neoplastic samples were available, FT samples were preferred for RNA sequencing.

Data and Statistical analyses. After mapping to the feline genome, read counts for annotated genes were obtained using the Gage-R package (http://bioconductor.org/packages/gage/package). Subsequently, read counts for all protein-coding genes were analysed using the Edge-R package (http://bioconductor.org/packages/edgeR/). Analyses started with the generation of MDS plots to obtain an overview of homogeneity among the different samples groups (FFPE, FT, and cell lines). Two types of DEG analyses were conducted; first, an additive model was fitted that adjusts for any differences between the FFPE and FT samples

This analysis only detects genes differentially expressed between tumour (FFPE and FT) and control (FFPE and FT) groups after adjusting for the differences between FFPE and FT samples. Second, a classic group comparison without adjusting for specimen type was performed with tumour (FFPE and FT) or control (FFPE and FT) as single covariate. Additionally, the same type of analyses were conducted to identify DEG between cell lines and control samples (FFPE and FT). Afterwards, differentially expressed genes with FDR < 0.05 were uploaded to the DAVID Bioinformatics server (http://david.abcc.ncifcrf.gov), which was employed to identify enriched pathways (from the Kyoto encyclopaedia of genes and genomes [KEGG]) and for functional annotation clustering analyses. Additionally, up- and downregulated genes were compared with those previously reported as poor survival indicators in human breast cancers using UALCAN online tool (http://ualcan.path.uab.edu/)[38].

References

1. Ellis, M. J. *et al.* Whole-genome analysis informs breast cancer response to aromatase inhibition. *Nature* **486,** 353–360 (2012).
2. Nik-Zainal, S. *et al.* Mutational processes molding the genomes of 21 breast cancers. *Cell* **149,** 979–993 (2012).
3. Jonsson, G. *et al.* High-resolution genomic profiles of breast cancer cell lines assessed by tiling BAC array comparative genomic hybridization. *Genes. Chromosomes Cancer* **46,** 543–558 (2007).
4. Weigelt, B. *et al.* Metastatic breast carcinomas display genomic and transcriptomic heterogeneity. *Mod. Pathol.* **28,** 340–351 (2015).
5. Hennessy, B. T. *et al.* Characterization of a naturally occurring breast cancer subset enriched in epithelial-to-mesenchymal transition and stem cell characteristics. *Cancer Res.* **69,** 4116–4124 (2009).
6. Horpaopan, S. *et al.* Genome-wide CNV analysis in 221 unrelated patients and targeted high-throughput sequencing reveal novel causative candidate genes for colorectal adenomatous polyposis. *Int. J. Cancer* **136,** E578–E589 (2015).
7. Blighe, K. *et al.* Whole genome sequence analysis suggests intratumoral heterogeneity in dissemination of breast cancer to lymph nodes. *PLoS One* **9,** 1–11 (2014).
8. Zappulli, V. *et al.* Prognostic Evaluation of Feline Mammary Carcinomas: A Review of the Literature. *Vet. Pathol.* **52,** 46–60 (2015).
9. Hughes, K. & Dobson, J. M. Prognostic histopathological and molecular markers in feline mammary neoplasia. *Vet. J.* **194,** 19–26 (2012).
10. Adega, F., Borges, A. & Chaves, R. Cat Mammary Tumors: Genetic Models for the Human Counterpart. *Vet. Sci.* **3,** 17 (2016).
11. MacEwen, E. G. Spontaneous tumors in dogs and cats: models for the study of cancer biology and treatment. *Cancer Metastasis Rev.* **9,** 125–36 (1990).
12. Borrego, J. F., Cartagena, J. C. & Engel, J. Treatment of feline mammary tumours using chemotherapy, surgery and a COX-2 inhibitor drug (meloxicam): a retrospective study of 23 cases (2002-2007)*. *Vet. Comp. Oncol.* **7,** 213–21 (2009).
13. McNeill, C. J. *et al.* Evaluation of adjuvant doxorubicin-based chemotherapy for the treatment of feline mammary carcinoma. *J. Vet. Intern. Med.* **23,** 123–9 (2009).
14. Stephens, P. J. *et al.* Complex landscapes of somatic rearrangement in human breast cancer genomes. *Nature* **462,** 1005–1010 (2009).
15. Showler, K. *et al.* Analysis of genes involved in the PI3K/Akt pathway in radiation- and MNU-induced rat mammary carcinomas. *J. Radiat. Res.* **58,** 183–194 (2016).
16. Badve, S. *et al.* Basal-like and triple-negative breast cancers: a critical review with an emphasis on the implications for pathologists and oncologists. *Mod. Pathol.* **24,** 157–67 (2011).
17. Hennessy, B. T. *et al.* Characterization of a naturally occurring breast cancer subset enriched in epithelial-to-mesenchymal transition and stem cell characteristics. *Cancer Res.* **69,** 4116–4124 (2009).
18. Prat, A. *et al.* Phenotypic and molecular characterization of the claudin-low intrinsic subtype of breast cancer. *Breast Cancer Res.* **12,** R68 (2010).

19. Burrai, G. P. *et al.* Spontaneous feline mammary intraepithelial lesions as a model for human estrogen receptor- and progesterone receptor-negative breast lesions. *BMC Cancer* **10,** 156 (2010).
20. Sorenmo, K. U., Worley, D. R. & Goldschmidt, M. H. in *Withrow and MacEwen's Small Animal Clinical Oncology* (eds. Withrow, S. & MacEwen, E. G.) 538–556 (Elsevier, 2013). doi:10.1016/B978-1-4377-2362-5.00027-X
21. Novosad, C. A. *et al.* Retrospective evaluation of adjunctive doxorubicin for the treatment of feline mammary gland adenocarcinoma: 67 cases. *J. Am. Anim. Hosp. Assoc.* **42,** 110–20 (2006).
22. Cunha, S. C., Corgozinho, K. B., Souza, H. J., Silva, K. V. & Ferreira, A. M. R. Adjuvant chemotherapy with mitoxantrone for cats with mammary carcinomas treated with radical mastectomy. *J. Feline Med. Surg.* 1–5 (2015). doi:10.1177/1098612X14567159
23. Hayes, A. A. & Mooney, S. Feline mammary tumors. *Vet. Clin. North Am. Small Anim. Pract.* **15,** 513–20 (1985).
24. Prat, A. *et al.* Characterization of cell lines derived from breast cancers and normal mammary tissues for the study of the intrinsic molecular subtypes. *Breast Cancer Res. Treat.* **142,** 237–55 (2013).
25. Taher, L. *et al.* Comparative High-Resolution Transcriptome Sequencing of Lymphoma Cell Lines and de novo Lymphomas Reveals Cell-Line-Specific Pathway Dysregulation. *Sci. Rep.* **8,** 1–12 (2018).
26. Borges, A., Adega, F. & Chaves, R. Establishment and characterization of a new feline mammary cancer cell line, FkMTp. *Cytotechnology* **68,** 1529–43 (2016).
27. Granados-Soler, J. L. *et al.* TiHo-0906: a new feline mammary cancer cell line with molecular, morphological, and immunocytological characteristics of epithelial to mesenchymal transition. *Sci. Rep.* **8,** 13231 (2018).
28. Minke, J. M. *et al.* Isolation of two distinct epithelial cell lines from a single feline mammary carcinoma with different tumorigenic potential in nude mice and expressing different levels of epidermal growth factor receptors. *Cancer Res.* **51,** 4028–37 (1991).
29. Muleya, J. S. *et al.* Establishment and characterization of a new cell line derived from feline mammary tumor. *J. Vet. Med. Sci.* **60,** 931–5 (1998).
30. Uyama, R. *et al.* Establishment and characterization of eight feline mammary adenocarcinoma cell lines. *J. Vet. Med. Sci.* **67,** 1273–6 (2005).
31. Barbieri, F. *et al.* Isolation of stem-like cells from spontaneous feline mammary carcinomas: Phenotypic characterization and tumorigenic potential. *Exp. Cell Res.* **318,** 847–860 (2012).
32. Pang, L. Y. *et al.* Feline mammary carcinoma stem cells are tumorigenic, radioresistant, chemoresistant and defective in activation of the ATM/p53 DNA damage pathway. *Vet. J.* **196,** 414–423 (2013).
33. Pongor, L. *et al.* A genome-wide approach to link genotype to clinical outcome by utilizing next generation sequencing and gene chip data of 6,697 breast cancer patients. *Genome Med.* **7,** 1–11 (2015).
34. Huang, D. W., Sherman, B. T. & Lempicki, R. A. Systematic and integrative analysis of large gene lists using DAVID bioinformatics resources. *Nat. Protoc.* **4,** 44 (2008).
35. Gao, Y. *et al.* Cross-validation of genes potentially associated with overall survival and drug resistance in ovarian cancer. *Oncol. Rep.* **37,** 3084–3092 (2017).
36. Elston, C. & Ellis, I. Pathological prognostic factors in breast cancer. I. The value of histological grade in breast cancer: experience from a large study with long-term follow-up. *Histopathology* **19,** 403–410 (1991).
37. Castagnaro, M. *et al.* Tumour grading and the one-year post-surgical prognosis in feline mammary carcinomas. *J. Comp. Pathol.* **119,** 263–75 (1998).
38. Chandrashekar, D. S. *et al.* UALCAN : A Portal for Facilitating Tumor Subgroup Gene Expression. *Neoplasia* **19,** 649–658 (2017).
39. Mutlu, M. *et al.* MiR-564 acts as a dual inhibitor of PI3K and MAPK signaling networks and inhibits proliferation and invasion in breast cancer. *Sci. Rep.* **6,** 1–14 (2016).
40. Beck, J. *et al.* Genome Aberrations in Canine Mammary Carcinomas and Their Detection in Cell-Free Plasma DNA. **8,** (2013).
41. Maniscalco, L. *et al.* Activation of AKT in feline mammary carcinoma: a new prognostic factor for feline mammary tumours. *Vet. J.* **191,** 65–71 (2012).
42. Norton, N. *et al.* Assessment of tumor heterogeneity, as evidenced by gene expression profiles, pathway activation, and gene copy number, in patients with multifocal invasive lobular breast tumors. *PLoS One* **11,** 1–20 (2016).

43. Meißner, T. *et al.* Metastatic triple-negative breast cancer patient with TP53 tumor mutation experienced 11 months progression-free survival on bortezomib monotherapy without adverse events after ending standard treatments with grade 3 adverse events. *Cold Spring Harb. Mol. case Stud.* **3,** 1–23 (2017).
44. Dong, Z. & Zhang, J. T. Initiation factor eIF3 and regulation of mRNA translation, cell growth, and cancer. *Crit. Rev. Oncol. Hematol.* **59,** 169–180 (2006).
45. Rahman, M. A. *et al.* RRM2 Regulates Bcl-2 in Head and Neck and Lung Cancers: A Potential Target for Cancer Therapy. *Clin Cancer Res.* **19,** 3416–3428 (2014).
46. Furuta, E., Okuda, H., Kobayashi, A. & Watabe, K. Metabolic genes in cancer: their roles in tumor progression and clinical implications. *Biochim Biophys Acta* **1805,** 141–152 (2011).
47. Rahman, M. A. *et al.* Systemic Delivery of siRNA-Nanoparticles Targeting RRM2 Suppresses Head and Neck Tumor Growth. *J Control Release.* **159,** 384–392 (2013).
48. Lang, J. E. *et al.* Expression profiling of circulating tumor cells in metastatic breast cancer Julie. *Breast Cancer Res Treat.* **149,** 121–131 (2016).
49. Young, J. Metabolic flux rewiring in mammalian cell cultures. *Curr Opin Biotechnol* **24,** 1–16 (2014).
50. Huber, A. L. *et al.* CRY2 and FBXL3 Cooperatively Degrade c-MYC. *Mol. Cell* **64,** 774–789 (2016).
51. Su, X. *et al.* The circadian clock gene PER2 plays an important role in tumor suppression through regulating tumor-associated genes in human oral squamous cell carcinoma. 472–480 (2017). doi:10.3892/or.2017.5653
52. Masri, S. & Sassone-corsi, P. The emerging link between cancer, metabolism, and circadian rhythms. *Nat. Med.* **24,** (2018).
53. Tökés, A. M. *et al.* Expression of tight junction molecules in breast carcinomas analysed by array PCR and immunohistochemistry. *Pathol. Oncol. Res.* **18,** 593–596 (2012).
54. Flores, A. R., Rêma, A., Carvalho, F., Faustino, A. & Dias Pereira, P. Reduced expression of claudin-2 is associated with high histological grade and metastasis of feline mammary carcinomas. *J. Comp. Pathol.* **150,** 169–74 (2014).
55. Thiery, J. P. & Huang, R. Linking epithelial-mesenchymal transition to the well-known polarity protein par6. *Dev. Cell* **8,** 456–458 (2005).
56. Cursons, J. *et al.* Stimulus-dependent differences in signalling regulate epithelial-mesenchymal plasticity and change the effects of drugs in breast cancer cell lines. *Cell Commun. Signal.* **13,** 26 (2015).
57. Caliari, D. *et al.* Triple-negative vimentin-positive heterogeneous feline mammary carcinomas as a potential comparative model for breast cancer. *BMC Vet. Res.* **10,** 1–12 (2014).
58. Misdorp, W., Else, R., Hellmen, E. & Lipscomb, T. *Histological classification of mammary tumors of the dog and cat*. (1999).
59. Hammer, S. C. *et al.* Longitudinal claudin gene expression analyses in canine mammary tissues and thereof derived primary cultures and cell lines. *Int. J. Mol. Sci.* **17,** 1655 (2016).

Acknowledgments. The authors wish to thank Heike Thiemeyer, Eva Packeiser, Kerstin Rohn and Jan Torben Schille for their excellent technical assistance, valuable comments and suggestions.

Author Contributions. José Luis Granados-Soler, Ingo Nolte, Hugo Murua Escobar, and Marion Hewicker-Trautwein performed the primary study design; Ingo Nolte, Hugo Murua Escobar, Bertram Brenig, Johannes Junginger, Daniela Betz, and Marion Hewicker-Trautwein performed the manuscript revision and final approval; Kirsten Bornemann-Kolatzki, Julia Beck, Ekkehard Schütz and Bertram Brenig performed the RNA sequencing and bioinformatics; José Luis Granados-Soler retrieved the data, performed the RNA isolation, and RNA sequencing data analysis, analysed the data and wrote the paper.

Competing Interest. The author(s) declare no competing interests.

"General discussion"

Massive parallel sequencing—also referred to as next- or second-generation sequencing (NGS)—is rapidly evolving and is starting to be utilized in small animal medicine research with promising clinical and diagnostic applications[14,77,101]. This thesis aimed to molecularly characterise FMC tissues and derived cell lines in order to identify reliable prognostic biomarkers and therapeutic targets besides classical histopathological classifications. Herein different NGS approaches were used to identify subsets of patients that would benefit from individualised patient-tailored therapies.

Massively parallel sequencing platforms allow comprehensive analyses of genes in individual tumour genomes. Among possible genomic alterations, somatic-CNVs deregulate the largest number of genes influencing the gene expression patterns by altering the gene dosage[3,105–107]. The genomic approach used in this study revealed non-previously reported genomic aberrations in FMCs and cell lines. Among the 140 structural rearrangements detected, CNLs in FCA "B1 1–23 Mb" and CNGs in FCAs "B4 1–29 Mb" and "F2 63–84 Mb" were highly correlated with malignancy and poor prognosis. Our findings provide a solid support for the use of these specific genomic aberrations as useful prognostic biomarkers in FMCs, and open new avenues for the study of multiple deleted tumour-suppressors (*CSMD1*, *MSR1*, *MTUS1*, *TUSC3*, *DLC1*, *NRG1* and *LZTS1*) and amplified EMT-associated genes (*VIM*, *ZEB1*, *KRAS*, *HMGA2*, *ESRP1*, *MTDH*, *YWHAZ*, and *MYC*) in FMCs and derived cell lines. In agreement with previous findings in different types of human cancer, amplified regions were typically enriched with genes related to cell motility, transcription factors, and driver-genes providing selective growth advantage. On the other hand, deleted regions commonly involved tumour-suppressors, tight-junction components, and epithelial cell adhesion molecules[6,107–109].

The amplification of EMT-related genes was correlated with the immunohistochemical co-expression of epithelial and mesenchymal markers in the TiHo-0906 cell line, and with a high absolute q-PCR expression of EMT-related markers *HMGA2* and *CD44*. The co-expression of epithelial and mesenchymal markers in correlation with EMT-elicitation, CSCs-features acquisition, resistance against chemotherapeutic agents and malignancy have been previously reported in human breast cancer[110–117]. In FMCs the co-expression of epithelial and mesenchymal markers has been reported as common[46,118–120], and frequently associated with hormone negative status[46]. Additionally, a potential bilineage progenitor co-expressing epithelial markers and Vim was identified in non-neoplastic feline mammary tissue[46]. In the

first manuscript included in this thesis characterising the TiHo-0906 cell line and additional manuscripts analysing the genomic and transcriptomic features of FMCs, the expression of specific CSCs-associated markers was not evaluated due to the unavailability of cross-reacting antibodies (e.g. CD24 and CD133). However, CD44-positive FMC-isolated cultured cells—as in the case of TiHo-0906 cells—have been reported to survive and proliferate *in vitro* as spheres and display additional CSCs-features[81]; further studies evaluating the expression of CSCs-related markers and the growing behaviour of TiHo-0906 cells under stem cells permissive conditions are still necessary. At the genomic and transcriptomic level, we did not detect patterns correlated with CSCs enrichment in FMCs and cell lines evaluated. This may be related to the fact that CSCs often represent a small proportion of the cell populations enclosed in the tumour microenvironment[81,121], and that nucleic acids isolated from neoplastic samples represent a mixture of all cellular subpopulations included in the sample[19].

Immunohistochemically, all tumours included in this study were positive to the epithelial markers employed. In line with previous reports[46,119], the expression pattern of mesenchymal and basal markers was variable depending on the histological type. In tubular carcinomas—generally characterised by better outcomes—positive cells to Vim were predominantly detected at a basal location and between acinar structures, while the luminal expression of Vim was only observed in a small subset of tubular carcinomas displaying worst outcomes. On the other hand, solid carcinomas and comedocarcinomas—characterised by poor survival—showed a diffuse pattern of Vim expression with a variable grade of intensity. At the genomic level, all solid carcinomas and comedocarcinomas, and a subset of tubular carcinomas with luminal expression of Vim showed amplifications in genomic regions harbouring EMT-related genes (FCAs B4 1–29 Mb and F2 63–84 Mb), and CNLs in FCA B1 1–23 Mb harbouring important tumour-suppressors. Others have shown that cats with solid carcinomas have a reduced survival in comparison with patients affected by tubular carcinomas[54,122], our results suggest that this characteristic malignancy may be attributable to the aforementioned structural rearrangements; and moreover that these specific aberrations are also detectable in some cases with tubular carcinomas characterised by worst outcome. At the transcriptomic level different pathways associated with EMT were enriched in FMC tissues and cell lines evaluated. However, samples did not cluster according to histological diagnosis or any feature correlated with EMT. Consequently, further studies are necessary to establish a clear association between the concurrent immunoexpression of epithelial and mesenchymal markers, the presence of structural rearrangements harbouring EMT-related genes and a possible transcriptomic profile characterising these features in FMCs.

After comparing the human and feline karyotypes, we identified the human homologue regions and disclose possible useful biomarkers and potential therapeutic targets (e.g.*TUSC3* and *ESRP1*) encompassed in aberrant chromosomic regions strongly correlated with poor prognosis (i.e. CNLs in FCA B1 1–23 Mb and CNGs in FCAs B4 1–29 Mb and F2 63–84 Mb).

The tumour suppressor candidate *3*—*TUSC3*—deletion is associated with poor prognosis and has been reported as useful biomarker and therapeutic target in different types of human cancer[97,123–126]. Loss of *TUSC3* is associated with protein maturation disturbances resulting in malignant cell transformation[97,124]. In this study, *TUSC3* deletion (detected by CNVs analysis) was correlated with poor survival. At the transcriptomic level, *TUSC3* was downregulated in both FMC tissues and cell lines, although its downregulation was not significant. Due to its functional significance in the development of multiple tumour types; *TUSC3* deletion and downregulation is here proposed as an useful biomarker and poor prognosis indicator in FMCs. Recombinant Ad-*TUSC3* gene therapy, mutant-specific *TUSC3* rescue drugs and targeting the negative regulators of *TUSC3* have been proposed as molecularly-tailored therapeutic options to restore *TUSC3* protein function in patients with tumours carrying this specific genomic aberration[97,124,126].

The epithelial splicing regulatory protein 1—*ESRP1*—regulates *CD44* alternative splicing producing a more malignant isoform (CD44v), promoting invasiveness and distant metastasis in human breast cancer stem cells[127]. Furthermore, in human non-small cell lung cancer (NSCLC) cell lines the loss of *ESRP1* has been recently proposed as the direct mechanism underlying Snail-induced EMT and cancer-associated phenotypes currently attributed to Snail expression[128]. TiHo-0906 cell line showed amplifications in the genomic region harbouring *ESRP1* and overexpressed CD44. Using CNVs analysis, we detected amplifications and deletions of *ESRP1* in different patients. However, structural aberrations of the genomic region harbouring this gene (FCA F2 17–63 Mb) were not correlated with poor survival. At the transcriptomic level, a significant downregulation of *ESPR1* was detected in cell lines analysed, while its expression was non-significantly upregulated in FMC tissues. Considering the importance of *ESRP1* in CSCs invasiveness and Snail-induced EMT, future studies evaluating the role of this gene in FMC-isolated CSCs are required.

Genes included in commonly amplified and deleted genomic regions detected by CNVs analysis were further investigated with clustering analysis to identify enriched biological processes and KEGG pathways. Our results from CNVs analysis revealed that amplified genes were mainly related to cell proliferation and motion (e.g. *SBDS*, *ITGAM*, *PDGFA* and *RAC1*), and transcription regulation and DNA binding (e.g. *GATA3, HMGN1, ZEB1, MYC* and *MYCN)*. Similarly, upregulated genes at the transcriptomic level were mainly involved in pathways related to cell growth and death regulation (e.g. *CDK1, CCNB2, RRM2* and *CHEK1*), and DNA replication and repair (e.g. *MCM2, RRM2* and *TYMS*). Interestingly, genes such as *RRM1, RRM2* and *TYMS* participate in the reprogramming of metabolic pathways associated to nucleotide synthesis and their upregulation have been correlated with tumour progression in multiple types of human cancer including breast cancer[129–131].

The ribonucleotide reductase regulatory subunit M2—*RRM2*—upregulation have been recently reported in human breast cancer[132–134]. Circulating tumour cells (CTCs) isolated from patients with metastatic breast cancer overexpress *RRM2* suggesting a potential usefulness as biomarker and patient-tailored therapeutic indicator[135]. The mediated siRNA silencing of *RRM2* by nanoparticles systemic delivery has been reported to suppress head and neck tumour growth[131].

Additional *in vitro* studies have demonstrated that knockdown of *RRM2* induces apoptosis in head and neck squamous cell carcinoma (HNSCC) and NSCLC cell lines[129]. Considering that several tumours included in this study and the TiHo-0906 cell line overexpress *RRM2*, future experiments using this cell line for the *in vitro* testing of this therapeutic strategy may be valuable.

Clustering and pathway analyses of genes in amplified and deleted genomic regions, and DEGs after transcriptomic analysis revealed similar alterations to those previously reported in human and canine mammary cancers, including those in p53 and PI3K-Akt signalling pathways[1,84,136,137]. The role of p53 in preventing tumour development has been previously reported in nearly all types of cancer in humans and animals, and is typically characterised by the presence of different mutations in multiple members of the p53 signalling pathway[138–141]. Using CNVs, we identified different amplifications in important cancer-related genes involved in the p53 pathway such as *MDM2*, *CDK4*, *CCND2* and *MYC*. Moreover, a differential expression of *MYC* and additional components of this signalling pathway like. *TGFB2*, *CCND1*, *CHEK1* were detected in both FMCs and derived cell lines. Additionally, important cancer-related genes such as *LAMA3*, *FLT4*, *PDGFD* and *BRCA1* participating in the PI3K-Akt signalling pathway were differentially expressed between FMCs and healthy mammary tissues. Using CNVs analysis amplifications of *AKT1* and deletions of *PTEN* were observed in the TiHo09-06 cell line making this cellular model suitable for the *in vitro* testing of PI3K inhibitors (e.g. pictilisib, buparlisib, idelalisib, toceranib, copanlisib and duvelisib) and AKT inhibitors (e.g. ipatasertib, MK-2206 and ARQ-092).

These results must be carefully interpreted considering the sample size. Additional constraints such as the poor quality of the RNA isolated from FFPE samples and the limited amount of available cell lines must be considered. Besides the characterization of the structural rearrangements and gene expression patterns, the regulation of the expression and the interaction of potential molecular markers is still a novel field of intensive research in general. Herein, especially microRNAs have moved into the spotlight. Future studies focusing on the identification of miRNAs may provide potential for new therapeutic approaches for FMCs.

Our results confirm that massive parallel DNA and RNA sequencing can be reliably used to identify pivotal biological processes correlated with FMC malignancy, especially those pathways governing the FMCs progression and dissemination. Moreover, DNA and RNA high-throughput sequencing prove to be of major importance to identify important biomarkers and target genes susceptible of therapeutic intervention. Our genomic and transcriptomic analyses provide more detailed information confirming previously proposed similarities between FMCs and molecular subtypes of breast cancer with worse outcomes (i.e. hTNBCs, metaplastic breast carcinomas, and claudin-low breast tumours). Furthermore, genomic, transcriptomic and immunohistochemical comparison of FMC tissues with derived cell lines provide important information about the usefulness and limitations of *in vitro* models for the study of FMCs.

"Molecular Characterisation of Feline Mammary Tumours"

José Luis Granados-Soler

FMCs are highly malignant tumours characterised by local invasion and early dissemination. Considering the poor outcome of affected cats, identification of useful biomarkers to predict clinical behaviour and suitable therapeutic targets is of major importance. In this study, we used massive-parallel DNA and RNA sequencing to identify structural rearrangements and differentially expressed genes enriching key biological processes characterising FMC-associated malignancy and poor outcome. Important structural rearrangements (CNLs in FCA B1 and CNGs in FCAs B4 and F2) were detected and correlated with poor prognosis. Immunohistochemical and transcriptomic findings showed a high level of correlation with genomic aberrations detected. Different potential biomarkers and therapeutic targets were identified including *TUSC3, RRM2, ESRP1, HMGA2* and *MYC* as well as different components of the p53 and PI3K-Akt signalling pathways. Amplified and upregulated genes were typically involved in pathways correlated with cell motion (*SBDS*, *ITGAM*, *PDGFA, RAC1, FGFR1, APC* and *ITGB2*), transcription modulation (*GATA3, HMGN1, ZEB1, MYC* and *MYCN)*, DNA replication and repairing (*RFC3, AK2, NUDT5. MCM2, RRM2* and *TYMS*) and EMT-elicitation (*VIM, ZEB1, KRAS, HMGA2, ESRP1, MTDH, YWHAZ,* and *MYC*). On the other hand, deleted and down-regulated genes were typically tumour-suppressors (*CSMD1*, *MSR1*, *MTUS1*, *TUSC3, DLC1, NRG1* and *LZTS1*) or genes involved in biological processes that would normally prevent tumour spreading such as tight junction components (*CLDN4, CLDN5 CLDN7, CLDN8, CLDN23, LMO7, PCDH17, PCDH20* and *PCDH9*) and cell adhesion molecules (*CD2, CD8A, CD34, CD40, CDH1, CDH4, CDH5, ICAM2, ITGAM, ITGB2, PECAM1, ESAM* and *JAM2*). FMCs included in this study shared some clinical and molecular similarities with specific molecular subtypes of human breast cancer characterised by worse outcome (i.e. hTNBCs, metaplastic breast carcinomas, and claudin-low breast tumours). Cellular models analysed shared a considerable amount of similarities with original tumours; however, specific alterations mainly correlated with endocrine regulation, circadian rhythm and metabolic pathways showed important differences. Despite the genomic characteristics associated with poor prognosis in solid carcinomas, no separation for the different histological grouping (tubular carcinomas, comedocarcinomas and solid carcinomas) was observed at the transcriptomic level. Molecular characteristics associated with malignancy were more typically observed in solid carcinomas and comedocarcinomas. However, specific cases with tubular carcinomas also shared these molecular characteristics and had a poor survival. DNA and RNA high-throughput sequencing prove to be useful to identify important biomarkers and target genes, resemblances between FMCs and human breast cancer, and advantages and limitations of *in vitro* models.

"*Molekulare Charakterisierung von feline Mammatumoren*"

José Luis Granados-Soler

FMCs sind hoch maligne Tumore, die durch lokale Invasion und frühe Metastasierung gekennzeichnet sind. In Anbetracht der schlechten Prognose der betroffenen Katzen ist die Identifizierung von Biomarkern zur Differenzierung und frühen Diagnose sowie für die Suche nach therapeutischen Ansätzen auf molekularer Ebene von großer Bedeutung. In der vorliegenden Studie sind FMCs und Zelllinien aus diesen Tumoren über die Hochdurchsatz-Sequenzierungen von DNA und RNA charakterisiert worden. Hierbei konnten strukturelle Chromosomenveränderungen und unterschiedlich exprimierte Gene gefunden werden, die in wichtigen biologischen Prozessen involviert sind. Sie sind der FMC-assoziierten Malignität und Überlebensraten gegenübergestellt worden. Wichtige strukturelle Chromosomenveränderungen (CNLs in FCA B1 und CNGs in FCAs B4 und F2) wurden erkannt, die mit einer schlechten Prognose korrelieren. Befunde aus der Immunhistochemie und der Transkriptomsequenzierung zeigten eine hohe Korrelation mit nachgewiesenen genomischen Aberrationen. Verschiedene potenzielle Biomarker und therapeutische Ziele wurden identifiziert, darunter *TUSC3*, *RRM2*, *ESRP1*, *HMGA2* und *MYC* sowie verschiedene Komponenten der Signalwege p53 und PI3K-Akt. Die amplifizierten und hochregulierten Gene sind häufig an biologischen Prozessen beteiligt. Diese können mit Zellmigration (*SBDS*, *ITGAM*, *PDGFA*, *RAC1*, *FGFR1*, *APC* und *ITGB2*), Transkriptionsmodulation (*GATA3*, *HMGN1*, *ZEB1*, *MYC* und *MYCN*), DNA-Replikation und -Reparatur (*RFC3*, *AK2*, *NUDT5*. *MCM2*, *RRM2* und *TYMS*) und EMT-Auslösung (*VIM*, *ZEB1*, *KRAS*, *HMGA2*, *ESRP1*, *MTDH*, *YWHAZ* und *MYC*) korrelieren. Dagegen sind die deletierten und herunterregulierten Gene meist Tumorsuppressoren (*CSMD1*, *MSR1*, *MTUS1*, *TUSC3*, *DLC1*, *NRG1* und *LZTS1*) oder sie sind an biologischen Prozessen beteiligt, die eine Tumorausbreitung verhindern sollten, wie z. B. Zellverbindungskomponenten (*CLDN4*, *CLDN5 CLDN7*, *CLDN8*, *CLDN23*, *LMO7*, *PCDH17*, *PCDH20* und *PCDH9*) und Zelladhäsionsmoleküle (*CD2*, *CD8A*, *CD34*, *CD40*, *CDH1*, *CDH4*, *CDH5*, *ICAM2*, *ITGAM*, *ITGB2*, *PECAM1*, *ESAM* und *JAM2*). Die in dieser Studie eingeschlossenen FMCs weisen klinische und molekulare Ähnlichkeiten mit spezifischen molekularen Subtypen von humanem Brustkrebs auf, der durch eine schlechtere Prognose gekennzeichnet ist (d. h. hTNBCs, metaplastische Brustkarzinome und Brusttumore mit niedriger Claudin-Expression). Die analysierten Zelllinien weisen eine weitgehende Übereinstimmung mit den Ursprungstumoren auf. Jedoch bestehen bedeutende Unterschiede hinsichtlich der endokrinen Regulation, dem zirkadianen Rhythmus und den Stoffwechselwegen. Trotz der genomischen Merkmale, die mit einer schlechten Prognose bei soliden Karzinomen verbunden sind, konnte auf Transkriptom-Ebene keine Unterscheidung zwischen den verschiedenen histologischen Entitäten (tubuläre Karzinome, Komedokarzinome und solide Karzinome) gefunden werden. Die mit Malignität verbundenen molekularen Charakteristiken, sind typischerweise beim soliden Karzinom und Komedokarzinom zu finden. Aber auch einzelne tubuläre Karzinome besitzen diese molekularen Eigenschaften und sind mit einer verkürzten Überlebenszeit assoziiert. Die Hochdurchsatz-Sequenzierung von DNA und RNA ist geeignet, um aus FMCs wichtige Biomarker und Zielgene zu identifizieren. Die Ergebnisse sind als Grundlage geeignet, Ähnlichkeiten zwischen Mammatumoren von Mensch und Katze herauszuarbeiten. Außerdem konnte über eine tiefergehende molekulare Differenzierung die Eignung von Zelllinien dieser Spezies für ein in vitro Modell verifiziert werden.

"General References"

1. Ellis, M. J. *et al.* Whole-genome analysis informs breast cancer response to aromatase inhibition. *Nature* **486,** 353–360 (2012).
2. Nik-Zainal, S. *et al.* Mutational processes molding the genomes of 21 breast cancers. *Cell* **149,** 979–993 (2012).
3. Jonsson, G. *et al.* High-resolution genomic profiles of breast cancer cell lines assessed by tiling BAC array comparative genomic hybridization. *Genes. Chromosomes Cancer* **46,** 543–558 (2007).
4. Weigelt, B. *et al.* Metastatic breast carcinomas display genomic and transcriptomic heterogeneity. *Mod. Pathol.* **28,** 340–351 (2015).
5. Hennessy, B. T. *et al.* Characterization of a naturally occurring breast cancer subset enriched in epithelial-to-mesenchymal transition and stem cell characteristics. *Cancer Res.* **69,** 4116–4124 (2009).
6. Horpaopan, S. *et al.* Genome-wide CNV analysis in 221 unrelated patients and targeted high-throughput sequencing reveal novel causative candidate genes for colorectal adenomatous polyposis. *Int. J. Cancer* **136,** E578–E589 (2015).
7. Blighe, K. *et al.* Whole genome sequence analysis suggests intratumoral heterogeneity in dissemination of breast cancer to lymph nodes. *PLoS One* **9,** 1–11 (2014).
8. Ross, J. S. *et al.* Genomic Profiling of Advanced-Stage, Metaplastic Breast Carcinoma by Next-Generation Sequencing Reveals Frequent, Targetable Genomic Abnormalities and Potential New Treatment Options. *Arch. Pathol. Lab. Med.* **139,** 642–649 (2015).
9. Taherian-Fard, a., Srihari, S. & Ragan, M. A. Breast cancer classification: linking molecular mechanisms to disease prognosis. *Brief. Bioinform.* **16,** bbu020- (2014).
10. Norton, N. *et al.* Assessment of tumor heterogeneity, as evidenced by gene expression profiles, pathway activation, and gene copy number, in patients with multifocal invasive lobular breast tumors. *PLoS One* **11,** 1–20 (2016).
11. Hart, C. D., Tenori, L., Luchinat, C. & Di Leo, A. Metabolomics in Breast Cancer: Current Status and Perspectives. *Adv. Exp. Med. Biol.* **882,** 217–234 (2016).
12. Günther, U. L. Metabolomics Biomarkers for Breast Cancer. *Pathobiology* **82,** 153–165 (2015).
13. Pongor, L. *et al.* A genome-wide approach to link genotype to clinical outcome by utilizing next generation sequencing and gene chip data of 6,697 breast cancer patients. *Genome Med.* **7,** 1–11 (2015).
14. Taher, L. *et al.* Comparative High-Resolution Transcriptome Sequencing of Lymphoma Cell Lines and de novo Lymphomas Reveals Cell-Line-Specific Pathway Dysregulation. *Sci. Rep.* **8,** 1–12 (2018).
15. Huang, D. W., Sherman, B. T. & Lempicki, R. A. Systematic and integrative analysis of large gene lists using DAVID bioinformatics resources. *Nat. Protoc.* **4,** 44 (2008).
16. Gao, Y. *et al.* Cross-validation of genes potentially associated with overall survival and drug resistance in ovarian cancer. *Oncol. Rep.* **37,** 3084–3092 (2017).
17. Soares, M. *et al.* Molecular based subtyping of feline mammary carcinomas and clinicopathological characterization. *The Breast* **27,** 44–51 (2016).
18. Goldschmidt, M. H., Peña, L., Rasotto, R. & Zappulli, V. Classification and grading of canine mammary tumors. *Vet. Pathol.* **48,** 117–31 (2011).
19. Nieto, a. *et al.* Immunohistologic Detection of Estrogen Receptor Alpha in Canine Mammary Tumors: Clinical and Pathologic Associations and Prognostic Significance. *Vet. Pathol.* **37,** 239–247 (2000).
20. Zappulli, V. *et al.* Immunohistochemical Expression of E-Cadherin and b-Catenin in Feline Mammary Tumours. *J. Comp. Pathol.* **147,** 161–170 (2012).
21. Zappulli, V. *et al.* Proposed Classification of the Feline 'Complex' Mammary Tumors as Ductal and Intraductal Papillary Mammary Tumors. *Vet. Pathol.* **50,** 1070–1077 (2013).
22. Shafiee, R. *et al.* Diagnosis, classification and grading of canine mammary tumours as a model to study human breast cancer: an Clinico-Cytohistopathological study with environmental factors influencing public health and medicine. *Cancer Cell Int.* **13,** 79 (2013).

REFERENCES

23. Misdorp, W., Else, R., Hellmen, E. & Lipscomb, T. *Histological classification of mammary tumors of the dog and cat*. (1999).
24. Zappulli, V. *et al.* Prognostic Evaluation of Feline Mammary Carcinomas: A Review of the Literature. *Vet. Pathol.* **52,** 46–60 (2015).
25. Wiese, D., Thaiwong, T., Yuzbasiyan-gurkan, V. & Kiupel, M. Feline mammary basal-like adenocarcinomas: a potential model for human triple-negative breast cancer (TNBC) with basal-like subtype. *BMC Cancer* **13,** 403 (2013).
26. Brunetti, B. *et al.* Molecular Phenotype in Mammary Tumours of Queens: Correlation between Primary Tumour and Lymph Node Metastasis. *J. Comp. Path.* **148,** 206–13 (2013).
27. Beha, G. *et al.* Molecular phenotype of primary mammary tumours and distant metastases in female dogs and cats. *J. Comp. Pathol.* **150,** 194–197 (2014).
28. Soares, M., Correia, J., Rodrigues, P., Simões, M. & Matos, A. De. Feline HER2 Protein Expression Levels and Gene Status in Feline Mammary Carcinoma: Optimization of Immunohistochemistry (IHC) and In Situ Hybridization (ISH) Techniques. *Microsc. Microanal.* **19,** 876–882 (2013).
29. Dias Pereira, P. & Gärtner, F. Expression of E-cadherin in normal, hyperplastic and neoplastic feline mammary tissue. *Vet. Rec.* **153,** 297–302 (2003).
30. Tanabe, S. *et al.* Expression of mRNA of chemokine receptor CXCR4 in feline mammary adenocarcinoma. *Vet. Rec.* **151,** 729–33 (2002).
31. Adega, F., Borges, A. & Chaves, R. Cat Mammary Tumors: Genetic Models for the Human Counterpart. *Vet. Sci.* **3,** 17 (2016).
32. Flores, A. R., Rêma, A., Carvalho, F., Faustino, A. & Dias Pereira, P. Reduced expression of claudin-2 is associated with high histological grade and metastasis of feline mammary carcinomas. *J. Comp. Pathol.* **150,** 169–74 (2014).
33. Hughes, K. & Dobson, J. M. Prognostic histopathological and molecular markers in feline mammary neoplasia. *Vet. J.* **194,** 19–26 (2012).
34. Borrego, J. F., Cartagena, J. C. & Engel, J. Treatment of feline mammary tumours using chemotherapy, surgery and a COX-2 inhibitor drug (meloxicam): a retrospective study of 23 cases (2002-2007)*. *Vet. Comp. Oncol.* **7,** 213–21 (2009).
35. Penzo, C., Ross, M., Muirhead, R., Else, R. & Argyle, D. J. Effect of recombinant feline interferon-ω alone and in combination with chemotherapeutic agents on putative tumour-initiating cells and daughter cells derived from canine and feline mammary tumours. *Vet. Comp. Oncol.* **7,** 222–229 (2009).
36. Cunha, S. C., Corgozinho, K. B., Souza, H. J., Silva, K. V. & Ferreira, A. M. R. Adjuvant chemotherapy with mitoxantrone for cats with mammary carcinomas treated with radical mastectomy. *J. Feline Med. Surg.* 1–5 (2015). doi:10.1177/1098612X14567159
37. Sorenmo, K. U., Worley, D. R. & Goldschmidt, M. H. in *Withrow and MacEwen's Small Animal Clinical Oncology* (eds. Withrow, S. & MacEwen, E. G.) 538–556 (Elsevier, 2013). doi:10.1016/B978-1-4377-2362-5.00027-X
38. Hayes, A. A. & Mooney, S. Feline mammary tumors. *Vet. Clin. North Am. Small Anim. Pract.* **15,** 513–20 (1985).
39. Misdorp, W. & Weijer, K. Animal model of human disease: breast cancer. *Am. J. Pathol.* **98,** 573–6 (1980).
40. Zappulli, V., De Zan, G., Cardazzo, B., Bargelloni, L. & Castagnaro, M. Feline mammary tumours in comparative oncology. *J. Dairy Res.* **72,** 98 (2005).
41. Hahn, K. A., Bravo, L. & Avenell, J. S. Feline breast carcinoma as a pathologic and therapeutic model for human breast cancer. *In Vivo* **8,** 825–8 (1994).
42. Hahn, K. A. & Adams, W. H. Feline mammary neoplasia: biological behavior, diagnosis, and treatment. *Feline Pr.* **25,** 5–11 (1977).
43. Overley, B., Shofer, F. S., Goldschmidt, M. H., Sherer, D. & Sorenmo, K. U. Association between Ovarihysterectomy and Feline Mammary Carcinoma. *J. Vet. Intern. Med.* **19,** 560–563 (2005).
44. Ito, T. *et al.* Prognosis of malignant mammary tumor in 53 cats. *J. Vet. Med. Sci.* **58,** 723–6 (1996).
45. Weijer, K. & Hart, A. A. Prognostic factors in feline mammary carcinoma. *J. Natl. Cancer Inst.* **70,** 709–716 (1983).
46. Caliari, D. *et al.* Triple-negative vimentin-positive heterogeneous feline mammary carcinomas as a potential comparative model for breast cancer. *BMC Vet. Res.* **10,** 1–12 (2014).
47. Elston, C. & Ellis, I. Pathological prognostic factors in breast cancer. I. The value of histological grade in breast cancer: experience from a large study with long-term follow-up. *Histopathology* **19,** 403–410 (1991).

48. Castagnaro, M. *et al.* Tumour grading and the one-year post-surgical prognosis in feline mammary carcinomas. *J. Comp. Pathol.* **119,** 263–75 (1998).
49. McNeill, C. J. *et al.* Evaluation of adjuvant doxorubicin-based chemotherapy for the treatment of feline mammary carcinoma. *J. Vet. Intern. Med.* **23,** 123–9 (2009).
50. Viste, J. R., Myers, S. L., Singh, B. & Simko, E. Feline mammary adenocarcinoma : tumor size as a prognostic indicator. *Can Vet J* **43,** 33–37 (2002).
51. Morris, J. Mammary tumours in the cat: size matters, so early intervention saves lives. *J. Feline Med. Surg.* **15,** 391–400 (2013).
52. Soares, M. *et al.* Ki-67 as a Prognostic Factor in Feline Mammary Carcinoma: What Is the Optimal Cutoff Value? *Vet. Pathol.* **53,** 37–43 (2016).
53. Maniscalco, L. *et al.* Activation of AKT in feline mammary carcinoma: a new prognostic factor for feline mammary tumours. *Vet. J.* **191,** 65–71 (2012).
54. Seixas, F., Palmeira, C., Pires, M. A., Bento, M. J. & Lopes, C. Grade is an independent prognostic factor for feline mammary carcinomas: a clinicopathological and survival analysis. *Vet. J.* **187,** 65–71 (2011).
55. Burrai, G. P. *et al.* Spontaneous feline mammary intraepithelial lesions as a model for human estrogen receptor- and progesterone receptor-negative breast lesions. *BMC Cancer* **10,** 156 (2010).
56. Novosad, C. A. *et al.* Retrospective evaluation of adjunctive doxorubicin for the treatment of feline mammary gland adenocarcinoma: 67 cases. *J. Am. Anim. Hosp. Assoc.* **42,** 110–20 (2006).
57. Dias Pereira, P., Carvalheira, J. & Gärtner, F. Cell proliferation in feline normal, hyperplastic and neoplastic mammary tissue--an immunohistochemical study. *Vet. J.* **168,** 180–5 (2004).
58. Rutteman, G. R., Blankenstein, M. A., Minke, J. & Misdorp, W. Steroid receptors in mammary tumours of the cat. *Acta Endocrinol. (Copenh).* **125 Suppl,** 32–7 (1991).
59. Millanta, F., Calandrella, M., Vannozzi, I. & Poli, A. Papers & Articles Steroid hormone receptors in normal , dysplastic and neoplastic feline mammary tissues and their prognostic significance. *Vet. Rec.* **158,** 821–824 (2006).
60. Martín de las Mulas, J. *et al.* Progesterone receptors in normal, dysplastic and tumourous feline mammary glands. Comparison with oestrogen receptors status. *Res. Vet. Sci.* **72,** 153–61 (2002).
61. Hamilton, J. M., Else, R. W. & Forshaw, P. Oestrogen receptors in feline mammary carcinomas. *Vet. Rec.* **99,** 477–9 (1976).
62. Lana, S., Rutteman, G. & Withrow, S. in *Withrow and MacEwen's Small Animal Clinical Oncology* (eds. Withrow, S. & Vail, D.) 619–636 (Saunders Elsevier, 2007).
63. Santos, S. *et al.* ERBB2 in cat mammary neoplasias disclosed a positive correlation between RNA and protein low expression levels: A model for erbB-2 negative human breast cancer. *PLoS One* **8,** e83673 (2013).
64. Sayasith, K., Sirois, J. & Doré, M. Molecular characterization of feline COX-2 and expression in feline mammary carcinomas. *Vet. Pathol.* **46,** 423–429 (2009).
65. Petterino, C., Ratto, A., Podestà, G., Drigo, M. & Pellegrino, C. Immunohistochemical evaluation of STAT3-p-tyr705 expression in feline mammary gland tumours and correlation with histologic grade. *Res. Vet. Sci.* **82,** 218–24 (2007).
66. Petterino, C. *et al.* Expression of Stat3 in Feline Mammary Gland Tumours and its Relation to Histological Grade. *Vet. Res. Commun.* **30,** 599–611 (2006).
67. Rogalla, P. *et al.* Expression of HMGI-C, a member of the high mobility group protein family, in a subset of breast cancers: relationship to histologic grade. *Mol. Carcinog.* **3,** 153–156 (1997).
68. Ahmed, K. M., Tsai, C. Y. & Lee, W.-H. Derepression of HMGA2 via removal of ZBRK1/BRCA1/CtIP complex enhances mammary tumorigenesis. *J. Biol. Chem.* **285,** 4464–71 (2010).
69. Morishita, A. *et al.* HMGA2 is a driver of tumor metastasis. *Cancer Res.* **73,** 4289–4299 (2013).
70. Iida, N. & Bourguignon, L. Y. New CD44 splice variants associated with human breast cancers. *J. Cell. Physiol.* **162,** 127–33 (1995).
71. Ricardo, S. *et al.* Breast cancer stem cell markers CD44, CD24 and ALDH1: expression distribution within intrinsic molecular subtype. *J. Clin. Pathol.* **64,** 937–946 (2011).
72. Moody, S. E. *et al.* The transcriptional repressor Snail promotes mammary tumor recurrence. *Cancer Cell* **8,** 197–209 (2005).
73. Im, K. S. *et al.* Possible Role of Snail Expression as a Prognostic Factor in Canine Mammary Neoplasia. *J. Comp. Pathol.* **147,** 121–128 (2012).
74. Vuong, D., Simpson, P. T., Green, B., Cummings, M. C. & Lakhani, S. R. Molecular classification of breast cancer. *Virchows Arch* **465,** 1–14 (2014).

REFERENCES

75. Pontius, J. U. *et al.* Initial sequence and comparative analysis of the cat genome. *Genome Res.* **17,** 1675–1689 (2007).
76. Borges, A., Adega, F. & Chaves, R. Establishment and characterization of a new feline mammary cancer cell line, FkMTp. *Cytotechnology* **68,** 1529–43 (2016).
77. Granados-Soler, J. L. *et al.* TiHo-0906: a new feline mammary cancer cell line with molecular, morphological, and immunocytological characteristics of epithelial to mesenchymal transition. *Sci. Rep.* **8,** 13231 (2018).
78. Minke, J. M. *et al.* Isolation of two distinct epithelial cell lines from a single feline mammary carcinoma with different tumorigenic potential in nude mice and expressing different levels of epidermal growth factor receptors. *Cancer Res.* **51,** 4028–37 (1991).
79. Muleya, J. S. *et al.* Establishment and characterization of a new cell line derived from feline mammary tumor. *J. Vet. Med. Sci.* **60,** 931–5 (1998).
80. Uyama, R. *et al.* Establishment and characterization of eight feline mammary adenocarcinoma cell lines. *J. Vet. Med. Sci.* **67,** 1273–6 (2005).
81. Barbieri, F. *et al.* Isolation of stem-like cells from spontaneous feline mammary carcinomas: Phenotypic characterization and tumorigenic potential. *Exp. Cell Res.* **318,** 847–860 (2012).
82. Pang, L. Y. *et al.* Feline mammary carcinoma stem cells are tumorigenic, radioresistant, chemoresistant and defective in activation of the ATM/p53 DNA damage pathway. *Vet. J.* **196,** 414–423 (2013).
83. Prat, A. *et al.* Characterization of cell lines derived from breast cancers and normal mammary tissues for the study of the intrinsic molecular subtypes. *Breast Cancer Res. Treat.* **142,** 237–55 (2013).
84. Sun, Y. & Liu, Q. Deciphering the correlation between breast tumor samples and cell lines by integrating copy-number changes and gene expression profiles. *Biomed Res. Int.* **2015,** 1–22 (2015).
85. Lacroix, M. & Leclercq, G. Relevance of breast cancer cell lines as models for breast tumours: an update. *Breast Cancer Res. Treat.* **83,** 249–289 (2004).
86. Domcke, S., Sinha, R., Levine, D. A., Sander, C. & Schultz, N. Evaluating cell lines as tumour models by comparison of genomic profiles. *Nat. Commun.* **4,** 1–10 (2013).
87. Gillet, J.-P. *et al.* Redefining the relevance of established cancer cell lines to the study of mechanisms of clinical anti-cancer drug resistance. *Proc. Natl. Acad. Sci.* **108,** 18708–18713 (2011).
88. Burdall, S. E., Hanby, A. M., Lansdown, M. R. J. & Speirs, V. Breast cancer cell lines: Friend or foe? *Breast Cancer Res.* **5,** 89–95 (2003).
89. Calles, K., Svensson, I., Lindskog, E. & Häggström, L. Effects of conditioned medium factors and passage number on Sf9 cell physiology and productivity. *Biotechnol. Prog.* **22,** 394–400 (2006).
90. Thomas, R. Cytogenomics of Feline Cancers : Advances and Opportunities. *Vet. Sci.* **2,** 246–258 (2015).
91. Mayr, B., Ortner, W., Breeding, A., Reifinger, M. & Loupal, G. Loss of chromosome B2-material in three cases of feline mammary tumours. *Res. Vet. Sci.* **60,** 61–63 (1995).
92. Lebok, P. *et al.* 8P Deletion Is Strongly Linked To Poor Prognosis in Breast Cancer. *Cancer Biol. Ther.* **16,** 1080–1087 (2015).
93. Moelans, C. B., Maldegem, C. M. G. Van & Wall, E. Van Der. Copy number changes at 8p11-12 predict adverse clinical outcome and chemo- and radiotherapy response in breast cancer. *Oncotarget* **9,** 17078–17092 (2018).
94. Cai, Y. *et al.* Loss of Chromosome 8p Governs Tumor Progression and Drug Response by Altering Lipid Metabolism. *Cancer Cell* **29,** 751–766 (2016).
95. Saito, S., Morita, K. & Hirano, T. High frequency of common DNA copy number abnormalities detected by bacterial artificial chromosome array comparative genomic hybridization in 24 breast cancer cell lines. *Hum. Cell* **22,** 1–10 (2009).
96. Iddawela, M. *et al.* Integrative analysis of copy number and gene expression in breast cancer using formalin-fixed paraffin-embedded core biopsy tissue: A feasibility study. *BMC Genomics* **18,** 1–13 (2017).
97. Yu, X. *et al.* TUSC3: a novel tumour suppressor gene and its functional implications. *J. Cell. Mol. Med.* **21,** 1711–1718 (2017).
98. Wienberg, J. *et al.* Conservation of human vs. feline genome organization revealed by reciprocal chromosome painting. *Cytogenet. Cell Genet.* **77,** 211–7 (1997).
99. Yang, F. *et al.* Reciprocal chromosome painting illuminates the history of genome evolution of the domestic cat, dog and human. *Chromosom. Res.* **8,** 393–404 (2000).
100. Le Scouarnec, S. & Gribble, S. M. Characterising chromosome rearrangements: Recent technical advances in molecular cytogenetics. *Heredity (Edinb).* **108,** 75–85 (2012).
101. Beck, J. *et al.* Genome Aberrations in Canine Mammary Carcinomas and Their Detection in Cell-Free Plasma DNA. **8,** (2013).

102. Chandrashekar, D. S. *et al.* UALCAN : A Portal for Facilitating Tumor Subgroup Gene Expression. *Neoplasia* **19,** 649–658 (2017).
103. Singh, R. R. *et al.* Clinical massively parallel next-generation sequencing analysis of 409 cancer-related genes for mutations and copy number variations in solid tumours. *Br. J. Cancer* **111,** 2014–2023 (2014).
104. Zaman, N. *et al.* Signaling Network Assessment of Mutations and Copy Number Variations Predict Breast Cancer Subtype-Specific Drug Targets. *Cell Rep.* **5,** 216–223 (2013).
105. Korkola, J. & Gray, J. W. Breast cancer genomes - form and function. *Curr. Opin. Genet. Dev.* **20,** 4–14 (2010).
106. Pinkel, D. *et al.* High resolution analysis of DNA copy number variation using comparative genomic hybridization to microarrays. *Nat. Genet.* **20,** 207–211 (1998).
107. Zhao, M., Liu, Y. & Qu, H. Expression of epithelial-mesenchymal transition-related genes increases with copy number in multiple cancer types. *Oncotarget* **7,** 24688–99 (2016).
108. Haverty, P. M. *et al.* High-resolution genomic and expression analyses of copy number alterations in breast tumors. *Genes, Chromosom. Cancer* **47,** 530–542 (2008).
109. Shlien, A. & Malkin, D. Copy number variations and cancer. *Genome Med.* **1,** 1–9 (2009).
110. Oon, M. L., Thike, A. A., Tan, S. Y. & Tan, P. H. Cancer stem cell and epithelial–mesenchymal transition markers predict worse outcome in metaplastic carcinoma of the breast. *Breast cancer Res. Treat. Treat* **150,** 31–41 (2015).
111. Gobbi, H., Simpson, J. F., Borowsky, A., Jensen, R. A. & Page, D. L. Metaplastic breast tumors with a dominant fibromatosis-like phenotype have a high risk of local recurrence. *Cancer* **85,** 2170–2182 (1999).
112. Adem, C., Reynolds, C., Adlakha, H., Roche, P. & Nascimento, A. Wide spectrum screening keratin as a marker of metaplastic spindle cell carcinoma of the breast: an immunohistochemical study of 24 patients. *Histopathology* **40,** 556–562 (2002).
113. Shankar, J. & Nabi, I. R. Actin cytoskeleton regulation of epithelial mesenchymal transition in metastatic cancer cells. *PLoS One* **10,** 1–12 (2015).
114. Hennessy, B. T. *et al.* Characterization of a naturally occurring breast cancer subset enriched in epithelial-to-mesenchymal transition and stem cell characteristics. *Cancer Res.* **69,** 4116–4124 (2009).
115. Singh, A. & Settleman, J. EMT, cancer stem cells and drug resistance: an emerging axis of evil in the war on cancer. *Oncogene* **29,** 4741–4751 (2010).
116. Vora, H. H. *et al.* Cytokeratin and vimentin expression in breast cancer. *Int. J. Biol. Markers* **24,** 38–46 (2009).
117. Korsching, E. *et al.* The origin of vimentin expression in invasive breast cancer: Epithelial- mesenchymal transition, myoepithelial histogenesis or histogenesis from progenitor cells with bilinear differentiation potential? *J. Pathol.* **206,** 451–457 (2005).
118. Arahana, V., Arteaga, H., Tobar, J., Jaramillo, V. & Torres, M. D. L. Efecto de la temperatura, medios de cultivo y reguladores de crecimiento en la germinación de embriones cigóticos de durazno (Prunus persica) var. Diamante. **4,** 24–35 (2012).
119. Mulas, J. M. De, E, A. & Monteros, D. L. Immunohistochemical Distribution Pattern of Intermediate Filament Proteins and Muscle Actin in Feline and Human Mammary Carcinomas. *J. Comp. Path.* **111,** 365–381 (1994).
120. Sarli, G., Brunetti, B. & Benazzi, C. Mammary mucinous carcinoma in the cat. *Vet. Pathol.* **43,** 667–673 (2006).
121. Morel, A.-P. *et al.* Generation of Breast Cancer Stem Cells through Epithelial-Mesenchymal Transition. *PLoS One* **3,** 1–7 (2008).
122. Mills, S. W. *et al.* Prognostic Value of Histologic Grading for Feline Mammary Carcinoma: A Retrospective Survival Analysis. *Vet. Pathol.* **52,** 238–249 (2014).
123. Conway, K. *et al.* Racial variation in breast tumor promoter methylation in the carolina breast cancer study. *Cancer Epidemiol. Biomarkers Prev.* **24,** 921–930 (2015).
124. Yuan, J. *et al.* Tumor suppressor candidate 3: A novel grading tool and predictor of clinical malignancy in human gliomas. *Oncol. Lett.* **15,** 5655–5661 (2018).
125. Vaňhara, P. *et al.* Loss of the oligosaccharyl transferase subunit TUSC3 promotes proliferation and migration of ovarian cancer cells. *Int. J. Oncol.* **42,** 1383–1389 (2013).
126. Horak, P. *et al.* TUSC3 Loss Alters the ER Stress Response and Accelerates Prostate Cancer Growth in vivo. *Sci. Rep.* **4,** 1–9 (2014).

127. Hu, J., Li, G., Zhang, P., Zhuang, X. & Hu, G. A CD44v+ subpopulation of breast cancer stem-like cells with enhanced lung metastasis capacity. *Cell Death Dis.* **8,** e2679 (2017).
128. Walser, T. C. *et al.* Silencing the snail-dependent RNA splice regulator ESRP1 drives malignant transformation of human pulmonary epithelial cells. *Cancer Res.* **78,** 1986–1999 (2018).
129. Rahman, M. A. *et al.* RRM2 Regulates Bcl-2 in Head and Neck and Lung Cancers: A Potential Target for Cancer Therapy. *Clin Cancer Res.* **19,** 3416–3428 (2014).
130. Furuta, E., Okuda, H., Kobayashi, A. & Watabe, K. Metabolic genes in cancer: their roles in tumor progression and clinical implications. *Biochim Biophys Acta* **1805,** 141–152 (2011).
131. Rahman, M. A. *et al.* Systemic Delivery of siRNA-Nanoparticles Targeting RRM2 Suppresses Head and Neck Tumor Growth. *J Control Release.* **159,** 384–392 (2013).
132. Thanmalagan, R. R., Naorem, L. D. & Venkatesan, A. Expression Data Analysis for the Identification of Potential Biomarker of Pregnancy Associated Breast Cancer. *Pathol. Oncol. Res.* **23,** 537–544 (2017).
133. Meißner, T. *et al.* Metastatic triple-negative breast cancer patient with TP53 tumor mutation experienced 11 months progression-free survival on bortezomib monotherapy without adverse events after ending standard treatments with grade 3 adverse events. *Cold Spring Harb. Mol. case Stud.* **3,** 1–23 (2017).
134. Cejalvo, J. M. *et al.* Intrinsic subtypes and gene expression profiles in primary and metastatic breast cancer. *Cancer Res.* **77,** 2213–2221 (2017).
135. Lang, J. E. *et al.* Expression profiling of circulating tumor cells in metastatic breast cancer Julie. *Breast Cancer Res Treat.* **149,** 121–131 (2016).
136. Uva, P. *et al.* Comparative expression pathway analysis of human and canine mammary tumors. *BMC Genomics* **10,** 135 (2009).
137. Showler, K. *et al.* Analysis of genes involved in the PI3K/Akt pathway in radiation- and MNU-induced rat mammary carcinomas. *J. Radiat. Res.* **58,** 183–194 (2016).
138. He, L. *et al.* A microRNA component of the p53 tumour suppressor network. *Nature* **447,** 1130–1134 (2007).
139. Chung, W. C., Zhang, S., Challagundla, L., Zhou, Y. & Xu, K. Lunatic Fringe and p53 Cooperatively Suppress Mesenchymal Stem-Like Breast Cancer. *Neoplasia (United States)* **19,** 885–895 (2017).
140. Leszczynska, K. B. *et al.* Hypoxia-induced p53 modulates both apoptosis and radiosensitivity via AKT. *J. Clin. Invest.* **125,** 2385–2398 (2015).
141. Mayr, B., Schaffner, G., Kurzbauer, R., Reifinger, M. & Schellander, K. Sequence of an exon of tumour suppressor p53 gene--a comparative study in domestic animals: mutation in a feline solid mammary carcinoma. *Br. Vet. J.* **151,** 325–9 (1995).

1st Manuscript

"Supplementary information"

Marker	Negative control	Positive control
vimentin	IgG1	feline skin
pan-CK	IgG1	feline skin
CK8/18	IgG1	feline normal mammary gland
CK14	rabbit serum	feline skin
CK5/6	IgG1	feline skin
SMA	IgG2a	feline urinary bladder
calponin	IgG1	feline normal mammary gland
p63	IgG2a	feline normal mammary gland
E-cadherin	IgG2a	feline skin
Ki67	IgG1	feline normal small intestine
p53	IgG2a	feline transitional cell carcinoma
COX-2	rabbit serum	feline normal lymph node, feline transitional cell carcinoma
HER-2/c-erbB2	IgG1	human mammary tissue and pellets from cell lines overexpressing HER-2*, feline mammary carcinoma
progesteron receptor	IgG2a	feline normal mammary gland
estrogen receptor	IgG1	feline normal mammary gland
claudin-2	IgG2b	feline and canine normal mammary gland
HMGA2	rabbit serum	Feline and canine neonatal tissue
CD44	rat serum	feline lymph node
*kindly provided by Prof. Dr. H.-H. Kreipe, Department of Pathology, Hannover Medical School		

Supplementary table 1. Antibodies and corresponding negative and positive controls used in this study.

2nd Manuscript

"Supplementary information"

FCA (Mb)	HSA	Size (Mb)	Animals affected				Relevant genes
			CNGs TC	CNGs SC	CNLs TC	CNLs SC	
A1 1–28	13	28	0	1	0	3	*ZMYM2, XPO4, LATS2, EFHA1, FGF9, SGCG, SACS, TNFRSF19, MIPEP, C1QTNF9, SPATA13, CDK8, USP12, RPL21, SNORD102(LOC111557008), SNORA27, RASL11A, GTF3A, MTIF3, LNX2, POLR1D, GSX1, PDX1, CDX2, FLT3, PAN3, FLT1, POMP, SLC46A3, MTUS2, KATNAL1, HMGB1, USPL1, ALOX5AP, MEDAG, TEX26, HSPH1, B3GLCT, BRCA2, PDS5B, KL, RFC3, NBEA, DCLK1, POSTN, LHFPL6, FOXO1, NEK3, RB1, LPAR6, LRCH1, LCP1, COG3, TPT1, KCTD4, NUFIP1*
A1 28–30	13	2	0	1	3	4	*TNFSF11, ELF1*
A1 65–68	13	3	1	1	5	3	*GPR180, SOX21, ABCC4, CLDN10, DZIP1, DNAJC3, HS6ST3*
A1 68–73	13	5	1	1	4	3	*OXGR1, MBNL2, RAP2A, FARP1, STK24, UBAC2, EBI2,(LOC101101025), ZIC5, ZIC2, PCCA, ITGBL1, FGF14*
A1 73–75	13	2	1	1	3	3	*KDELC1, ERCC5,(LOC101085685)*
A1 75–78	13	3	1	1	2	2	*EFNB2*
A1 78–80	13	2	1	1	1	2	*TNFSF13B, IRS2*
A1 80–85	13 1	5	2	1	0	2	*RAB20, SOX1, GRK1, SH3BP5L, ZNF692*
A1 85–87	1	2	3	1	0	2	
A1 87–95	1 5	8	3	0	1	3	*NLRP3, RNF187, FLT4, MGAT1*
A1 95–100	5 7	5	3	0	0	5	*CCDC112, TMED7, LVRN, DMXL1, PPP1R9A*
A1 100–105	5 7	5	2	0	1	5	*PON1, PDK4, SNCAIP, CEP120*

A1 105–124	5	19	1	0	2	5	*MEGF10, FBN2, RAPGEF6, ACSL6, RAD50, AFF4, ZCCHC10, JADE2, SEC24A, ETF1, ARHGAP26*
A1 124–146	5	22	1	0	2	6	*IL6ST, MAP3K1, MIER3, PLK2, GAPT, ERCC8, IPO11, HTR1A, RGS7BP, PIK3R1, ADAMTS6, MAST4, PIK3R1, BDP1, FCHO2, SV2C, PDE8B, TBCA, AP3B1, DMGDH, BHMT2, CMYA5*
A1 146–149	5	3	1	0	4	6	*ATP6AP1L, ACOT12*
A1 149–171	5	22	1	0	6	3	*ERAP2*
A1 171–173	5	2	2	0	2	6	*SLC25A46*
A1 173–179	5	6	2	0	2	7	*APC, NSD1*
A1 179–181	5	2	2	0	3	7	*NPM1, TLX3, RANBP17*
A1 181–199	5	18	2	0	4	7	*SLIT3, WWC1, MAT2B, HMMR, CCNG1, PTTG1, PWWP2A, ADRA1B, IL12B, EBF1, SOX30, CYFIP2, ITK, MED7, GEMIN5, LARP1, HAND1, CD74, PDGFRB*
A1 200–207	5	8	2	0	3	6	*FGF10*
A1 207–215	5	8	2	0	1	6	*GHR, PLCXD3, MROH2B, CARD6, C9, FYB1, RICTOR, LIFR, WDR70, CPLANE1, SLC1A3, IL7R, PRLR, RXFP3*
A1 215–221	5	6	2	0	1	5	
A1 221–241	5	20	2	0	1	3	*CTNND2, MARCH6, SEMA5A, TERT, AHRR,TRIP13, BRD9, SLC9A3*
A2 1–21	193	21	1	1	6	4	*FSTL3, STK11, TCF3, GNA11, MAP2K2, SH3GL1, CHAF1A, CNOT3, TFPT, MLLT1, DNM2, CARM1, SMARCA4, CALR, LYL1, BRD4, TPM4, BST2, JAK3 ELL, CRTC1, SETD2, LAMB2, CEBPA, CEP89, BAP1*
A2 21–40	3	19	0	0	7	7	*PBRM1, CACNA1D, FHIT, PTPRG, C30rf14, SUCLG2, EOGT, MITF, FOXP1*
A2 40–49	3	9	0	0	7	6	
A2 49–52	3	3	0	0	5	5	*SRGAP3, FANCD2, VHL*
A2 52–69	37	17	0	0	4	2	*PPARG, RAF1, XPC, CNBP, RPN1, GATA2, IKZF1*
A2 69–73	7	4	0	0	5	3	*EGFR*
A2 73–93	7	20	0	0	3	5	*CD36*

A2 93–114	7	21	1	1	4	6	*AKAP9, CDK6, ASB4, DLX5, ASNS, ETV1*
A2 114–145	7	31	1	0	4	7	*GPNMB, HNRNPA2B1, HOXA9, HOXA11, HOXA13, JAZF1, FOXP2, MET, SLC13A1, POT1*
A2 145–151	7	6	1	0	3	4	*PAX4, SND1, IMPDH1, FAM71F1, CALU, CCDC136, KCP, SMO, CPA4, CPA5, PLXNA4*
A2 151–171	7	20	1	0	4	4	*CHRM2, CREB3L2, TRIM24 (LOC101089090), KIAA1549, TTC26, BRAF, KLRG2, EPHB6, TRPV5, CASP2, FAM131B, TAS2R41, EZH2, ZNF783, SSPO, GIMAP4 (LOC101101043), ASB10, ABCF2, WDR86, KMT2C, DPP6, PAXIP1, MNX1, PTPRN2, WDR60*
A3 1–22	20	22	5	4	1	0	*MYT1, SLC2A4RG, ZGPAT, PTK6, EEF1A2, KCNQ2, CHRNA4, ARFGAP1, ADARB1, GATA5, CABLES2, RPS21, LAMA5, SS18L1 GNAS (LOC101098453), TMEPAI, ZBP1, PCK1, SPO11, TFAP2C, CSTF1, AURKA, DOK5, PFDN4, CYP24A1, BCAS1, ZNF217, TSHZ2, NFATC2, SDC4, PLCG1, TOP1, MAFB*
A3 22–31	20	9	5	4	0	0	*SRC, ASXL1*
A3 31–41		10	1	1	3	2	
A3 41–55		14	1	1	4	2	
A3 55–60		5	1	1	3	2	
A3 60–62		2	1	1	2	2	
A3 62–70	2	8	1	1	2	2	*AFF3, MSH2, MSH6, FBXO11*
A3 70–91	2	21	1	2	1	2	*BCL11A, REL, XPO1*
A3 91–113	2	22	1	2	0	0	*DCTN1, PAX8, TTL, EML4*
A3 113–119							*RRM2*
B1 51–115	84	64	1	0	5	5	*CLU, EXTL3, MSRA, GATA4, NEIL2, FDFT1, CTSB, PDGFC, PRSS48, FBXW7, GATB, FAM160A1*
B1 115–121	4	6	1	0	4	5	*FGF2, IL2, TET2, TACR3*
B1 121–142	4	21	2	0	4	5	*RAP1GDS1, AFF1, ARHGAP24*

B1 142–184	4	42	1	0	4	5	*RCHY1, PARM1, BTC, AREG, EREG, EPGN, MTHFD2L, CXCL8, RASSF6, AFP, AFM, ALB, ANKRD17, COX18 (LOC101095576), KDR, KIT, PDGFRA, CHIC2, FIP1L1, PHOX2B, RHOH*
B2 1–21	6	21	1	0	2	2	*TRIM27, CDKAL1, DEK*
B2 21–25	6	4	1	0	3	2	
B2 25–48	6	23	1	0	2	2	*IRF4, POU5F1, DAXX, HMGA1, FANCE, SRSF3, PIM1, TFEB, CCND3, HSP90AB1*
B2 48–120	6	72	0	0	5	6	*DPPA5, KHDC3L, DDX43, EEF1A1, PRDM1, FOXO3, CDC40, RPF2, FYN, WISP3, VGLL2, ROS1, DCBLD1, GOPC, RSPO3, PTPRK*
B2 120–134	6	14	1	0	3	5	*MYB, IFNGR1, TNFAIP3, EBP2, ECT2L, HECA*
B2 134–136	6	2	1	0	5	5	
B2 135–156	6	20	1	0	2	0	*ESR1, SYNE1, MYCT1, SYNJ2, EZR, MRPL18, PNLDC1, MAS1, FGFR1OP, IGF2R, PLG, MAP3K4, AFDN*
B3 1–21	15	21	2	0	2	1	*CRTC3, BLM, IDH2, NTRK3*
B3 21–38	15	17	1	0	2	2	*PML*
B3 38–40	15	2	1	0	1	2	
B3 40–60	15	20	0	0	1	3	*MAP2K1, TCF12,*
B3 60–85	15 14	25	0	0	2	5	*MYO5A, RAD51, KNL1, BUB1B, CCNB1IP1, AKAP6*
B3 85–99	14	14	1	0	2	5	*EGLN3, NFKBIA, NKX2-1, FOXA1, NUTM1*
B3 99–105	14	6	1	0	2	4	*NIN*
B3 105–112	14	7	0	0	3	4	*KTN1*
B3 112–115	14	3	0	0	3	3	*ESR2, MAX, GPHN*
B3 115–130	14	15	0	0	3	4	*MPP5, EIF2S1, PLEKHH1, ARG2, RAD51B, MAP3K9, NUMB, ACOT2 (LOC101092274), ACOT4, VSX2, TSHR*
B3 130–150	14	20	1	0	2	1	*FOXN3, TRIP11, GOLGA5, DICER1, TCL1A, BCL11B, HSP90AA1, AKT1*

B4 40–60	12	21	5	4	1	0	*ZNF384, ETV6, CDKN1B*
B4 60–105	12	45	3	1	2	1	*KRAS, PPFIBP1, SLC38A1, ARID2, COL2A1, KMT2D, ATF1, CDK4, PFDN5, HOXC13, HOXC11, ERBB3, NACA, STAT6, NAB2, DDIT3, CDK4, LRIG3, WIF1, HMGA2, MDM2, RAB3IP, CNOT2, KCNMB4, PTPRB, PTPRR, TSPAN8, LGR5,*
B4 105–125	12	20	3	1	3	1	*BTG1', C120rf74, PLEKHG7*
B4 125–146	22	21	8	6	0	0	*MCM5, RASD2, APOL6, APOL5, MYH9, EIF3D, EIF3L, MAFF, PDGFB, ATF4, MRTFA, EP300, BIK*
C1 1–20	1	20	2	0	3	1	*TNFRSF14, PRDM16, RPL22, CAMTA1, TNFRSF9, PIK3CD, EPHA2, SDHB, PAX7, ECE1, WNT4, E2F2*
C1 20–23	1	3	3	0	3	1	*ARID1A, EPB41, MECR, PTPRU*
C1 23–25	1	2	3	0	3	1	*LCK, S100PBP*
C1 25–45	1	22	2	0	3	3	*SFPQ, THRAP3, CSF3R, TMEM200B, SFRS4, MYCL, MPL, MUTYH, TAL1, STIL, CDKN2C, EPS15*
C1 45–91	1	46	0	0	4	6	*JUN, JAK1, FUBP1, BCL10, RPL5*
C1 104–121	1 2	17	0	0	3	7	*BCL9, ENSA, CTSS, CTSK, ARNT', MLLT11, SEMA6C, PI4KB, ERCC3, GLI2, INHBB*
C1 121–127	2	6	0	0	5	7	
C1 127–132	2	5	0	0	5	6	
C1 132–200	2	68	0	0	4	6	*CHN1, HOXD13, HOXD11, NFE2L2, PMS1, SF3B1, CASP8, CREB1, IDH1*
C1 200–202	2	2	1	0	2	2	*ATIC*
C1 202–223	2	21	2	0	2	1	*FEV, PAX3, ACSL3, ACKR3, HDAC4*
C2 50–69	3	20	1	0	6	3	*CBLB*
C2 69–81	3	12	4	0	1	1	*TFRC, HRASLS*
C2 81–89	3	8	7	0	1	1	*LPP, BCL6, EIF4A2, ETV5, SOX2*
C2 89–92	3	3	4	0	1	3	*PIK3CA*

C2 92–101	3	9	4	0	2	3	*TBL1XR1, MECOM*
C2 101–127	3	26	1	0	2	3	*MLF1, GMPS, WWTR1, FOXL2*
C2 127–138	3	11	1	1	2	3	
D1 1–20	11	20	1	0	4	5	*BIRC3 (LOC101083444), MMP7, PDGFD, CASP4, ATM', DDX10, POU2AF1, SDHD, ZBTB16, PAFAH1B2, PCSK7, KMT2A, DDX6, CBL (LOC101096508), ARHGEF12*
D1 20–40	11	20	0	0	6	6	*FLI1, KCNJ5, PGR, MAML2*
D1 40–79	11	39	0	0	5	7	*FZD4, PRSS23, ME3, EED, PICALM, SYTL2, CREBZF, ANKRD42, PCF11, RAB30, PRCP, TENM4, NARS2, GAB2, USP35, KCTD21, INTS4, AAMDC, RSF1, CLNS1A, AQP11, PAK1, GDPD4, OMP, CAPN5, WNT11, UVRAG, DGAT2, MAP6, SERPINH1, GDPD5, KLHL35, RPS3, ARRB1, NEU3, POLD3, PPME1, UCP2, RAB6A, RELT, FCHSD2, ATG16L2, CLPB, PHOX2A, INPPL1, FOLR1, NUMA1, NUP98, LMO1, NAV2, DBX1, SLC6A5, NELL1, CAPRIN1, NAT10, ABTB2, CAT, ELF5, EHF, HRAS*
D1 79–97	11	18	0	0	4	7	*FANCF, WT1, LMO2*
D1 97–118	11	21	1	1	3	1	*API5, TTC17, EXT2, CREB3L1, DDB2, CLP1, STX3, SDHAF2, BAD, RPS6KA4, MEN1, RPS6KB2, AIP, CPT1A, CCND1, FGF19, FGF4, FGF3, FADD, CARS*
D2 20–33	10	13	1	1	1	2	*CCDC6, TET1*
D2 33–91	10	58	2	1	2	3	*PRF1, KAT6B, BMPR1A, NCOA4, RET, HTR7, ANKRD1, RPP30, PPP1R3C, TNKS2, BTAF1, IDE, KIF11, HHEX, MYOF, SLIT1, ARHGAP19, FRAT1, FRAT2, RRP12, PGAM1, EXOSC1, ZDHHC16, MMS19, UBTD1, ANKRD2, COX15 (LOC101085408), CUTC, ABCC2, ENTPD7, DNMBP, CPN1, ERLIN1, CHUK, CWF19L1, SNORA12 (LOC111557193), BLOC1S2, PKD2L1, SCD, WNT8B, SEC31B, NDUFB8, HIF1AN, PAX2, SEMA4G, MRPL43, TWNK, LZTS2, PDZD7, SFXN3, KAZALD1, TLX1, GBF1, NFKB2, SUFU, NT5C2, SLK, SORCS3, VTI1A, TCF7L2, ATE1, SHTN1, FGFR2*
D3 1–35	12 22	35	1	2	3	1	*ZCCHC8, CLIP1, BCL7A, SH2B3, ALDH2, PTPN11, HNF1A, BCR, PATZ1, NF2', EWSR1, CHEK2, MN1, ASPHD2, SEZ6L, MYO18B, CRYBB2, SEPT5, CLTCL1, SMARCB1*

D3 35–76	18	41	1	0	4	3	*RAB31, RAB12, YES1, LAMA3, ZNF521, SS18, BRUNOL4, SETBP1, SLC14A2 (LOC101084395), SLC14A1(LOC101101172), LOXHD1, ST8SIA5, MYO5B, CFAP53, CXXC1, MAPK4, ELAC1, SMAD4, DCC, POLI*
D3 76–97	18	21	1	1	2	3	*TCF4, ZNF532, TXNL1, WDR7, ST8SIA3, FECH, NARS, ATP8B1, NEDD4L, ALPK2, MALT1, CDH20, RNF152, PIGN, BCL2, KDSR, NFATC1, CTDP1*
D4 17–37	9	20	2	1	3	4	*GNAQ, FANCC, PTCH1, KDM4C, PTPRD*
D4 37–43	9	6	2	0	2	4	*TYRP1*
D4 43–47	9	4	1	0	3	4	*NFIB, PSIP1, BNC2, SH3GL2*
D4 47–57	9	10	0	0	4	4	*MLLT3, MTAP, CDKN2A, CDKN2B, ELAVL2, TUSC1, IFNK, TEK*
D4 69–73	9	4	0	0	5	4	*TAL2, KLF4*
D4 73–75	9	2	0	0	5	2	
D4 75–77	9	2	1	2	4	2	*CDC26, PRPF4, RNF183*
E1 1–18	17	18	4	4	1	0	*RABEP1, TP53', PER1, AURKB, GLP2R, PIK3R5, RCVRN, GAS7, MAP2K4, PMP22, SPECC1, ULK2, SHMT1, TOP3A, FLCN, MAP2K3, YWHAE*
E1 18–37	17	19	2	2	0	0	*NF1, SUZ12, TAF15, ACACA, HEATR6, USP32, RPS6KB1, CLTC, BRIP1, RPS6KB1, RNF43, LPO, SFRS1, MSI2, COIL, DGKE, NOG, ANKFN1, PCTP, MMD, HLF, COX11 (LOC101085843)*
E1 37–44	17	7	5	5	0	0	*COL1A1, KAT7, NGFR, MLLT6, CDK12, LASP1, PPP1R1B, STARD3, ERBB2, GRB7, RARA, TOP2A, IGFBP4, SMARCE1, EIF1, STAT5B, STAT5A, STAT3, BRCA1, ETV4*
E1 44–65	17	21	6	5	0	0	*DDX42, GH1, CD79B, ICAM2, ERN1, TEX2, DDX5', SMURF2, PRKCA, APOH, AXIN2, PRKAR1A, KCNJ16, KCNJ2, H3F3B (LOC101080845), SRSF2, SEPT9, RNF213, ASPSCR1*
E2 1–18	19	18	4	4	1	1	*ZNF586 (LOC102902115), ZNF671, ZSCAN4 (LOC102901659), ZNF211, ZNF134, ZNF550, ZNF419 (LOC101098592), ZNF772, ZNF304, ZNF543 (LOC101095625), AURKC, PEG3, ZIM2, ZNF331, PPP2R1A, KLK2 (LOC101097936), ERCC2, CBLC, BCL3, CD79A, CIC, AKT2*

E2 18–39	19 16	21	0	2	2	1	*LSM14A, CCNE1, CYLD, RBL2, FTO, IRX5, MMP2, HERPUD1, NLRC5, CPNE2, CIAPIN1, DOK4, MMP15*
E2 39–44	16	5	0	1	2	2	*CDH8 (LOC101094809), CDH11 (LOC101095064)*
E2 44–66	16	22	2	1	2	1	*CDH5, PDP2, CES2, CBFB, TRADD, E2F4, PARD6A, CDH1, BCAR1, MAF, CBFA2T3, CDK10, FANCA, PRDM7*
E3 36–45	16	9	4	4	5	1	*CREBBP, IL32, MMP25, TNFRSF12A, PDPK1, CCNF, TRAF7, PKD1, TSC2, MCRIP2, AXIN1*
F1 1–23	1	23	0	3	1	0	*TP53BP2, EPHX1, H3F3A, SMYD3, EFCAB2, AKT3, EXO1, GREM2, PRRX1, RASAL2, ANGPTL1, ABL2*
F1 23–49	1	26	0	2	1	0	*PTGS2, PDC, TPR', RNF2, PLXNA2, PTPRC', DDX59, PKP1, PTPN7, UBE2T, SYT2, RABIF, BTG2, FMOD, PIK3C2B, MDM4, ELK4, SLC45A3, IKBKE, CFH (LOC101089505)*
F1 49–70	1	21	1	2	1	0	*CDC73, FAM5C, TGFB2, RAB3GAP2, PBX1, DDR2, ATF6, DUSP12, FCRLB, FCRLA, FCGR2B, SDHC, PCP4L1, APOA2 (LOC101088457), USP21, DEDD, CD48, DUSP23, APCS, FCRL4, RAB25, NTRK1, PRCC, SEMA4A, LMNA, CLK2, MUC1, EFNA4, IL6R, TPM3*
F2 17–63	8	46	3	0	1	3	*MYBL1, SGK3, COPS5, SULF1, NCOA2, TRAM1, EYA1, MSC, TERF1, PKIA, IL7, HEY1, FABP4 (LOC101087449), E2F5, NBN, RUNX1T1, CDH17, MDM4', ESRP1, CCNE2, TP53INP1, MTDH, STK3, COX6C (LOC101096876), RGS22, FBXO43, POLR2K, SPAG1, RNF19A, YWHAZ, UBR5, ODF1, KLF10, AZIN1, BAALC, DCAF13, RIMS2, ZFPM2, ABRA, OXR1, ANGPT1, EIF3E', RSPO2, TRHR, NUDCD1, ENY2, PKHD1L1, EBAG9, KCNV1, CSMD3, TRPS1*
FCA, feline chromosome; HSA, homologue human chromosomes; TC, tubulopapillary carcinoma group; SC, solid carcinoma and comedocarcinoma group.							

Supplementary table 1. CNVs observed in this study

3rd Manuscript

"Supplementary information"

Biological process	KEGG pathway	Count	Genes	*p*-value	FDR
Cell growth and death	Cell cycle	49	*E2F1, E2F2, E2F3, DBF4, PKMYT1, TTK, TGFB2, CDC45, CDKN2A, RAD21, MCM7, CDKN2B, CDKN2C, MYC, CDC6, CDK1, TP53, ESPL1, MCM2, CDK4, MCM3, MCM4, CDK2, MCM5, MCM6, CCND1, MAD2L1, CCND2, MDM2, BUB1B, GADD45A, CHEK1, BUB1, BUB3, TFDP1, YWHAB, CDC25C, YWHAE, CDC25B, CCNB1, YWHAG, CDKN1A, CCNB3, YWHAH, CCNB2, HDAC2, PLK1, PCNA, SMC1A*	4.11E-15	5.04E-12
	p53 signalling pathway	25	*BID, STEAP3, CHEK1, SESN2, GTSE1, CDKN2A, THBS1, CDK1, TP53, CDK4, CDK2, CCNB1, CDKN1A, CCND1, EI24, CCNB3, CCNB2, SERPINB5, CCND2, BAX, RRM2, MDM2, SIAH1, PERP, GADD45A*	2.37E-07	2.91E-04
Metabolism	Citrate cycle (TCA cycle)	13	*SDHA, DLST, ACO2, CS, IDH3B, IDH1, ACLY, PDHA2, PDHA1, DLAT, PCK2, IDH3A, MDH1*	9.32E-05	0.1
	Glycolysis / Gluconeogenesis	16	*LDHB, PFKL, HK2, PFKP, HK1, ALDH3B2, DLAT, PCK2, ALDH3B1, AKR1A1, PGAM4, ALDH1A3, PGM1, PDHA2, PDHA1, ENO1*	0.05	6.2
	Valine, leucine and isoleucine biosynthesis	6	*IARS, BCAT1, LARS, PDHA2, PDHA1, VARS*	0.01	55.1
	Biosynthesis of unsaturated fatty acids signalling pathway	8	*PECR, ELOVL5, FADS1, SCD, ELOVL2, FADS2, TECR, ACOT4*	0.009	11.3
	Glyoxylate and dicarboxylate metabolism	6	*MTHFD1, MTHFD2, ACO2, CS, MTHFD1L, MDH1*	0.02	24.8
	Oxidative phosphorylation	24	*ATP5D, UQCRC1, NDUFB6, NDUFA8, NDUFB9, CYC1, ATP6V1G1, ATP6V1B2, NDUFA10, UQCRFS1, COX5A, ATP5G3, COX5B, SDHA, ATP6V0C, ATP6V1E1, NDUFV1, NDUFS8, ATP5C1, ATP5A1, ATP6V1G3, COX17, NDUFS1, UQCRB*	0.02	26.1
	One carbon pool by folate	6	*MTHFD1, TYMS, MTHFD2, SHMT2, MTHFD1L, GART*	0.03	31.5
	N-Glycan biosynthesis	11	*MGAT1, MGAT2, STT3A, ALG2, ALG3, DAD1, RPN1, DPAGT1, RPN2, ALG12, DDOST*	0.03	35.3

Translation	Aminoacyl-tRNA biosynthesis	15	*CARS, YARS, NARS, AARS, GARS, EPRS, VARS, IARS, WARS, TARS, RARS, LARS, HARS, MARS2, MARS*	1.21E-04	0.1
DNA replication and repair	DNA replication	13	*POLA2, MCM2, RNASEH2A, MCM3, MCM4, MCM5, MCM6, POLE4, RFC3, MCM7, POLD1, PCNA, FEN1*	4.78E-04	0.5
	Pyrimidine metabolism	18	*POLR2G, POLR2F, POLR2E, DTYMK, DCK, POLR1C, CAD, POLA2, CMPK1, TK1, POLR3D, TYMS, POLE4, UMPS, POLD1, RRM2, RRM1, UCK1*	0.04	42.5
	Purine metabolism	26	*ADCY3, POLR2G, POLR2F, POLR2E, DCK, POLA2, HPRT1, PFAS, POLE4, PAPSS1, PAPSS2, IMPDH2, ADSSL1, NUDT5, AK2, POLR1C, AMPD2, PDE6H, GART, POLR3D, POLD1, RRM2, RRM1, ADSL, PAICS, PRPS1*	0.04	44.3
Cancer	Bladder cancer	14	*E2F1, E2F2, E2F3, CDKN1A, CCND1, CDKN2A, VEGFA, TP53, MDM2, CDK4, THBS1, MYC, DAPK3, MMP1*	6.30E-04	0.7
	Pathways in cancer	48	*HSP90AB1, E2F1, BID, E2F2, CKS1B, E2F3, EGLN3, ITGB1, MMP1, CTNNB1, TGFB2, AKT1, CDC42, MAX, CDKN2A, CDKN2B, SLC2A1, RAC1, LAMB1, MYC, TRAF4, FN1, DVL2, CTBP1, COL4A2, BMP2, COL4A1, RXRB, TP53, ITGA3, BIRC5, FGF21, CDK4, DAPK3, CDK2, FZD6, CCND1, CDKN1A, HSP90B1, HDAC2, HIF1A, LAMA5, BAX, VEGFA, MDM2, WNT11, TCEB1, WNT7A*	0.07	59.6
	Small cell lung cancer	21	*E2F1, E2F2, CKS1B, E2F3, COL4A2, COL4A1, RXRB, TP53, ITGA3, CDK4, ITGB1, CDK2, AKT1, MAX, CCND1, CDKN2B, LAMA5, LAMB1, MYC, TRAF4, FN1*	0.001	1.4
KEGG, Kyoto Encyclopaedia of Genes and Genomes; FDR, False Discovery Rate					

Supplementary table 1. KEGG pathway analysis for upregulated genes in FMC-derived cell lines. Data analysed with DAVID Bioinformatics.

Biological process	KEGG pathway	Count	Genes	*p*-value	FDR
Signal transductio n	Calcium signalling pathway	59	*PLCZ1, ADCY4, GNA14, GNA15, ADCY2, TACR3, TNNC2, PHKB, ADCY8, TACR1, ITPKB, EDNRA, AGTR1, ATP2B2, EDNRB, PLCB4, GRIN2C, PLCB1, HTR5A, PRKCA, EGFR, PTGER3, BST1, GRIN2A, PRKCB, CD38, GNAQ, CAMK4, RYR3, HTR7, PDGFRA, PDGFRB, CYSLTR1, ADORA2A, CYSLTR2, CAMK2G, PHKA1, OXTR, PTK2B, CALML3, PDE1A, GRPR, PPP3CC, PPP3CA, CALML5, CAMK2A, SLC8A1, SPHK1, PTGFR, ITPR1, P2RX7, P2RX1, ATP2A3, AVPR1A, ADRA1A, CACNA1C, CACNA1D, CACNA1A, HTR2A*	1.10E-07	1.35E-04
	Phosphatidylinosi tol signalling system	23	*PRKCA, PIK3CG, PLCZ1, IMPA2, PIK3C2G, PIP5K1B, DGKH, ITPKB, DGKI, CDS1, ITPR1, PRKCB, DGKB, PLCB4, CALML3, DGKG, PIK3C3, PIK3R5, INPP4B, CALML5, INPP5D, PLCB1, PIK3R1*	0.004	5.3

Signal transduction	MAPK signalling pathway	60	*MEF2C, FGF5, FGF7, FGF10, FGF12, MAPT, MAP3K8, FGF1, MAP2K6, AKT3, PRKCA, EGFR, BRAF, CACNG7, CACNG2, CACNG1, PRKCB, MAP4K3, ARRB1, RASGRF1, GADD45G, PDGFRA, PDGFRB, MAPK7, PLA2G5, FGFR1, PPM1B, KRAS, MAP3K3, RAC2, RASGRP4, MAP3K1, PLA2G12B, RASGRP2, PPP3CC, NFATC4, PPP3CA, NFATC2, EGF, RASA2, CACNA2D1, NTF4, NTF3, TAOK1, NLK, PTPN5, TAOK3, MAPK10, CACNA2D3, CACNA2D2, RPS6KA5, RPS6KA6, RPS6KA3, RPS6KA2, NTRK2, CACNA1C, CACNA1D, CACNA1A, PLA2G4E, CD14*	0.01	18
	Jak-STAT signalling pathway	36	*CRLF2, LEPR, STAT5B, IL21R, IL7R, STAT4, CSF3R, CSF2RB, IL2RG, PIK3R5, IL13RA1, AKT3, CSF2RA, PIK3R1, GHR, PIK3CG, IL4, PTPN6, IL2RA, IL23R, SOCS2, IL7, LIFR, IL6R, IL11RA, CISH, STAT3, CBLC, CBLB, PRLR, IL20RA, EPOR, JAK3, IL5RA, PIAS1, IL22RA2*	0.04	40.7
	VEGF signalling pathway	20	*PRKCA, PIK3CG, SPHK1, SRC, KDR, PRKCB, SH2D2A, KRAS, RAC2, PLA2G12B, PPP3CC, PIK3R5, NFATC4, PPP3CA, NFATC2, NFATC3, PLA2G5, PIK3R1, PLA2G4E, AKT3*	0.04	41.2
	mTOR signalling pathway	15	*PIK3CG, CAB39L, BRAF, PGF, IGF1, RICTOR, VEGFC, RPS6KA6, RPS6KA3, RPS6KA2, RHEB, PIK3R5, PRKAA2, PIK3R1, AKT3*	0.04	45
	Wnt signalling pathway	34	*CER1, NKD1, WNT16, BTRC, CAMK2G, DAAM1, TCF7L2, TCF7L1, WNT2, WNT4, PLCB4, WNT3, RAC2, PPP3CC, NFATC4, PPP3CA, NFATC2, PLCB1, NFATC3, CAMK2A, APC, PRKCA, WNT10A, NLK, MAPK10, PRKCB, SFRP5, DKK2, FZD10, SFRP2, GSK3B, PRICKLE2, WNT9B, PPP2R5E*	0.06	58.7
	ErbB signalling pathway	21	*PRKCA, EGFR, PIK3CG, BRAF, CAMK2G, STAT5B, MAPK10, SRC, PRKCB, CBLC, CBLB, KRAS, EREG, GSK3B, PIK3R5, AREG, SHC3, EGF, CAMK2A, PIK3R1, AKT3*	0.09	68.9
Immune response	Complement and coagulation cascades	29	*C7, A2M, F13A1, C6, C5, C1R, C1S, C1QC, FGG, CFD, KNG1, C5AR1, F8, SERPING1, C4BPB, F7, C4BPA, PLG, C8A, C1QA, C1QB, VWF, C8B, THBD, F5, F3, TFPI, SERPIND1, PLAU*	2.63E-06	0.03
	Leukocyte transendothelial migration	39	*CLDN8, ITGAL, CLDN7, OCLN, MYL2, CLDN4, MMP9, CLDN5, ITGB2, MMP2, CXCL12, CDH5, ITGAM, RAC2, PTK2B, ESAM, RAPGEF4, PIK3R5, RAPGEF3, PIK3R1, PIK3CG, PRKCA, ITK, NOX3, VAV3, NCF1, NCF4, MYLPF, ACTN2, ACTN3, ITGA4, PRKCB, THY1, RASSF5, CYBB, PECAM1, TXK, JAM2, JAM3*	3.20E-05	0.03
	Hematopoietic cell lineage	31	*CD8A, MME, KIT, IL7R, ITGAM, GP9, MS4A1, CD2, CSF3R, CD5, CSF2RA, CD7, CSF1R, IL4, IL2RA, CD3G, CD3D, CD3E, IL7, ITGA4, IL6R, IL11RA, CD38, CD37, CD36, CD34, ITGA5, EPOR, IL5RA, CD14, ITGA2B*	4.06E-05	0.05

Immune response	T cell receptor signalling pathway	33	*CD8A, NFKBIA, KRAS, MAP3K8, ZAP70, PPP3CC, NFATC4, PIK3R5, PPP3CA, NFATC2, NFATC3, AKT3, PIK3R1, TEC, PIK3CG, IL4, PTPRC, ITK, PTPN6, VAV3, CD3G, CD3D, CD3E, CTLA4, CARD11, CBLC, PRKCQ, CBLB, CD40LG, GSK3B, LCK, GRAP2, LCP2*	7.15E-04	0.8
	Chemokine signalling pathway	49	*ADCY4, ADCY2, ADCY8, ADCY5, STAT5B, CXCR3, CXCL12, PLCB4, CXCR5, TIAM1, PLCB1, SHC3, AKT3, PIK3CG, BRAF, NCF1, WAS, PRKCB, ELMO1, ARRB1, WASL, CCL1, PARD3, CCL2, CCR1, CXCL9, NFKBIA, CCL8, DOCK2, CCL22, KRAS, RAC2, PTK2B, CCL21, RASGRP2, PIK3R5, PIK3R1, ITK, VAV3, CCL19, STAT3, GNGT2, CCL14, CXCL14, GSK3B, GRK7, GRK4, JAK3, GRK5*	0.001	1.7
	Fc gamma R-mediated phagocytosis	27	*WASF2, PIP5K1B, ASAP3, AMPH, DOCK2, RAC2, PIK3R5, INPP5D, AKT3, PIK3R1, SYK, PIK3CG, PRKCA, PTPRC, PLD1, VAV3, NCF1, SPHK1, PRKCE, WAS, PRKCB, SCIN, PLA2G4F, WASL, PLA2G4E, DNM1, PLA2G4D*	0.007	8.4
	Primary immunodeficiency	13	*CIITA, PTPRC, CD3D, CD8A, CD3E, CD40LG, LCK, ZAP70, IL2RG, JAK3, CD40, IL7R, BTK*	0.009	11.5
	B cell receptor signalling pathway	22	*PIK3CG, PTPN6, VAV3, NFKBIA, BTK, PRKCB, CARD11, KRAS, RAC2, GSK3B, PPP3CC, PIK3R5, CD79B, NFATC4, PIK3AP1, PPP3CA, INPP5D, NFATC2, NFATC3, PIK3R1, AKT3, SYK*	0.01	13
	Fc epsilon RI signalling pathway	21	*PRKCA, IL4, PIK3CG, FCER1A, VAV3, MAPK10, PRKCE, BTK, PRKCB, KRAS, RAC2, PLA2G12B, PIK3R5, INPP5D, PLA2G5, PIK3R1, MAP2K6, PLA2G4E, AKT3, LCP2, SYK*	0.03	34
Cellular interaction	Focal adhesion	57	*PGF, VTN, PDGFD, SHC3, AKT3, PARVG, EGFR, PRKCA, PIK3CG, BRAF, ACTN2, ACTN3, PRKCB, VEGFC, LAMC3, RASGRF1, COL1A2, PDGFRA, PDGFRB, LAMC2, COL1A1, PARVB, ITGA2B, CAV3, MYL2, COL3A1, ITGA11, SRC, LAMB4, DOCK1, COL6A6, RAC2, ITGB8, TNR, COL6A3, COL6A1, PIK3R5, EGF, THBS2, PIK3R1, COL4A4, VAV3, MYLPF, IGF1, MAPK10, HGF, ITGA4, BIRC3, COL4A6, KDR, LAMA2, VWF, ITGA9, LAMA3, ITGA5, GSK3B, ITGA8*	5.81E-05	0.07
	Cell adhesion molecules (CAMs)	40	*CLDN8, ITGAL, CLDN7, OCLN, CD8A, CLDN4, CLDN5, CDH1, ITGB2, CDH4, HLA-DMA, CDH5, ITGAM, ITGB8, CD2, ESAM, CNTNAP1, HLA-DOB, NEGR1, MAG, PTPRC, PTPRM, ICAM2, NLGN1, CTLA4, NFASC, ITGA4, CD40, PDCD1LG2, SIGLEC1, NCAM2, ITGA9, CD80, CD34, CD40LG, ITGA8, PECAM1, CNTN1, JAM2, JAM3*	2.08E-04	0.25

Cellular interaction	Cytokine-cytokine receptor interaction	65	*LEPR, IL18, IL21R, TNFSF15, CXCR3, CXCL12, IL17RB, TNFRSF11A, CXCR5, IL1RAP, CSF3R, CSF2RB, IL13RA1, LTB, CSF2RA, GHR, EGFR, LIFR, TNFRSF17, CD40, IL6R, IL11RA, VEGFC, ACVR2A, TNFSF13B, IL20RA, CD40LG, PDGFRA, PDGFRB, CCL1, TNFRSF6B, CCL2, CCR1, CRLF2, CXCL9, BMPR2, CCL8, KIT, IL7R, CCL22, IL17B, CCL21, TNFRSF19, IL2RG, EGF, CD27, CSF1R, IL4, IL18R1, IL2RA, IL23R, IL7, CCL19, HGF, KDR, TNFSF8, TNFSF10, CCL14, TNFSF11, PRLR, CXCL14, EPOR, IL5RA, IL22RA2, BMPR1A*	0.001	1.2
	ECM-receptor interaction	27	*COL3A1, ITGA11, VTN, GP9, LAMB4, COL6A6, ITGB8, TNR, COL6A3, COL6A1, SV2B, THBS2, COL4A4, ITGA4, COL4A6, LAMA2, ITGA9, VWF, LAMA3, CD36, ITGA5, LAMC3, ITGA8, COL1A2, LAMC2, COL1A1, ITGA2B*	0.001	1.3
	Tight junction	35	*CLDN8, CLDN7, PARD3, OCLN, MYH15, MYL2, CLDN4, CLDN5, CASK, SRC, KRAS, AKT3, PRKCA, MAGI3, MAGI1, HCLS1, MYH3, MYH2, MPP5, PRKCH, MYLPF, MYH7, ACTN2, ACTN3, PRKCE, MYH8, PRKCB, EPB41L3, IGSF5, PRKCQ, CGN, MYH11, MYH13, JAM2, JAM3*	0.008	9.7
	Gap junction	24	*PRKCA, EGFR, ADCY4, ADCY2, ADCY8, ADCY5, LPAR1, PRKG2, ITPR1, SRC, PRKCB, KRAS, PLCB4, GNAQ, PDGFRA, TUBA4A, GUCY1A3, PDGFRB, GUCY1B3, PDGFD, MAPK7, PLCB1, EGF, HTR2A*	0.02	23.7
Cell motility	Regulation of actin cytoskeleton	47	*ITGAL, FGFR1, FGF5, FGF7, MYL2, SSH2, WASF2, ITGA11, PIP5K1B, FGF10, ABI2, ITGB2, FGF12, ITGAM, KRAS, DOCK1, RAC2, ITGAX, ITGB8, TIAM1, PIK3R5, PDGFD, EGF, FGF1, FGD3, PIK3R1, APC, ARHGEF4, PIK3CG, EGFR, VAV3, BRAF, NCKAP1L, MYLPF, ACTN2, ACTN3, ITGA4, WAS, ITGA9, ITGA5, ITGA8, SCIN, PDGFRA, PDGFRB, WASL, CD14, ITGA2B*	0.05	47.5
KEGG, Kyoto Encyclopaedia of Genes and Genomes; FDR, False Discovery Rate					

Supplementary table 2. KEGG pathway analysis for downregulated genes in FMC-derived cell lines. Data analysed with DAVID Bioinformatics.

Marker	Negative control	Positive control
vimentin	IgG1	feline skin
pan-CK	IgG1	feline skin
CK8/18	IgG1	feline normal mammary gland
CK14	rabbit serum	feline skin
CK5/6	IgG1	feline skin
SMA	IgG2a	feline urinary bladder
calponin	IgG1	feline normal mammary gland
p63	IgG2a	feline normal mammary gland
E-cadherin	IgG2a	feline skin
Ki67	IgG1	feline normal small intestine
p53	IgG2a	feline transitional cell carcinoma
COX-2	rabbit serum	feline normal lymph node, feline transitional cell carcinoma
HER-2/c-erbB2	IgG1	human mammary tissue and pellets from cell lines overexpressing HER-2*, feline mammary carcinoma
progesteron receptor	IgG2a	feline normal mammary gland
estrogen receptor	IgG1	feline normal mammary gland
claudin-2	IgG2b	feline and canine normal mammary gland
HMGA2	rabbit serum	Feline and canine neonatal tissue
CD44	rat serum	feline lymph node
*kindly provided by Prof. Dr. H.-H. Kreipe, Department of Pathology, Hannover Medical School		

Supplementary table 3. Antibodies and corresponding negative and positive controls used in this study.

"List of abbreviations"

Abbreviation*	Explanation
DFS	Disease-free survival
ER	Oestrogen receptor
FMCs	Feline mammary carcinomas
HER2	Human epidermal growth factor receptor 2
HMG	Histological malignancy grade
hTNBC	Human late-stage hormone receptor-independent triple negative breast cancer
NGS	Next-generation sequencing
OS	Overall survival
PR	Progesterone receptor
FFPE	Formalin-fixed paraffin-embedded
FF	Fresh-frozen tissue
BS	British shorthair
DSH	Domestic Shorthair
TC	Tubulopapillary carcinomas
IPC	Intraductal papillary carcinomas
SC	Solid carcinomas
CC	Comedocarcinomas
hMBC	Human metaplastic breast carcinoma
CNV	Copy-number variations
FCAs	Feline chromosomes
WHO	World Health Organization
HMGA2	High-mobility group AT-hook 2 protein
E-cad	E-cadherin
Vim	Vimentin (antibody)
VIM	Vimentin (gene)
CKs	Cytokeratins
CALP	Calponin
SMA	Smooth muscle actin

CNGs	Copy-number gains
CNLs	Copy-number losses
H&E	Haematoxylin eosin
CK5/6	Cytokeratin 5/6
pan-CK	Pan-cytokeratin
COX-2	Cyclooxigenase-2
CLDN-2	Claudin 2
RT-PCR	Real-time polymerase chain reaction
BrdU	5-bromo-2'-deoxyuridine
CK8/18	Cytokeratin 8/18
CK14	Cytokeratin 14
HSA 8q	Human chromosome 8
FISH	Fluorescence in situ hybridization
FBS	Foetal bovine serum
EMT	Epithelial to mesenchymal transition
CGH	Comparative genome hybridisations
HAS	Homologue human chromosomes
TUSC3	Tumour suppressor candidate 3
EPV	Events per variable
DEGs	Differentially expressed genes
RIN	RNA integrity number
CTCs	Circulating tumour cells
KEGG	Kyoto Encyclopaedia of Genes and Genomes
NSCLC	Non-small cell lung cancer
HNSCC	Head and neck squamous cell carcinoma
CAMs	Cell adhesion molecules
ESRP1	Epithelial splicing regulatory protein 1
CSCs	Cancer stem cells
RRM2	Ribonucleotide reductase regulatory subunit M2

*This list does not include an extensive review of official gene names mentioned in the document and tables, for additional details please refer to:

https://www.ncbi.nlm.nih.gov/gene?cmd=Retrieve&dopt

ACKNOWLEDGMENTS

Conducting my research in Germany has been a dream come true and there is no possible way I can thank my main supervisor Prof. Dr. Ingo Nolte for giving me the opportunity to develop my work at the Small Animal Clinic/University of Veterinary Medicine Hannover—I will be forever grateful. His great contribution to this thesis with his experience and knowledge is invaluable. Besides my main supervisor, I would like to thank PD. Dr. Hugo Murua Escobar and Prof. Dr. Marion Hewicker-Trautwein for their comments and motivation, but overall for helping me to widen my research and to challenge myself. Thanks to Dr. Johannes Junginger for all of his comments and careful review of the manuscripts included in this thesis. I would like to express my most sincere gratitude to the team of Chronix Biomedical and the Institute of Veterinary Medicine/University of Göttingen, especially to Dr. Julia Beck, Dr. Kirsten Bornemann-Kolatzki, and Prof. Dr. Bertram Brenig for their invaluable contribution to this work.

I would like to thank the DAAD for providing the necessary funding to carry out my research. Your economic support is of immense value for scientists from all over the world. I hope that many other scientists from lower-income countries like mine will have the opportunity you granted me.

Thanks to Dr. Vladimir Galindo Zamora and Dr. Claudia Brieva Rico for their friendship and endless help since the moment I started my journey as a veterinary student. Thanks to everyone in the molecular biology research group at the Small Animal Clinic/TiHo, it was great sharing laboratory with you during the last three years. Thanks to Ms. Kerstin Rohn for her technical assistance, and to Dr. Selle and Tanja Czeslik for their help and support during the last three years. I also would like to thank the entire team of the Small Animal Clinic/National University of Colombia, especially to Doc Lu, Mary, Henry, Piero, Giovanni, Diego, and Angela; I hope to work again with you at some point of my life.

To my life-coaches, my parents Etelvina and Joaquín, who have always supported me all along the way—nothing would have been possible without you. Thanks to my beloved sisters, Diana, and Martha for always having a positive word and for encouraging me to be who I am. Many thanks to my beloved husband Félix Requena, you're my best friend, my eternal cheerleader, my favourite scientific consultant and my biggest support. Thanks to my family in Spain, Pilar, Antonio-padre, Jesús, Charlene, Antonio-hijo, Gema, Toñi, Paco and Javier for adopting me as another member of the family. Thanks to my little nieces and nephew, Isabella, Nathalia, Irene and Alejandro, life has never been so funny, I love you guys!

Thanks to all my dear friends in Colombia who have always been there for me especially to Andrés, Alex, Juan Lucas, Mayo, and Luis Angel. Thanks to my dearest friend Gudrun for visiting us on every occasion she came to Germany—your visits were always a way to refill batteries. Thanks to my favourite women, friends, and colleagues in Germany Heike, Lisa, Eva, Camila, Suhayla and Leona you are all awesome!

And finally, last but by no means least, thanks to my beloved dog Diablo for being so crazy and special, and for always making me feel happy and loved. Thanks to all my beloved friendly, fuzzy, smelly, loyal, protective, smart, ferocious, high-spirited, intelligent, playful, splendid, and not so obedient four-legged friends for being there during my whole life taking turns in this endless relay race.